

UNIVERSITY OF OKLAHOMA

GRADUATE COLLEGE

VARIABILITY OF TROPICAL CYCLONES IN THE PHILIPPINES

A DISSERTATION

SUBMITTED TO THE GRADUATE FACULTY

in partial fulfillment of the requirements for the

Degree of

DOCTOR OF PHILOSOPHY

By

IRENEA L. CORPORAL-LODANGCO

Norman, Oklahoma

2014

VARIABILITY OF TROPICAL CYCLONES IN THE PHILIPPINES

A DISSERTATION APPROVED FOR THE  
SCHOOL OF METEOROLOGY

BY

---

Dr. Peter J. Lamb, Co-Chair

---

Dr. Lance M. Leslie, Co-Chair

---

Dr. Michael B. Richman

---

Dr. Renee A. McPherson

---

Dr. Gerilyn S. Soreghan



To my beloved parents, Osias and Trinidad,  
who sacrificed and worked hard so their children could get the education they  
dreamed to have,

and to my three girls,  
Izabela, Izra, and Izandra,  
who are indeed beautiful gifts from the Lord.

*“Trust in the Lord with all your heart and lean not on your own understanding.”*  
*Prov. 3:5*

## **Acknowledgements**

I would like to express my heartfelt gratitude to the people who have provided their support and encouragement throughout my doctoral studies at OU.

First and foremost, I want to thank my advisors, Dr. Peter J. Lamb and Dr. Lance M. Leslie. Without them, this academic journey would not be possible. They believed in me when they decided to accept me as their student, and they have never failed to provide kind support, understanding and extensive knowledge. Similarly, I gratefully acknowledge the Cooperative Institute for Mesoscale Meteorological Studies (CIMMS) for funding my Ph. D. work.

I am thankful to Dr. Michael B. Richman, Dr. Renee A. McPherson and Dr. Gerilyn S. Soreghan for being part of my dissertation committee. Their academic input and encouragement are greatly appreciated.

I acknowledge Luwanda Byrd for all the help she extended to me and for the friendship that has been made through this process.

My deepest appreciation also goes to my Filipino friends who stood and served as my family during my early years in Oklahoma, as well as, to my American churchmates for their emotional support and friendship.

In addition, my earnest thanks goes to my best friend Mercy Johnson who stood with me through all my ups and downs. Thank you for always lending your ears when I need them.

My most special thank you goes to my family:

- To my parents, who told me to build a dream and chase after it. Thank you for believing and supporting me. I am eternally grateful for all your hard work and sacrifices. Without each of you, I'd be nowhere near where I am today.
- Also, to my sisters, Amelia and Elizabeth, for looking after my girls when I was out of the Philippines to pursue my graduate studies.
- To Nanay Doya, for staying faithful to my family. Thank you for taking care of us and giving my girls unconditional love.
- To my husband, Don, for being a father to my girls.
- And to my real treasures - Izabela, Izra and Izandra, my constant source of joy, and the reason why I pursue this dream, thank you.

Last but definitely not the least, I would like to express my sincerest gratitude to God. Without Him I cannot do anything, and thank you for giving me all these wonderful people who have made this journey much more brighter and enjoyable.

## Table of Contents

	<b>Page</b>
<b>Acknowledgements</b>	iv
<b>List of Tables</b>	x
<b>List of Illustrations</b>	xi
<b>Abstract</b>	xvii
<b>Chapter 1. Introduction</b>	1
<b>Chapter 2. Domain, Data, and Definitions</b>	
2.1 Study Region	5
2.2 TC Data Source	5
2.3 Large-scale Climate Data	6
2.4 Definitions	8
<b>Chapter 3. Climatology of Philippine Tropical Cyclone Activity</b>	
3.1 Introduction	9
3.2 Methodology	13
3.3 TC Statistics	15
3.4 TC Season Start/End Date and Length	18
3.5 TC Days	27

3.6 Landfall	27
3.7 Intensity	30
3.8 Variability	32
3.9 Genesis Positions and Tracks	35
3.10 The Role of ENSO	39
<b>Chapter 4. Impacts of ENSO on Philippine TC Activity</b>	
4.1 Introduction	44
4.2 Methodology	46
4.3 ENSO Impacts on Genesis, Tracks, and Frequency	
4.3.1 Genesis Positions	49
4.3.2 Tracks	54
4.3.3 Frequency	59
4.4 Impacts on Other TC Properties	
4.4.1 Intensity	61
4.4.2 TC days	66
4.4.3 Season ACE	68
4.4.4 Season Start/End date and Length	72
4.5 ENSO Influence on Large-scale Environmental Variables	
4.5.1 SST	77
4.5.2 Vorticity	81
4.5.3 Zonal Wind	86



4.5.4 Divergence	88
4.6 Summary and Conclusions	92
<b>Chapter 5. Cluster analysis of Philippine tropical cyclones</b>	
5.1 Introduction	98
5.2 Methodology	101
5.2.1 K-means Cluster Algorithm	102
5.2.2 Determining the Number Clusters	
5.2.2.1 Silhouette Coefficient	105
5.2.2.2 Total Sum of Point-to-Cluster Distances	109
5.2.2.3 Oceanic and Meteorological Variables	109
5.3 Results	
5.3.1 The Optimal Cluster Number	112
5.3.2 Clustering of Genesis Locations	115
5.3.3 Genesis Seasonality	118
5.3.4 Clustering of Decay Locations	120
5.3.5 Decay Seasonality	123
5.3.6 Clustering of Tracks	126
5.3.7 Tracks Seasonality	130
5.3.8 Monthly Analysis of TC Activity	133
5.4 Discussion and Conclusions	141

<b>Chapter 6. Future Work</b>	145
<b>Chapter 7. References</b>	147

## List of Tables

- Table 1: Quarterly number of tropical cyclones, percentage of number over the total, number of tropical cyclone landfalls, and the percentage of landfalls over the quarterly landfall total. The last line is the total and percentage of all tropical cyclones and landfalls for the period 1945-2011.
- Table 2: Quarterly number of tropical cyclones, percentage of the number over the total, quarterly number of tropical cyclones classified by intensity and its quarterly percentage. Intensity is classified into tropical depression (TD), tropical storm (TS), and typhoon (TY).
- Table 3: Same as Table 2, but for quarterly number of landfalls, percentage of landfalls over the quarterly total, quarterly number of landfalls classified by intensity and its quarterly percentage.
- Table 4: List of years for each ENSO phase in LAS and MAS.
- Table 5: Comparison of LAS start and end dates and length during El Niño and La Niña phases with Neutral phase.
- Table 6: Comparison of MAS start and end dates and length during El Niño and La Niña phases with Neutral phase.
- Table 7: Summary of ENSO impacts on Philippine TC activity in LAS and MAS.
- Table 8. Silhouette coefficients and total sum of point-to-centroid distances.

## List of Illustrations

- Figure 1: (a) Tropical storm (TS) Thelma just before its landfall in the Philippines, source://www.noaa.gov and (b) track of TS Thelma, source://http:commons.wikimedia.org
- Figure 2: The study region covers latitudes  $5^{\circ}$ - $25^{\circ}$ N and longitudes  $115^{\circ}$ - $135^{\circ}$ , shown as the black inset and referred to here as the Philippine domain. The irregular box (red broken line) shows the PAGASA area of responsibility for TCs. PAGASA monitors and forecasts TCs that affect the Philippines.
- Figure 3: Mean monthly TCs in the Philippines. The less active season (LAS) runs from January 1 to May 31, representing the quiet phase of TC activity in the Philippine domain, during which there is less than one TC on average per month. The more active season (MAS) is from June 1 to December 31, with monthly averages greater than one.
- Figure 4: Time series of annual number of TCs (in green line) plotted against the LAS (in blue line) and MAS (in red line) TCs. The MAS dominates the mean annual TC numbers, accounting for about 80% of the total. The linear trend lines are shown as dashed lines.
- Figure 5: The year-to-year TC activity in the Philippine domain. The TC frequency varies on an intraseasonal time scale, with alternating LAS, quiescent, and MAS periods. The blue and red bars denote the yearly season length of the LAS and the MAS, respectively. Season length is defined as starting from the day of the first TC genesis in the Philippine domain and ending when the last TC lies within the domain. The start date of the season (lower tip of the bar) is defined as the day when the first TC, during a particular season, is in the Philippine domain. The end date of the season (upper tip of the bar) is defined as the day when the last TC is inside the domain. The mean start and end dates for the LAS (MAS) are March 6<sup>th</sup> (June 20<sup>th</sup>) and May 5<sup>th</sup> (December 10<sup>th</sup>), respectively.
- Figure 6: (a) The length of less active season (LAS) is illustrated by the length of the bar in each year (b) the five-year running mean of the LAS length (c) the five-year running mean of LAS yearly earliest start date (d) the

five-year running mean of LAS yearly latest end date. The dash line in each graph represents the trend line.

- Figure 7: Same as Fig. 6, but for more active season (MAS). (a) The yearly season length as represented by the length of each bar (b) the five-year running mean of MAS length (c) the five-year running mean of MAS yearly earliest start date (d) the five-year running mean of MAS yearly latest end date. The dash line for each graph is the trend line.
- Figure 8: Frequency distribution of (a) length of the annual TC season, (b) LAS length, and (c) MAS length.
- Figure 9: Same as Fig. 8, but for the TC days.
- Figure 10: Interannual and interdecadal variations in the frequency of (a) all TCs and (b) landfalling TCs over the 1945-2011 period. Large amplitude variations are apparent in the time series. The maximum was 28 in 1993, and the minimum was 10 in 1946. Years with 5-year running mean below the long-term average of 18 are considered to be part of the below average period (BAP), and all years with above average TCs are part of the above average period (AAP).
- Figure 11: Seasonal variations in genesis positions of all TCs in (a) LAS, and (b) MAS. Tracks of all TCs in (c) LAS, and (d) MAS. Genesis positions of landfalling TCs in (e) LAS, and (f) MAS. Tracks of landfalling TCs in (g) LAS, and (h) MAS.
- Figure 12: (a) Wavelet analysis of the Philippine TC series. The black curve indicates the cone of influence, and (b) the corresponding global wavelet spectrum.
- Figure 13: Shows how TC-ENSO relationship varies with quarter (a) Standardized quarterly TC total during neutral, El Niño and La Niña conditions (b) same with (a) but for standardized TC landfall count.
- Figure 14: Niño 3.4 indices ( $^{\circ}\text{C}$ ) for the period 1950-2011 for (a) LAS and (b) MAS, the dashed lines show the negative and positive threshold of the index.

- Figure 15: TC genesis locations during (a)-(c) LAS, and (d)-(f) MAS for each ENSO phase. The black double circles are the mean genesis locations.
- Figure 16: TC birthplace cumulative density per  $5^\circ \times 5^\circ$  grid box during (a)-(c) LAS, and (d)-(f) MAS for each ENSO phase.
- Figure 17: Tracks of TCs formed in (a)-(d) Neutral, (e)-(h) El Niño, and (i-l) La Niña years during JFM, AMJ, JAS, and OND.
- Figure 18: Tracks of TCs formed in (a)-(d) Neutral, (e)-(h) El Niño, and (i-l) La Niña years during LAS and MAS.
- Figure 19: TC track density per  $5^\circ \times 5^\circ$  grid box during (a)-(c) LAS, and (d)-(f) MAS for each ENSO phase.
- Figure 20: Influence of ENSO to LAS and MAS TCs and landfalls (a) Standardized seasonal TC mean in LAS and MAS during ENSO conditions, (b) same with (a) but for standardized TC landfall mean.
- Figure 21: Standardized seasonal TC mean by intensity classification during various ENSO conditions (a) tropical depression (TD), (c) tropical storm (TS), and (c) typhoon.
- Figure 22: Standardized seasonal TC landfall mean by intensity classification in LAS and MAS during various ENSO conditions (a) tropical depression (TD), (c) tropical storm (TS), and (c) typhoon.
- Figure 23: Standardized seasonal number of TC days in LAS and MAS during various ENSO conditions.
- Figure 24: Climatological ACE per year for (a) LAS and (b) MAS. The dashed lines denote the 25<sup>th</sup>, median, and 75<sup>th</sup> percentiles.
- Figure 25: Standardized seasonal ACE in LAS and MAS during various ENSO conditions.

- Figure 26: The LAS start and end dates denoted by the lower and upper tip of the bar, respectively during (a) Neutral, (b) El Niño, and (c) La Niña phases of ENSO. The length of the bar also denotes the season length.
- Figure 27: Same as Fig. 26, but for MAS.
- Figure 28: Composite mean of surface SST during (a) LAS Neutral, (b) LAS La Niña, (c) LAS El Niño, (d) MAS Neutral, (e) MAS La Niña, and (f) MAS El Niño.
- Figure 29: SST differences (a) LAS Neutral minus LAS El Niño, (b) LAS Neutral minus LAS La Niña, (c) LAS El Niño minus LAS La Niña, (d) MAS Neutral minus MAS El Niño, (e) MAS Neutral minus MAS La Niña, and (f) MAS El Niño minus MAS La Niña.
- Figure 30: Same as Fig. 28, but for vorticity at .995 sigma level.
- Figure 31: Same as Fig. 29, but for vorticity differences.
- Figure 32: Same as Fig. 28, but for zonal wind at 200 mb.
- Figure 33: Same as Fig. 29, but for zonal wind differences.
- Figure 34: Same as Fig. 28, but for divergence at .2101 sigma level.
- Figure 35: Same as Fig. 29, but for divergence differences.
- Figure 36: Silhouette graphs for (a) genesis, (b) track, and (c) decay clusters.
- Figure 37: Key variables conducive to TC development and were used to subjectively decide on the most appropriate number of clusters. (a) SST, (b) vorticity, (c) relative humidity (RH), and (d) sea level pressure (SLP).
- Figure 38: K-means clusters of (a) genesis, (b) decay, and (c) tracks. The black asterisks are the centroid of each cluster.

- Figure 39: Cumulative density per 5°latitude by 5°longitude grid box of genesis locations.
- Figure 40: Corresponding TC tracks of each genesis cluster.
- Figure 41: Number of TCs per calendar month for each genesis cluster.
- Figure 42: Boxplots for each genesis cluster.
- Figure 43: Cumulative density of TCs decaying in each 5°latitude by 5°longitude grid box for each cluster and the percentage of decay per cluster.
- Figure 44: Corresponding TC tracks of each decay cluster.
- Figure 45: Same as Fig. 41, but for each decay cluster.
- Figure 46: Same as Fig. 42, but for decay clusters.
- Figure 47: Cumulative density of TC passages per 5° latitude by 5° longitude grid box.
- Figure 48: Track clusters after applying K-means clustering to Philippine TC tracks.
- Figure 49: Same as Fig. 45, but for each track cluster.
- Figure 50: Same as Fig. 46, but for each track cluster.
- Figure 51: Monthly variations of TC activity over the Philippine domain during JFM by cluster.
- Figure 52: Same as Fig. 51, but for AMJ.
- Figure 53: Same as Fig. 51, but for JAS.



Figure 54: Same as Fig. 51, but for OND.

## Abstract

The massive impacts of tropical cyclones (TCs) on the Philippines are well known. This study provides an improved understanding of TC activity in the country, allowing improved risk mitigation strategies that possibly can reduce the economic cost and fatalities from TCs. About 70% of tropical cyclones (TCs) in the western North Pacific (WNP) affect the Philippine region, with an annual median of 18 TCs for 1945-2011. The Philippine region has no TC free months, and here the calendar year is partitioned into the less active (LAS) and more active (MAS) seasons. A unique aspect that arose from this study is the nature of the transition periods between the LAS and the MAS. Philippine TC activity is defined by a comprehensive range of seasonal metrics, including: frequency, landfall, total days, earliest start/end dates, latest start/end dates, season lengths, genesis locations, and tracks.

The annual median for the LAS (MAS) frequency is 2 (15) with an interquartile range (IQR) 2 (4.5); the median LAS (MAS) landfalling frequency is 1 (5); and the median TC days is 8 (51). The median LAS (MAS) start and end dates are February 28<sup>th</sup> and May 20<sup>th</sup> (June 18<sup>th</sup> and December 16<sup>th</sup>). The median LAS (MAS) season length is 61 (176) days with IQR of 101 (28) days. The LAS (MAS) birthplaces are latitudinally bounded by 20°N (27°N) latitude and tracks by 46°N (55°N). A quiescent (TC free) period is identified between the LAS and MAS, varying from 2 days to 5 months (median 1.2 months) for LAS/MAS transition and 8 days to 5.6 months (median 2.85 months) for MAS/LAS transition.

Wavelet analysis reveals El Niño-Southern Oscillation (ENSO) as the

dominant global mode affecting Philippine TC activity. The impacts of ENSO depend on the season, the ENSO phase, and on the intensity of the TCs. Significant change in the median seasonal metrics is observed as different ENSO phases influence the region.

In Neutral conditions, both seasons have above average number of TCs and landfalls. During La Niña (El Niño) phase, above (below) average TC numbers are observed in LAS while both La Niña and El Niño phases observed below average in MAS. The landfalling TCs are above (below) average in La Niña (El Niño) years in both LAS and MAS.

Relative to Neutral years, the mean start date of the LAS is earlier (later) in La Niña (El Niño) years while the mean end date is later (earlier) in La Niña (El Niño) years. The average length of LAS is longer in La Niña years as compared with Neutral years; El Niño conditions have even shorter season length. In MAS, the average start date during La Niña years is much later relative to Neutral and El Niño years. El Niño conditions have the earliest end date but La Niña conditions end date is earlier than that of Neutral conditions. The MAS length during La Niña phase is the shortest as compared with El Niño and Neutral phases.

In both LAS and MAS, the TC birthplaces are closer to the Philippines in La Niña years and are found in broader latitude range as opposed during El Niño years. Most of the TC tracks during La Niña (El Niño) phase occupy a broader (narrower) longitude range in LAS but La Niña (El Niño) conditions have a narrower (broader) longitude range in MAS.

A cluster analysis using k-means was employed to analyze the TCs in the

Philippine region for the period 1945-2011. In this section, the clustering was implemented according to the TC genesis locations, decay locations, and tracks. The resultant silhouette coefficient values and key meteorological and oceanic variables have been examined to determine the optimal cluster number. The partitioning has revealed the following meaningful numbers of clusters: 4 for genesis locations, 5 for decay locations, and 6 for tracks.

The classification of TC genesis locations has captured the longitudinal separation of cyclogenesis regions. The formation region east of the Philippines (west of 140°E) is the most active, with 398 genesis points. TCs in the domain also exhibit distinct decay locations. The most prevalent area of dissipation is the cluster over Southeast Asia, with 352 decay points. Clustering the TC tracks has identified various track types by separating them into discrete numbers of patterns. Short, straight west-northwestward tracks heading towards Indochina have the highest density of trajectories, with 248 TCs.

To investigate the spatial and temporal behavior of Philippine TCs, monthly analyses of each cluster was carried out to show which cluster of genesis, decay, and tracks is most dominant during a specific month, which is a potentially useful forecast tool. The locations of TC formation determine the subsequent decay locations and TC paths. Once a TC is identified as belonging to one of the genesis clusters, the probable location of decay (including landfall location) along with the distinct trajectory type can be used as a forecasting guide. The monthly distribution of genesis, decay, and tracks also determines the variability in the seasonal cycles between clusters.

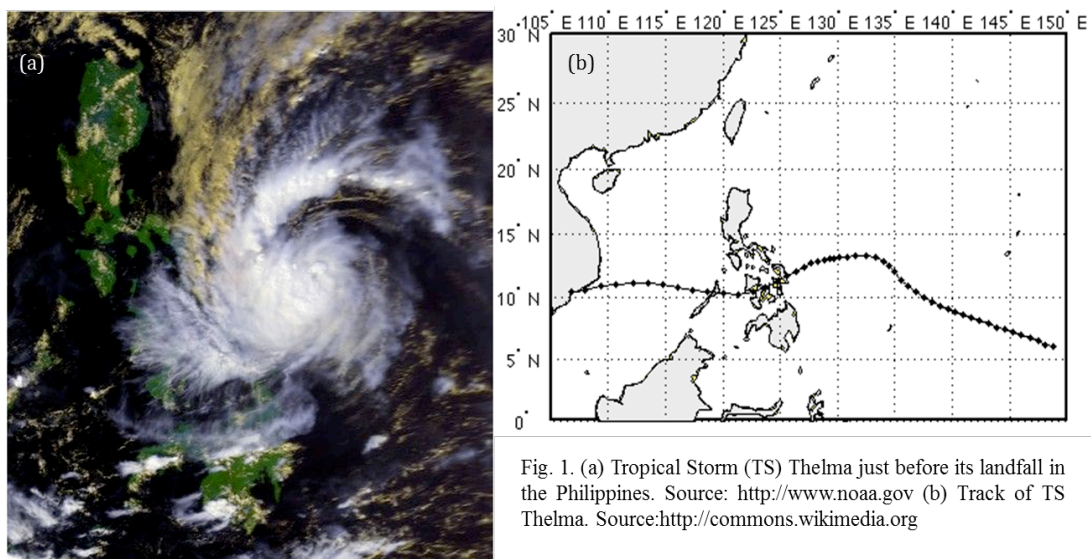
# **Chapter 1**

## **Introduction**

The Philippines lies in the typhoon belt of the WNP, the most active of the world's TCs basins (McBride 1996; Fink and Speth 1998). The country frequently experiences large and intense TCs (Hope 1979), and its geographical and topographical settings make the country's population and infrastructure susceptible to TCs and their associated natural hazards. The Philippines also is situated in the region where most TCs in the WNP reach maximum intensity (Xue and Neumann 1984). The maximum intensification of TCs is between 130°E-150°E (Gray 1968), just to the east of the Philippines. About 26 TCs form over the WNP each year (Richie and Holland 1999) and, of those, about 70% are located in the vicinity of the Philippines, with an annual median of 18 TCs over the 67-year period 1945-2011.

The susceptibility of the Philippines to the impacts of TCs is well known. With an area of 300,000 km<sup>2</sup> and almost 108 million people, it is the 13<sup>th</sup> most densely populated country in the world (USCIA World Factbook 2014). TCs are the most devastating and costly natural hazard affecting the Philippines, in terms of human casualties and socio-economic consequences. Destructive winds, storm surges, landslides and flooding are some TC impacts affecting the Philippines. For example, Typhoon (TY) Ike in September 1984 was one of the most damaging TCs to impact the Philippines in the 20<sup>th</sup> century, causing 1,363 fatalities. In November 1991, Tropical Storm (TS) Thelma showed that a TC below TY intensity could still be

lethal, producing over 5,000 casualties. Fig. 1a shows TS Thelma just before striking the Philippines on November 4, 1991 and Fig.1b shows its track, which remained close to the Philippines for 6 days. In December 2011, TS Washi caused catastrophic damage in the Philippines with an estimated 1,257 casualties. Most recently Typhoon Haiyan (2013) became the strongest and deadliest typhoon to make landfall in the Philippines, killing over 6,000 people and affecting over 4 million homeless. Typhoon Haiyan is the strongest TC to make landfall anywhere on the globe and possibly is the strongest TC ever recorded, in terms of wind speed.



Despite being the country most affected by TCs, there have been few detailed studies focusing exclusively on the Philippines TCs. There is an urgent need for a far more complete understanding of Philippine TC activity and its variability. This study is three-fold. The first part develops climatology of TCs affecting the Philippines that extends well beyond the relatively limited number and scope of existing studies of

Philippine TCs. The main aim here is to conduct a comprehensive investigation of Philippine TCs to extend the earlier work. Such climatology has vital social and economic significance to the country, and is necessary for planning and preparation, particularly before the start of each TC season.

The TC activity in the Philippine region has been observed to possess seasonal, interannual, and interdecadal variability. The second part of the study investigates how ENSO phenomenon contributes to the variability and examines the behavioral response of Philippine TC activity (i.e., seasonal statistics of TC number, landfalls, intensity, TC days, season start/end dates, season length, accumulated cyclone energy (ACE), cyclogenesis locations, and tracks) to various phases of ENSO. Here, the focus is to increase our understanding of the roles of ENSO on the climatology and variability of the TC activity in the Philippine domain. There is an extensive amount of literature addressing the issue on the influence of ENSO in WNP TC activity but no paper has emerged studying comprehensively the local consequences of ENSO to TCs although some studies have provided hints on the influence of ENSO to the Philippines, particularly to the TC activity.

The third part of the study is the classification of Philippine TCs by applying K-means cluster analysis. TCs are multifaceted hazards dependent on the oceanic and atmospheric conditions that contribute to their formation and development, movement, and decay. The seasonal variations in the large-scale atmospheric circulation also cause variations in the TC characteristics. Studying the formation and movement of Philippine TCs will provide valuable information necessary to understanding fully the behavior of the phenomenon. It is for this purpose that this section employs cluster

analysis using K-means method to investigate the underlying distinct characteristics of TCs. The aim of clustering is to partition a set of TC genesis and decay locations and tracks into homogenous groups such that the patterns within each group are similar, and will lead to the identification of different genesis and decay regions and track types.



## **Chapter 2**

### **Domain, Data, and Definitions**

#### **2.1 Study Region**

The study region covers latitudes  $5^{\circ}$  to  $25^{\circ}$ N and longitudes  $115^{\circ}$  to  $135^{\circ}$ E, as shown in Fig. 2 as the black inset, and referred to in this paper as the Philippine domain. The Philippine Atmospheric, Geophysical and Astronomical Services Administration (PAGASA) is the agency that monitors and forecasts TCs that affect the Philippines. PAGASA has its own domain, mandated by the World Meteorological Organization (WMO). It differs only very slightly from the Philippine domain defined in this paper. The irregular box (red broken line in Fig. 2) shows the PAGASA area of responsibility for TCs. For simplicity and data processing purposes, the domain in this study was chosen to be a conventional square latitude/longitude region closely approximating the PAGASA area.

#### **2.2 TC Data Sources**

The three major TC warning centers considered in the study are the PAGASA, the Japan Meteorological Agency (JMA), and the Joint Typhoon Warning Center (JTWC). However, disparities remain in TC statistics between these centers, as will be discussed below. TC records from PAGASA, JMA and JTWC were assessed and compared, to select the most appropriate TC data archive for this study. The JTWC data archive was chosen as it provides the most comprehensive coverage dating back

to 1945, and its observation record of mean sea level pressure (MSLP) provides an important advantage over the PAGASA data. Also, from 1951 to 1980, JMA did not include the actual values of maximum sustained winds. Instead just the intensity classifications were recorded. JMA began recording the maximum sustained winds in 1981, but only winds of at least 35 knots were included, and winds below that were recorded as 0 knots. Chan (2008) stated that JTWC best track dataset likely gives a better estimate of the number of intense TCs in the WNP than the JMA archive. The best-track data used in this study are extracted from the WNP archive of the JTWC ([http://www.usno.navy.mil/NOOC/nmfc-ph/RSS/jtwc/best\\_tracks/](http://www.usno.navy.mil/NOOC/nmfc-ph/RSS/jtwc/best_tracks/)). All Philippine TC metrics were calculated from the JTWC data set.

### **2.3 Large-scale Climate Data**

ENSO phenomenon such as El Niño is consistently reflected in the equatorial sea surface temperature (SST) from approximately 120°W westward to near the dateline (Barnston et al. 1997). Niño 3.4 is the most important region for WNP tropical cyclone activity (Camargo and Sobel 2005) and is one of the most popular indices used to monitor ENSO.

The SST monthly anomalies and Oceanic Niño Index (ONI) used in this study was obtained from the National Oceanic and Atmospheric Administration (NOAA, <http://www.cpc.ncep.noaa.gov/>) developed by Smith and Reynolds (2003). The ONI is defined as the three-month running mean of extended reconstructed sea surface temperature (ERSST) anomalies in the Niño 3.4 region (5°N-5°S; 170°-120°W), based

on the 1971-2000 period.

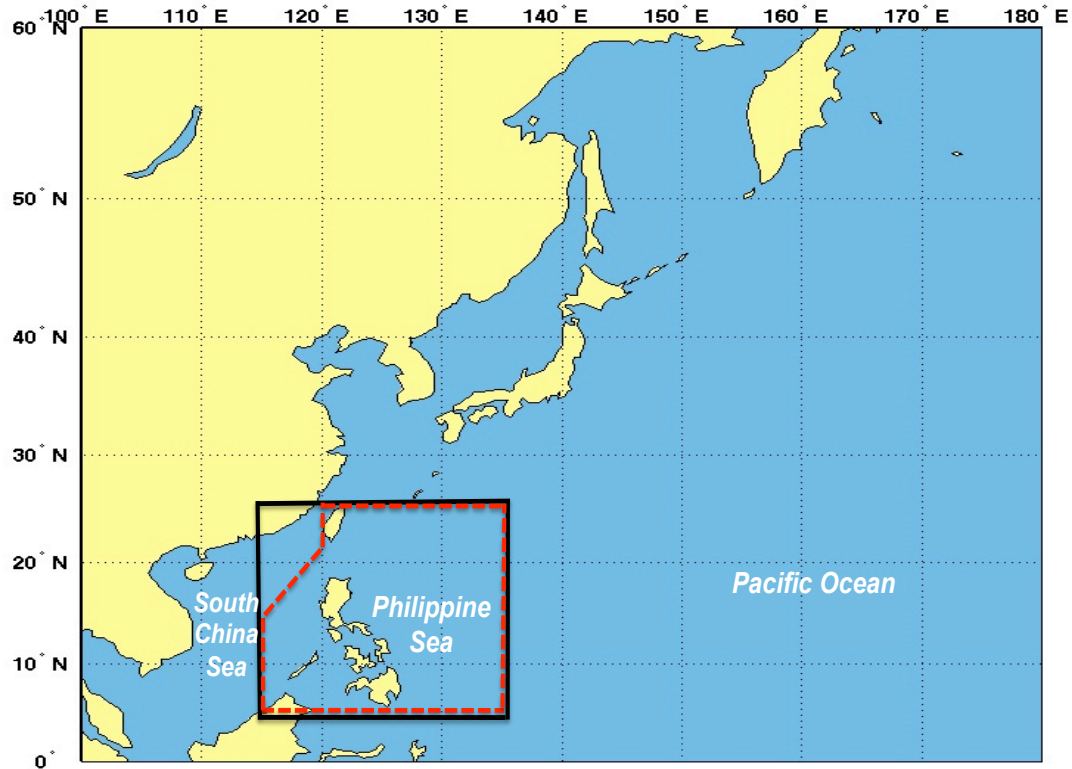


**Fig. 2.** The study region covers latitudes 5°-25°N and longitudes 115°-135°E, shown as the black inset and referred to here as the Philippine domain. The irregular box (red broken line) shows the PAGASA area of responsibility for TCs. PAGASA monitors and forecasts TCs that affect the Philippines.

Values of vorticity at .995 sigma level, sea level pressure (SLP), 200-mb zonal wind, and divergence at .2101 sigma level come from the monthly mean values of the National Centers for Environmental Prediction (NCEP)-National Center for Atmospheric Research (NCAR) reanalysis (Kalnay et al. 1996; Kistler et al. 2001).

## **2.4 Definitions**

All TCs in the Philippine domain for the period 1945-2011 are considered in this study. The TC archive is limited to the TCs that either formed in or moved into the defined domain. TCs were only included in the overall count if some part of their recorded tracks were within the Philippine domain. Overall, a total of 1199 TCs were analyzed for this study. The TC frequency is obtained by counting the annual number of TCs that spent any time within the study region, and the median provides the climatology. Here, the Philippine TC activity comprises three TC categories, namely, tropical depressions (TD), tropical storms (TS) and typhoons (TY). The TC intensity classification is based on the observed maximum sustained wind near the center. A TD is when the maximum sustained winds fall within the range of 35 to 64 kph, a TS has winds in the range 65 to 118 kph, and when the winds exceed 118 kph, the TC is classified as TY.

The best track data for each TC at 6-hour intervals includes: latitude-longitude position, maximum sustained surface wind speed, and minimum central pressure. Track parts that ventured outside the official domain were excluded from the TC days analysis, thus only the number of days that a system was actually within the domain was accumulated to represent the cumulative TC days. The birthplaces and tracks of TCs also are obtained from the JTWC dataset.

## Chapter 3

### Climatology of Philippine TC Activity

#### 3.1 Introduction

The pioneering work of Flores and Balagot (1969) is the groundwork for understanding the climate controls that define the Philippine climate, including TCs. They noted that the May to December rainfall is associated mainly with TC passages. They defined the TC season as extending from June to December, but mentioned that other months are also affected by TCs. Flores and Balagot (1969) described some of the seasonal features of TC tracks affecting the Philippines. Brand and Brelloch (1973) studied 30 typhoons to verify how the Philippine islands affect the TCs that cross the country and found that the intensity, speed of movement, and size characteristics of TCs are influenced largely by the topography over which the TC passes. They noted that the terrain of the Philippine islands varies significantly and that the central region of the Philippines has less effect on TCs. Brand and Brelloch (1973) also emphasized that in the later months of typhoon season, the South China Sea environment and mean synoptic conditions differ from those of the Philippine Sea. The different thermal structures of these two ocean basins are important because they determine the available energy for the TCs.

Shoemaker (1991) investigated the intensity, direction and speed of TCs affecting the Philippines, focusing on why TCs reach peak intensity hours before landfall and weaken after crossing the Philippines. Shoemaker (1991) also mentioned

that the majority of the TCs making landfall have a mean west-north-westward direction and only those coming from the South China Sea move eastwards. He also added that the direction of TC motion depends on its intensity prior to landfall. Shoemaker (1991) identified September to November as having maximum TC landfalls, also noting that the median landfall latitude has an annual cycle, with a maximum during August ( $\sim 15.5^{\circ}\text{N}$ ), and a minimum during February ( $\sim 9.0^{\circ}\text{N}$ ), similar to the monsoon trough.

Chan (2000) examined TC activity over the WNP to assess if variations occur prior to, during and after the occurrence of El Niño and La Niña events. The results of Chan (2000) suggest that TC activity over the Philippine region is likely to be above normal prior to an El Niño year, and that in October and November of an El Niño year, below normal numbers are observed. Furthermore, one year after an El Niño event, TC activity in the Philippines tends to be below normal. Chan (2000) further found that Philippine TC activity appears to be above normal in the year preceding a La Niña event and in September and October of a La Niña year, the Philippine region experiences more TCs. The same scenario was observed in the year following a La Niña event. Anomalous large-scale flow patterns at 850 and 500 hPa are linked to the variations in TC activity. The genesis and development are related to the 850-hPa flow. Anomalous cyclonic flow is associated with above normal TC activity, whereas anomalous anticyclonic flow is associated with below normal TC activity. The 500-hPa flow can steer a TC towards (away) from a region, making the TC activity in that region above (below) normal. Importantly, Chan (2000) also suggested that El Niño

and La Niña effects are not the sole factors that determine the anomalies in TC activity in the WNP.

The Philippine region is one of four areas considered by Wu et al. (2004) in their study of the impacts of ENSO on landfalling TCs in the WNP. They found that, relative to Neutral years, in September-November during El Niño years, fewer TCs make landfall in the Philippines, while in September-November of La Niña years, more TCs make landfall. Additionally, they attributed the reduced number of TC landfalls in El Niño years to the eastward shift in mean tropical cyclogenesis and development locations, along with a weaker subtropical ridge, whereas they associated increased landfalls in La Niña years with a westward shift in mean genesis position and a strong subtropical ridge.

Ribera et al. (2005) provided a high-resolution record of meteorological events in the WNP basin. Their chronology comprised 863 events, from 1901 to 1934, when the Manila Observatory and its associated network made most of its observations. They analyzed the geographical probability distribution of typhoon-passage frequency, revealing that the highest frequency of typhoon passage is over the northern part of Luzon Island, which they ascribed to the westward and poleward movement of the TCs. They also identified July to October as having the highest frequency of typhoons.

A similar study by Garcia-Herrera et al. (2007) is a high-resolution chronology of intense storms and typhoons in the Philippines and its vicinity during the period 1566–1900. It also was constructed mainly from the pioneering typhoon chronology of Miguel Selga, the last Spanish Jesuit director of Manila Observatory who served from 1926 to 1946.

Chan and Xu (2008) divided East Asia into sub-regions to examine variations in the annual number of landfalling TCs in the WNP TC basin. The Philippines is included in the south TC region, along with south China and Vietnam. Chan and Xu (2008) found that landfalling TC frequencies in the south TC region experience large interannual (2-8 years), interdecadal (8-16 years) and even multidecadal (16-32 years) variations. They noted that the interannual oscillation is the most dominant and the remainder of the variance is attributed to multidecadal oscillation.

Kubota and Chan (2009) assessed a database comprised of Philippine TCs with maximum surface wind intensities of 35 knots or higher and used the observed minimum pressures in the nearest station being less than 1000 hPa (if the surface wind speed is not available). They defined a Philippine landfall as occurring when a TC passed through the PAGASA TC area. The study identified interdecadal variability in Philippine TC activity, related to the various stages of ENSO and the Pacific Decadal Oscillation (PDO). Kubota and Chan (2009) found that the annual number of TCs that entered the Philippine landfall area had a period of about 32 years before 1939, and a period of about 10-22 years after 1945. They observed that the low PDO phase has decreasing (increasing) effect on the number of Philippine TCs during El Niño (La Niña) years, but that the same scenario is not seen during the high PDO phase, when its effect on Philippine TCs during different ENSO phases becomes uncertain. They also noted that ENSO effects on Philippine TCs are on seasonal time scales and not annual, as the ENSO phases in different phases of PDO alter Philippine Sea anticyclone intensity.



Recently, Zhang et al. (2012) studied the peak season (June-October) for landfalling TCs in East Asia during the central Pacific (CP) El Niño and compared it with landfalling frequencies during the eastern Pacific (EP) El Niño and La Niña. Zhang et al. (2012) found that TC landfall numbers in the Philippines are suppressed in the autumn seasons of CP El Niño years while more (less) TCs are expected to landfall during the peak TC season of La Niña (EP El Niño) years.

### **3.2 Methodology**

One aspect of this study is the partitioning of TC activity in the Philippines into two seasons based on the long-term monthly means. The twelve-month TC season was split into a less-active season (LAS) and a more-active season (MAS). The LAS runs from January 1 to May 31 and the MAS runs from June 1 to December 31.

Aside from the significant difference in the TC statistics between these two seasons, different environmental conditions, both thermodynamic and dynamic, also were observed. Measures such as the frequency, landfall, TC days, earliest start/end dates, latest start/end dates, season length, birthplace and track progression were important in defining the characteristics of each season. A unique aspect that arose from this study is the nature of the transition periods between the LAS and the MAS.

Basic statistical measures, such as medians, interquartile range (IQR) and trends, were used to investigate the TC activity in the Philippines. Over the 67-year period 1945-2011, the statistics were compiled for 3, 5, 7, and 12-month periods that correspond to the individual quarter, LAS, MAS and the calendar year, respectively.

The time series are simply the seasonal numbers of TCs in the domain over a particular period. Five-year running means were used to smooth out the year-to-year variability, and trends were analyzed by fitting linear regression to the running mean. The slopes of these trends were tested for statistical significance at the 95% confidence level.

For future discussion, the calendar year will be divided into four quarters. The four quarters are January-March (JFM), April-June (AMJ), July-September (JAS), and October-December (OND). To investigate the impacts of ENSO on TCs in the Philippine region, quarterly and seasonal numbers will be used for TCs that entered the Philippine domain, and also for the numbers of landfalling TCs. The quarterly and seasonal SST indices are used to define whether a particular period is an El Niño, La Niña or Neutral phase of ENSO. Then the quarterly and seasonal TC time series were standardized to provide a representative TC count during warm, cold, and Neutral episodes. Standardization involved subtracting the long-term mean from the individual TC count, and dividing the difference by the standard deviation. The standard score is defined as:

$$z = \frac{x - \mu}{\sigma}$$

where  $x$  is the raw score,  $\mu$  is the long-term mean of the population, and  $\sigma$  is the standard deviation of the population.

The number of TCs during Neutral years is greater than during El Niño and La Niña years, which would suggest falsely, without standardization, that ENSO has no

significant impact on the Philippine TCs. The standardized TC count indicates by how many standard deviations an observation is above or below the mean. Investigating the TC activity by season provides information on how ENSO affects early, mid, peak and late season TC activity.

The periodicities of the Philippine TCs were estimated using a wavelet analysis. Wavelet analysis is employed to identify the time frequency behavior of the TC count. It allows the identification of localized oscillations of various frequencies. Similarly, the global wavelet spectrum analysis is used to display the temporal features of time series on different timescales. For details of the wavelet technique, the reader is referred to Torrence and Compo (1998).

### **3.3 TC Statistics**

Over the period 1945-2011, the Philippines experienced a total of 1,199 TCs. TC activity is observed all year round in the region, with no month entirely free from TCs, so the TC season stretches from January to December. The annual long-term median (1945-2011) is 18. Fig. 3 shows the TC activity in the Philippine domain. The LAS represents the relatively quiet phase of TC activity in the Philippine domain, during which there is mean of less than one TC per month. The MAS has monthly means greater than one, so most TCs occur during the MAS.

The annual number of TCs fluctuated from a minimum of 10 in 1946 to a maximum of 28 in 1993 (Fig. 4). The green line in Fig. 4 is the mean annual TC numbers. The blue line is the mean LAS TC numbers and the red line is the mean

MAS TC numbers. Comparing the annual number of TCs with the number of TCs during the LAS and MAS, the mean annual total is dominated by the MAS (Fig. 4). The MAS experiences about 88% of the mean annual number of TCs affecting the Philippines. The linear trend lines for the three graphs all suggest an increase in TC frequency with time, which increased the motivation for this study.

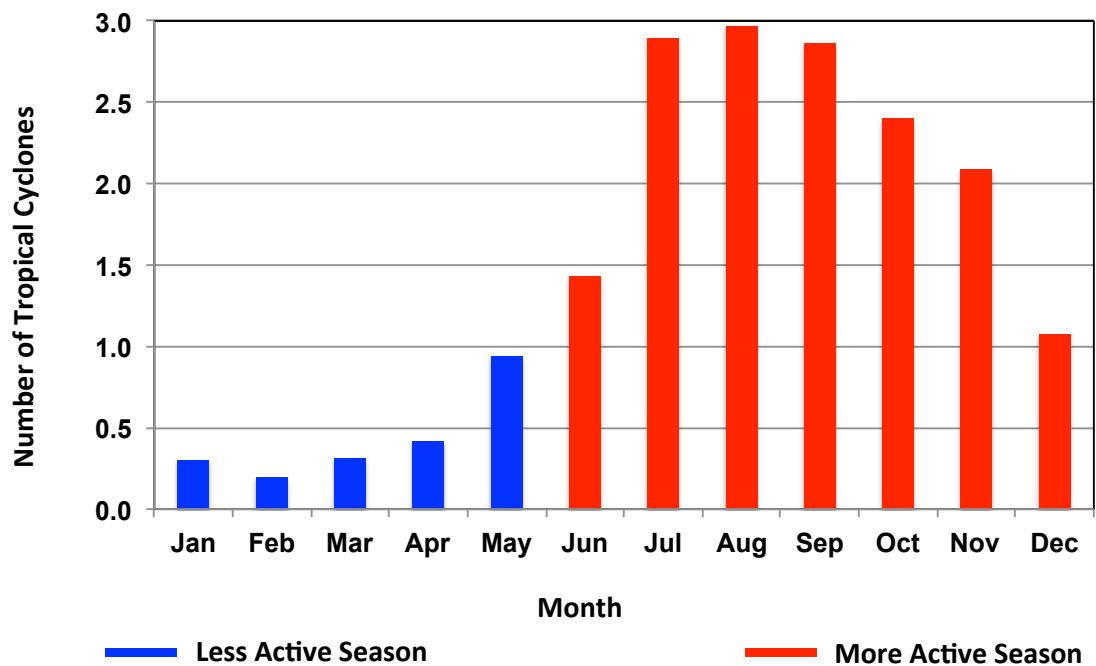


**Fig. 3.** Mean monthly TCs in the Philippines. The LAS (blue bars) runs from January 1 to May 31, representing the quiet phase of TC activity in the Philippine domain, during which there is less than one TC on average per month. The MAS (red bars) is from June 1 to December 31, with monthly averages greater than one.

The TC seasonal median for the LAS is 2 with an IQR of 2 and with a seasonal median landfall of 1 and an IQR of 2. February has the lowest TC frequency, and January-March is the least active TC period. February has the least TCs because, aside from being the peak month of the northeast monsoon, when there is cold air infusion, it also is the coldest month in the Northern Hemisphere and TCs often weaken before reaching the Philippine coastline (Shoemaker 1991). Lander (1994) found the same behavior over the entire WNP TC basin.

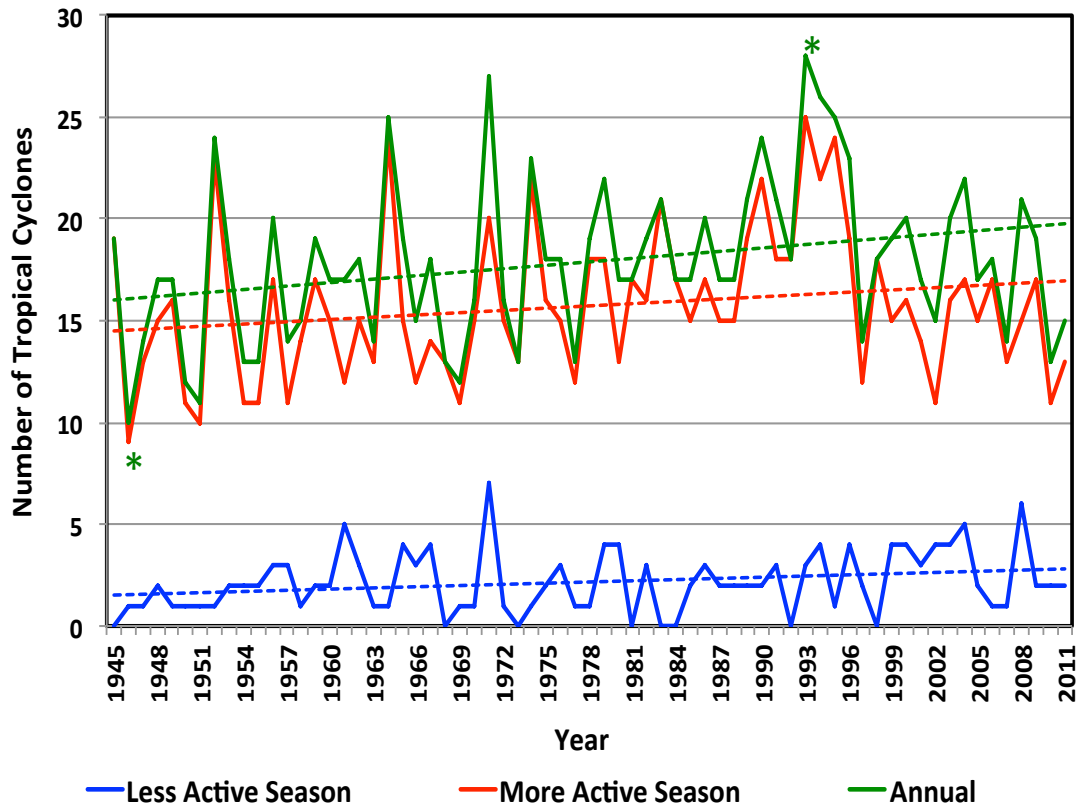


**Fig. 4.** Time series of mean annual number of TCs (in green line) plotted against the LAS (in blue line) and MAS (in red line) mean TCs. The MAS dominates the mean annual TC numbers, accounting for about 88% of the total. The linear trend lines are shown as dashed lines.

The MAS has a seasonal TC median of 15 with IQR of 4.5, and a seasonal median landfall of 5 and an IQR of 3. The peak months are July, August, and September, with monthly medians of 3 and an IQR of 2, and with August as the most active month. Neumann (1993) also found that for the entire WNP, TC activity is greatest from July to September. More TCs affect the Philippine domain during the MAS because environmental conditions over the WNP are more favorable for development of TCs. Neumann (1993) also indicated that in the WNP, the peak TC season covers summer and fall. This encompasses the MAS in the Philippines.

### **3.4 Season Start/End Date and Length**

The year-to-year spectrum of TC activity in the Philippine region is shown in Fig. 5. The TC frequency over the Philippine region varies on an intraseasonal time scale, with alternating less active, quiescent, and more active periods. The blue bars denote the yearly length of the LAS and red bars represent the yearly length of the MAS. The start date of the season is defined as the day during a particular season when the first TC is in the Philippine domain. The end date of the season is defined as the day when the last TC is inside the domain. Season length is defined as starting from the day of the first TC occurrence in the Philippine domain and ending when the last TC lies within the domain. The two seasons have very different season lengths. The season length for each year is the length of the bar. The start date of the season is the value at the lowest tip of the bar, and the end date of the season is the value at the upper tip of the bar.

Typically, LAS TCs have their last days within the season period. However, there are years when the end dates of LAS TCs occur in June, which already is part of the MAS. After the LAS ends, it takes a median of 1.5 months before the MAS commences. Notably, this gap between the LAS and MAS is as brief as 2 days and as long as about 5 months. The gap between the two seasons is referred to here as the “quiescent” period, in terms of TC activity. After the MAS, the quiescent period again is observed and is much longer than the quiescent period after the LAS. It ranges from 6 days to just over 7 months, with a median of about 3 months, and an IQR of 1.5 months.

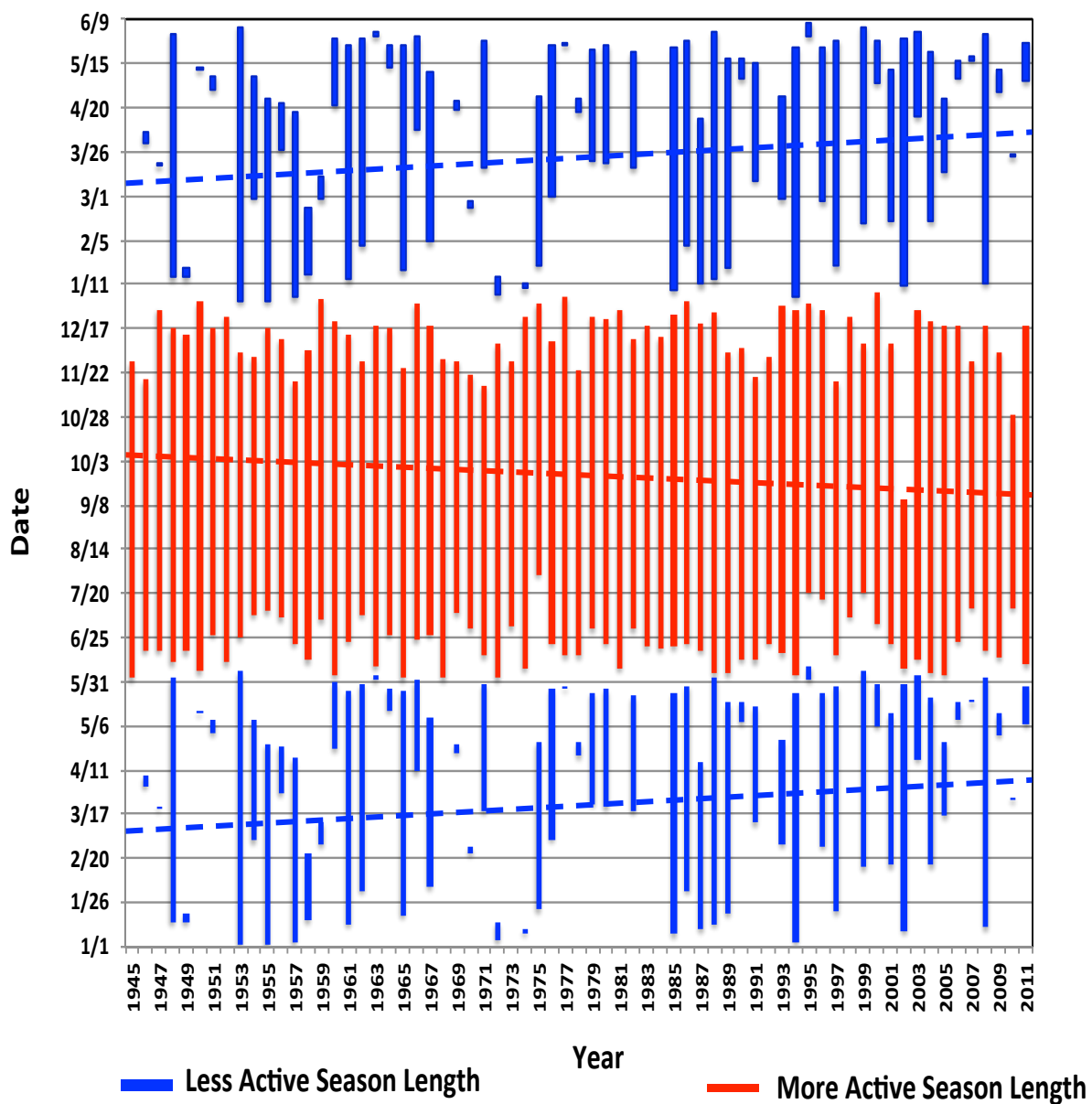


**Fig. 5.** The year-to-year TC activity in the Philippine domain. The TC frequency varies on an intraseasonal time scale, with alternating LAS, quiescent, and MAS periods. The blue and red bars denote the yearly season length of the LAS and the MAS, respectively. The start date of the season is the lower tip of the bar and the end date of the season is upper tip of the bar.



Figs. 6 and 7 compare the LAS and MAS. The yearly LAS length as shown in Fig. 6a, is the length of the blue bars and varies widely, from zero days in years when no TCs affect the Philippines, to 155 days, in 1953. The LAS TCs begin to form in or enter the Philippine domain as early as January 2<sup>nd</sup> and as late as May 31<sup>st</sup>. The median LAS start date is February 28<sup>th</sup>. However, TCs can leave the Philippine domain as early as January 11 and leave as late as June 6<sup>th</sup>. The median LAS end date is May 20<sup>th</sup>. The median LAS length is 38 days, with an IQR of 92 days. There is a slight increasing trend in the LAS length during 1945-2011. Interannual variability is very high in the LAS length time series. A 5-year running mean smooths out short-term fluctuations in the LAS length and highlights the long-term trend (Fig. 6b). The trend line shows a slight increase in the length of the LAS. The LAS length 5-year running mean has two peaks in 1952-1957 and 1984-1990 and declines to a trough extending from 1968-1983.

To remove the yearly periodicity in the time series of the LAS yearly start date, again a 5-year running mean is applied (Fig. 6c). The peaks in the time series appear in 1948-1953, 1961-1969, and 1976-1982 and the troughs in 1953-1960, 1972-1975, and 1983-1990. The linear trend line implies a slight increase in the start date of the LAS. The 5-year running mean of the LAS end date (Fig. 6d) suggests a slight increase, as shown by the linear trend line. The peaks are reached during the periods 1951-1955, 1961-1967, and 1977-2001 and the lowest point in the decline appears in 1956-1960 and 1968-1977.

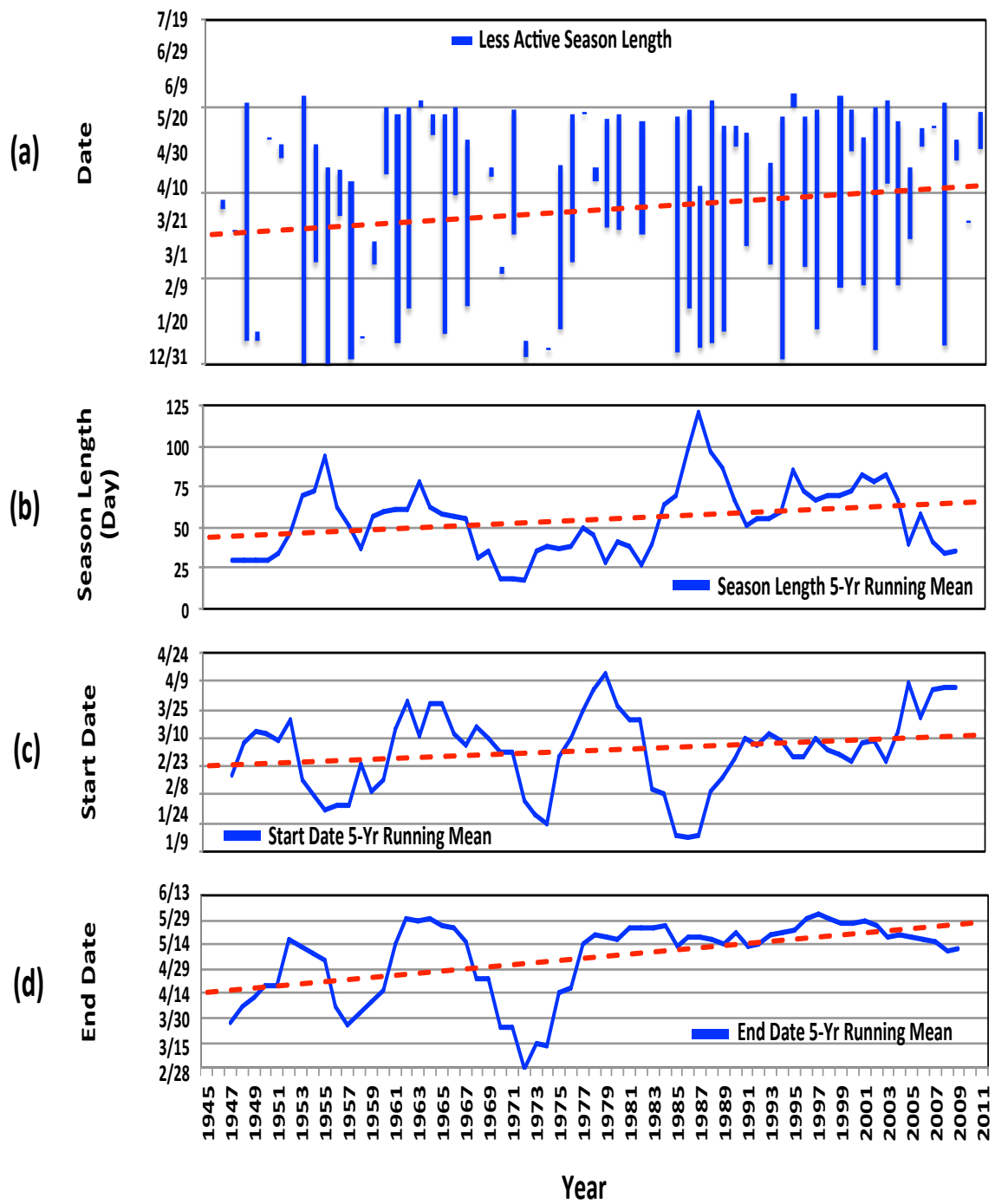


**Fig. 6.** (a) The length of LAS is illustrated by the length of the bar in each year (b) the 5-year running mean of the LAS length (c) the 5-year running mean of LAS yearly earliest start date (d) the 5-year running mean of LAS yearly latest end date. The dash line in each graph represents the trend line.

In the MAS (Fig. 7a), the earliest start date is June 1<sup>st</sup> and the latest start date is July 30<sup>th</sup>, June 18<sup>th</sup> the median start date. TCs begin to exit the domain as early as September 10<sup>th</sup>, and leave as late as January 5<sup>th</sup> of the following year, and the median MAS end date is December 16<sup>th</sup>. The median MAS length is 176 days, with an IQR of 28 days. There is no TC free year during the MAS. The linear trend line indicates a slight decrease in season length during 1945-2011.

The 5-year running mean of the MAS length is shown in Fig. 7b. The linear trend line suggests a slight decrease in the season length. The peaks of the time series occur in 1978-1995 and 2004-2007 while the dips appear in 1953-1958, 1967-1973, and 1996-2002. The peaks of the MAS start dates appear in 1952-1958 and 1994-2001 and the lowest points in 1985-1993 and 2002-2005 (Fig. 7c). The time series peaks of the MAS end dates are in 1948-1953, 1974-1988, and 1993-1999, and the troughs appear in 1954-1958, 1967-1973, 1989-1992, and 2000-2005 (Fig. 7d). Unlike the LAS, which has a highly irregular annual season length, the MAS length does not vary as greatly (Fig. 7a), consistent with the IQR. The minimum season length is 96 days in 2002, and the maximum is 209 days in 1950 with a median of 176 days and an IQR of 28 days.

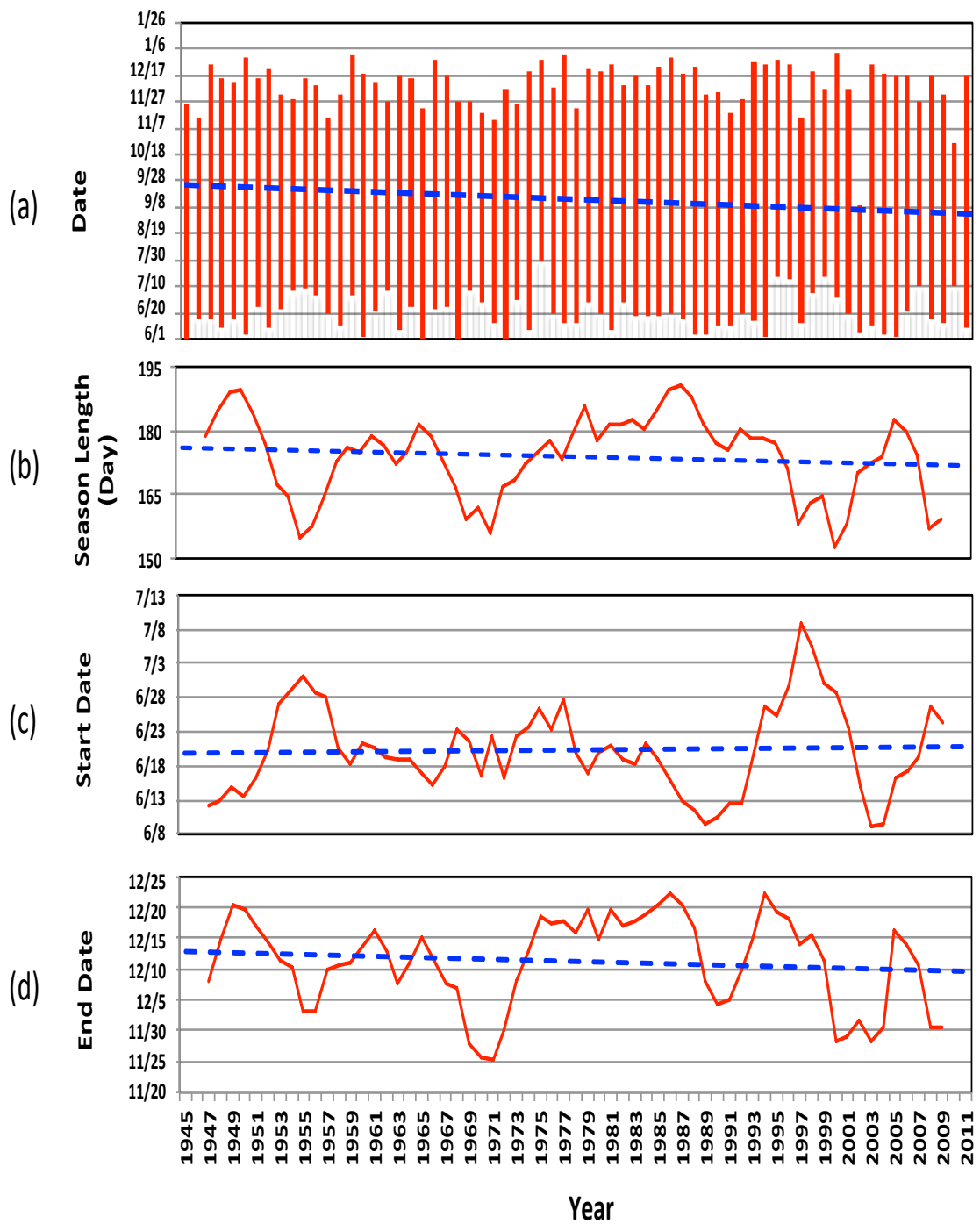


**Fig. 7.** Same as Fig. 6, but for MAS. (a) The yearly season length as represented by the length of each bar (b) the 5-year running mean of MAS yearly length (c) the 5-year running mean of MAS yearly earliest start date (d) the 5-year running mean of MAS yearly latest end date. The dash line for each graph is the trend line.

In Fig. 8, the length of the annual TC season is obtained by adding the LAS and MAS lengths (Fig.8a). The median annual season length is about 215 days, with an IQR of 71 days. The annual season length ranges from 110-350 days. About 64% of the annual season length falls within the range of 170-270 days. Only 13.5% lie below 170 days while 22.5% are above 270 days. Like the TC days, the length of the LAS is much shorter than the MAS; it extends from 0 to 180 days (Fig.8b). The median LAS length is 38 days. About 45% of the period are of 0-30 days length, and the remaining 55% lie between 31-180 days. Fig. 8c shows the MAS length. The median MAS length is 176 days. The largest percentage of about 21% is 170-180 days long. The ranges 90-100 days, 100-110 days, and 130-140 days all occupy ~1.5% of the whole period. Almost 33% have 140-170 days and the remaining 41.5% occupies 180 to 210 days. There are no years with MAS lengths of 110-130 days.

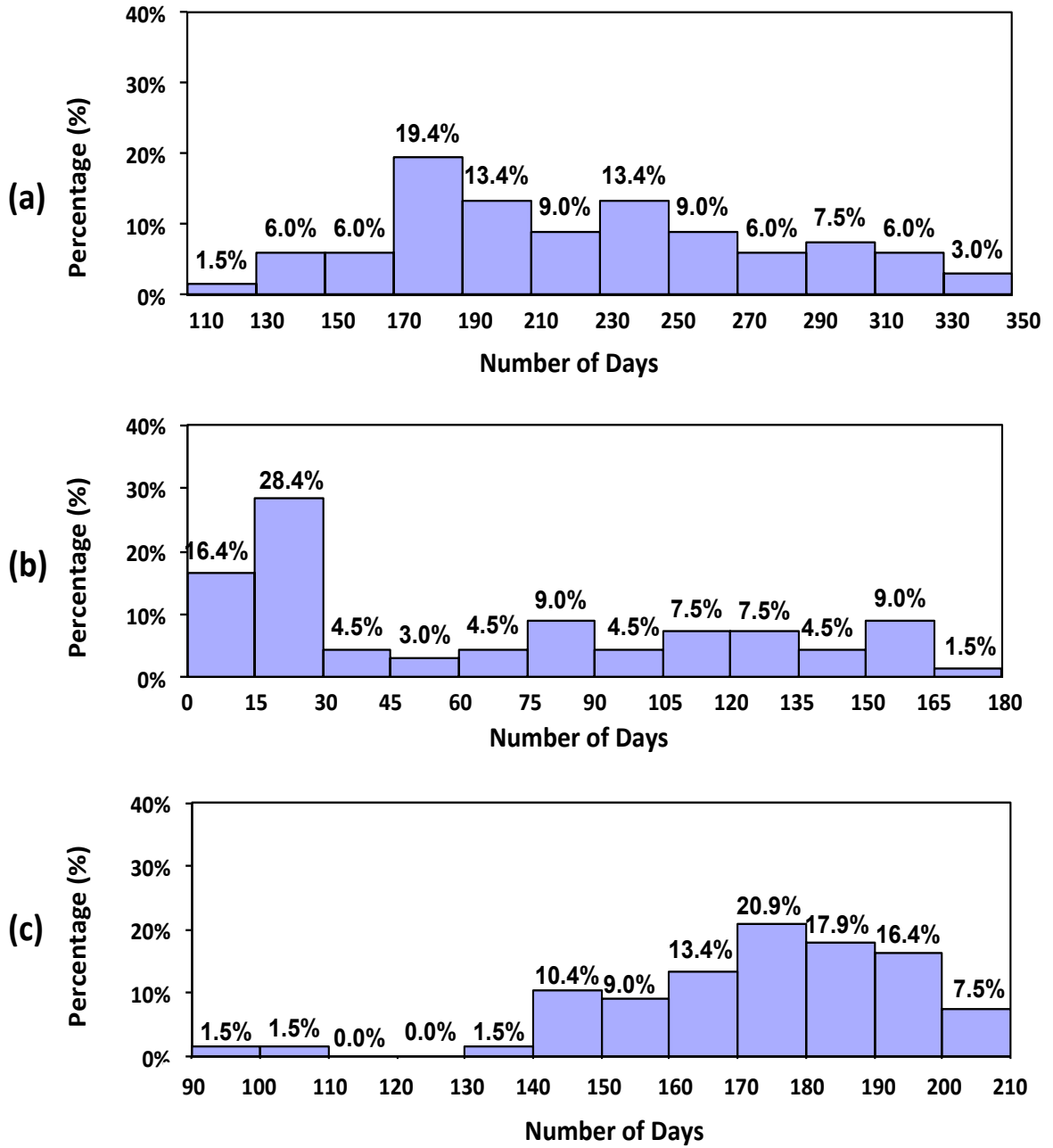


**Fig. 8.** Frequency distribution of (a) length of the annual TC season, (b) LAS length, and (c) MAS length.

### **3.5 TC Days**

A TC day is defined as one with at least one TC in the Philippine domain. A TC day varies from an hour to 24 hours. The annual TC days number is the sum of the TC days from both the MAS and the LAS (Fig. 9a). The median annual number of TC days is about 61 and the IQR is 26. There is a tendency for the annual TC days to lie in the range 40-80 days, as 77.5% of the annual TC days are in this range. Only 7.5% are below 40 days, and 15% are above 80 days. The median number of annual LAS TC days is about 8 days. The number of LAS TC days ranges from 0-30 days (Fig. 9b). The annual number of MAS TC days is much greater than the LAS TC days. The median number of MAS TC days is 51. Fig. 8c shows that the MAS TC days range annually from 10-110 with an IQR of 20 days. Note that the annual TC days are mostly from the MAS, with the above-mentioned MAS median of 51 days compared with 8 for the LAS.

### **3.6 Landfall**

About 49% of Philippine TCs occur in JAS, the busiest quarter of the year. There are more TCs during these months due to the environmental conditions over the WNP basin being favorable for the development of TCs. The definition of TC landfall is when the center of circulation of the TC reaches the Philippine coastline. Of the 1199 TCs that occurred in the Philippine domain, a remarkably high number (435, or 36%) struck the Philippines and many more came close to making landfall.

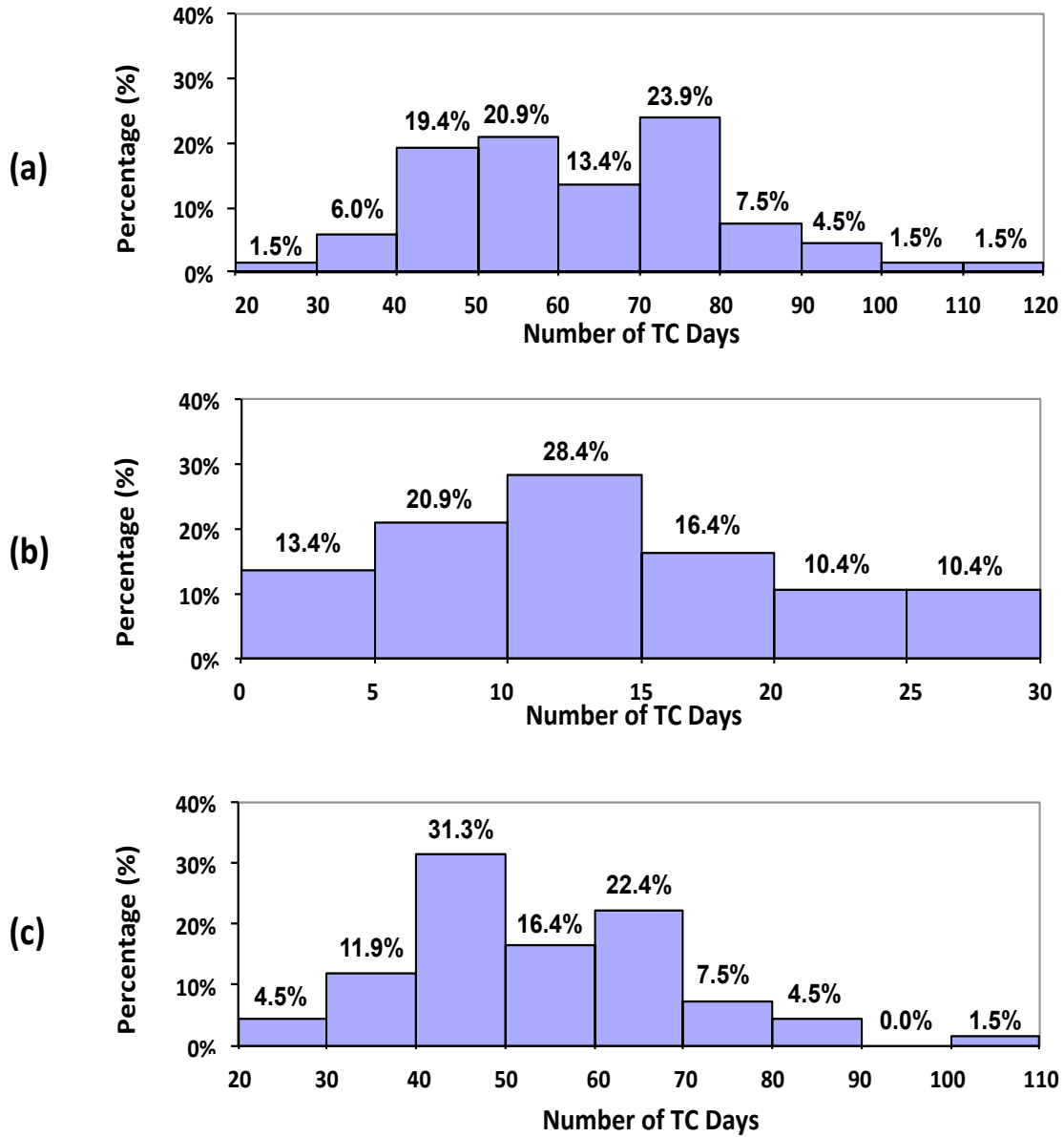


Fig. 9. Same as Fig. 8, but for the TC days.



Quarterly statistics for all TC and landfalling TCs are summarized in Table 1. The statistics indicate that JAS is more conducive to greater TC activity and this is attributed to the fact that during JAS, the necessary environmental elements for TC genesis are more likely to exist. The last quarter (OND), has a maximum percentage of landfalling TCs, accounting for 53% of the total TC landfalls (Table 1). The prevailing winds during OND are from the northeast (NE), influenced by the NE monsoon season, and prevent the TCs from recurving northeastward. Instead, the TCs are steered towards the coastlines of the Philippine archipelago.

<b>Seasonal Tropical Cyclones and Landfall</b>				
<b>Quarter</b>	<b>NTC</b>	<b>PTC</b>	<b>NLF</b>	<b>PLF</b>
<b>Jan-Mar</b>	<b>54</b>	<b>5%</b>	<b>25</b>	<b>46%</b>
<b>Apr-Jun</b>	<b>187</b>	<b>16%</b>	<b>70</b>	<b>37%</b>
<b>Jul-Sep</b>	<b>585</b>	<b>49%</b>	<b>143</b>	<b>24%</b>
<b>Oct-Dec</b>	<b>373</b>	<b>31%</b>	<b>197</b>	<b>53%</b>
<b>ALL</b>	<b>1199</b>	<b>100%</b>	<b>435</b>	<b>36%</b>

**Table 1.** Quarterly number of tropical cyclones, percentage of the number over the total, number of tropical cyclone landfalls, and the percentage of landfalls over the quarterly landfall total. The last line is the total and percentage of all tropical cyclones and landfalls for the period 1945-2011.

### **3.7 Intensity**

The Philippine TC intensity classification is based on the observed maximum sustained wind speed near the center. A tropical depression (TD) is when the maximum sustained winds fall within the range of 35 to 64 kph, a tropical storm (TS) has winds in the range 65 to 118 kph, and when the winds exceed 118 kph, the TC is classified as typhoon (TY). Table 2 shows the quarterly TC frequency based on its intensity classifications. Of the three intensity classifications, TDs are least likely to occur in each season, as only 16% of the total TCs are of TD intensity. There are 345 TSs in the Philippine domain, or about 29% of the total TCs. More than half, about 55%, of the total TCs that influenced the Philippines, were TYs, again a remarkably high percentage when compared with other TC basins. The TYs are most likely to occur in the Philippine domain during OND, comprising about 59% of TCs. Table 3 shows the quarterly TC landfall frequencies and the quarterly landfall intensity classifications. The greatest numbers of TC landfalls occur during OND. Of the 435 TC landfalls over the entire period, 103 (24%) are TDs, 132 (30%) are TSs and 201 (46%) are TYs. Most JFM landfalling TCs are TDs, comprising 36% of the total JFM TCs. The majority of the AMJ, JAS and OND quarterly TCs are TYs.

### Seasonal Tropical Cyclones With Intensity Classification

Quarter	NTC	PTC	NTD	PTD	NTS	PTS	NTY	PTY
Jan-Mar	54	5%	9	17%	24	44%	21	39%
Apr-Jun	187	16%	30	16%	58	31%	99	53%
Jul-Sep	585	49%	95	16%	169	29%	321	55%
Oct-Dec	373	31%	58	16%	94	25%	221	59%
ALL	1199	100%	192	16%	345	29%	662	55%

**Table 2.** Quarterly number of tropical cyclones, percentage of the number over the total, quarterly number of tropical cyclones classified by intensity and its quarterly percentage. Intensity is classified into tropical depression (TD), tropical storm (TS), and typhoon (TY).

### Seasonal Landfalls With Intensity Classification

Quarter	NLF	PLF	NTDLF	PTDLF	NTSLF	PTSLF	NTYLF	PTYLF
Jan-Mar	25	6%	9	36%	8	32%	8	32%
Apr-Jun	70	16%	21	30%	20	29%	30	43%
Jul-Sep	143	33%	39	27%	49	34%	56	39%
Oct-Dec	197	45%	34	17%	55	28%	107	54%
ALL	435	100%	103	24%	132	30%	201	46%

**Table 3.** Same as Table 2, but for quarterly number of landfalls, percentage of landfall over the quarterly total, quarterly number of landfalls classified by intensity and its quarterly percentage.

### 3.8 Variability

The interannual and interdecadal variations in the frequency of Philippine TCs over the 1945-2011 period were calculated and are shown in Fig. 10. Since 1945, large-amplitude variations are apparent in the time series of the annual number of TCs. The green line in Fig. 10a indicates the long-term mean of TCs in the Philippine domain. The pink line is the 5-year running mean. Years with 5-year running means below the long-term median of 18 are considered to be part of the below median period (BAP), and all years with above median TCs are part of the above median period (AAP). The BAP, as indicated by the yellow areas, can range from 1 to 16 years while the AAP, as indicated by the blue areas, ranges from 2 to 11 years. The orange line is the long-term trend line. The underlying trend appears to be positive throughout the entire period. There are significant variations in the time series. Short-term cycles are evident in the 5-year running mean of the annual number of TCs. Fig. 10b is for annual TC landfalls in the Philippine domain. The long-term median number of TC landfalls is 6 with an IQR of 3.5, and is represented by the green line in Fig. 10b. Almost 40% of the total number of TCs in the domain made landfall. The time-series of TC landfall also shows year-to-year variability. The trend line of the 5-year running mean suggests that there is a slight increase in the number of landfalling TCs over the whole period. The BAP can range from 1 to 20 years while the AAP ranges from 1 to 11 years. The interannual and interdecadal variability in the annual number of TCs is attributable to changes in large-scale environmental conditions over

the WNP basin. Chan (2000) and Wang and Chan (2002) suggested that the interannual variations of typhoon activity over the WNP are mainly influenced by ENSO phases, which alter the large-scale circulations. In the WNP, other modulating factors could be responsible for the variability in TC activity. For example, TCs preferentially occur during the convective phase of the Madden-Julian Oscillation (MJO).

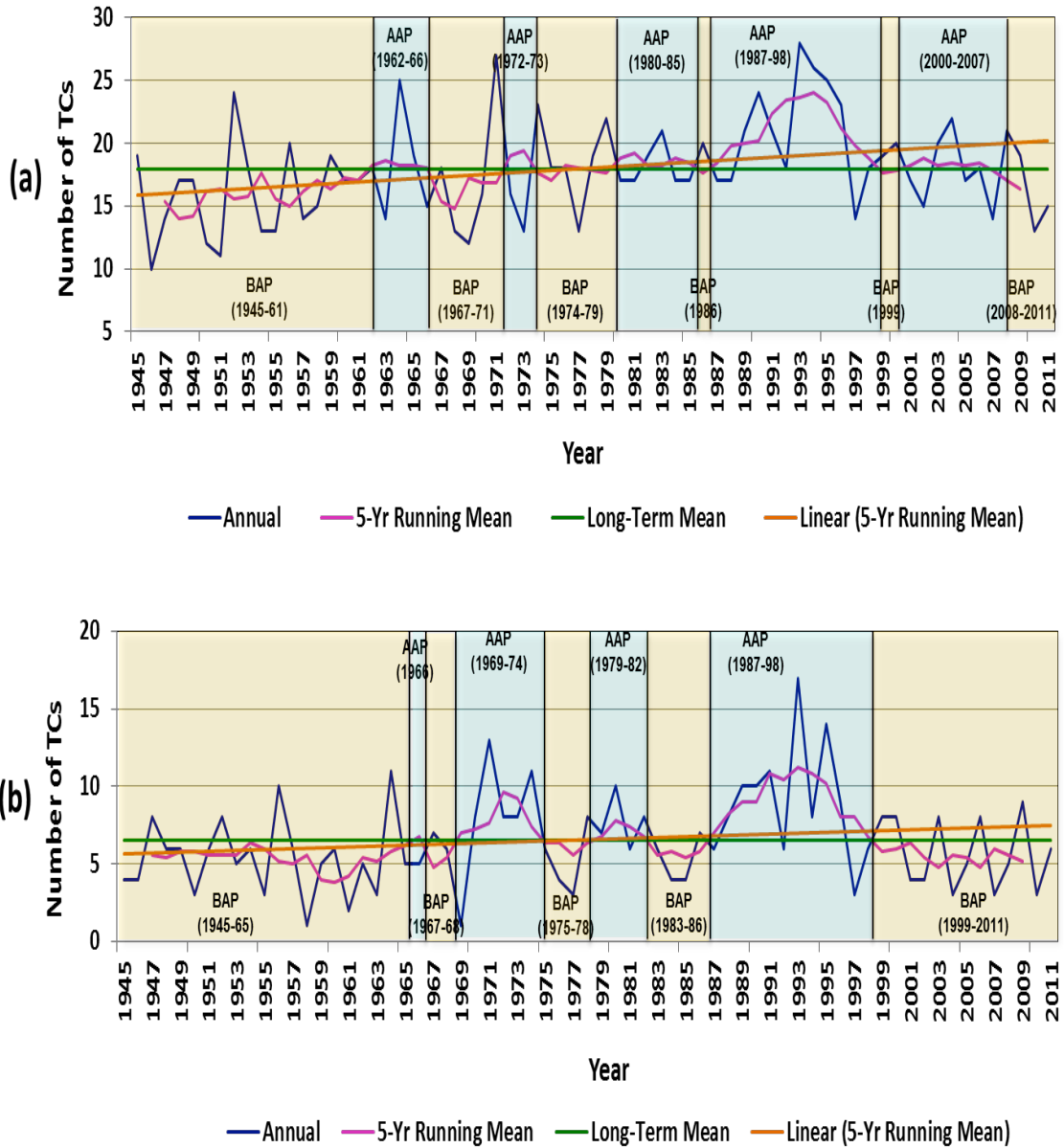


**Fig. 10.** Interannual and interdecadal variations in the frequency of (a) all TCs and (b) landfalling TCs over the 1945-2011 period. Years with 5-year running mean below the long-term average of 18 are considered to be part of the below average period (BAP), and all years with above average TCs are part of the above average period (AAP).

### **3.9 Genesis Positions and Tracks**

Over 80% of all TCs in the WNP form within 20° of the Equator (Frank et al. 2006). Briegel and Frank (1997) used the studies of Gray (1968, 1979, 1985) to define the climatological conditions necessary for tropical cyclogenesis. The required conditions include SST above 26.5°-27.0°C coupled with a relatively deep oceanic mixed layer, cyclonic low-level relative vorticity and planetary vorticity, weak to moderate, preferably easterly, vertical wind shear, and organized deep convection in an area of large-scale ascending motion and high midlevel humidity. The Philippines is in that part of the WNP where the above-mentioned necessary conditions can be satisfied all year, so TCs in the Philippine region can form in all months, but there is strong concentration in the MAS, especially in JAS. The Philippine TC birthplaces and tracks have regular spatial progressions. The birthplaces are the latitude-longitude positions where a TC is initially recorded by JTWC, even if it is outside the defined domain at the time of genesis.

Depending on the time of the year, birthplaces range widely from 2.5°N to 27.5°N. The genesis positions can also occur east as far as 179.5°E and west as far as 107°E. In the JFM, which represents the calm phase of TC activity in the region, the TC birthplaces are confined to between 3°N to 16°N latitude, and from 123°E to 179.5°E longitude. In JFM, no TCs developed in the western side of the country or in the South China Sea (Fig. 11a). Most of the tracks are straight-moving although some recurve (Fig. 11e). Like the birthplaces, the tracks are confined to the lower latitudes,

reaching 23°N at most. Some TC tracks reach the South China Sea. AMJ is marked by an increase in the genesis numbers (Fig. 11b); it has more TC birthplaces than JFM (Fig. 11a). The birthplaces extend farther north to 22°N, about 6° latitude higher than the JFM birthplaces. Their horizontal extent does not exceed 166°E and some TCs originate in the South China Sea, reaching as far west as 109°E. As the birthplaces move north, the tracks also extend north (Fig. 11f), up to 46°N. TC formation increases rapidly in JAS, the quarter with the greatest frequency of TC genesis. JAS therefore is the most active quarter, with the largest number of TCs. The birthplaces are denser than any other quarter (Fig. 11c) and the areal extent of TC birthplaces also is greatest in JAS. The genesis locations extend farthest north, to 27°N, about 5° latitude greater than for AMJ, and its horizontal extent stretches from 111°E to 177°E, 11° longitude farther eastward than AMJ. The JAS TC tracks spread farther northeast, beyond 55°N (Fig. 11g). The TC tracks also reach mainland China. The OND quarter is characterized by reduced TC genesis relative to JAS, but has the highest percentage of landfalling TCs. TCs birthplaces in OND reach almost to 25°N and extend from 107°E to 178°E (Fig. 11d). The TCs in OND exhibit both recurving and straight-moving tracks and can reach 53°N. The straight-moving tracks are denser than the recurving tracks (Fig. 11h). All year round, straight moving TCs are dominant in the Philippine domain, except in April. The quarterly birthplaces of Philippine landfalling TCs are given in Figs. 11(i-l). Only 36% of the total TCs that occurred in the Philippine domain struck the country; there is an evidently reduced number, of birthplace points as seen in Figs. 11(i-l). Birthplaces of landfalling TCs occupy narrower latitudinal and longitudinal scope, relatively closer to the Philippines



particularly prominent in AMJ and OND seasons. Landfalling TCs have a mean west-north-westward direction and some have an eastward direction, particularly those that developed from South China Sea. Landfalling TCs with recurving tracks hit the landmass of the northern Philippines before heading northeastward (Fig. 11m-p).

The tracks of the Philippine TCs can be grouped into three types: (1) straight-line, (2) recurving, and (3) free-moving. The TC track type is influenced by both the large-scale and synoptic-scale circulations (Harr and Elsberry 1991). Straight-moving TCs are confined to lower latitudes while recurving TCs form farther north and east of the Philippines. Straight-moving TCs occur when there are weak monsoon westerlies, strong trade easterlies and also a strong subtropical anticyclone to the north of the Philippines. Recurving TCs are present when there are strong monsoon westerlies, weak trade easterlies, a deep monsoon trough and the position of the subtropical anticyclone is to the far northeast of the Philippines (Chen et al. 2009). Most recurving TCs do not make landfall, unless the SW monsoon is weak. The free-moving TCs are those with neither recurving nor straight-line tracks.

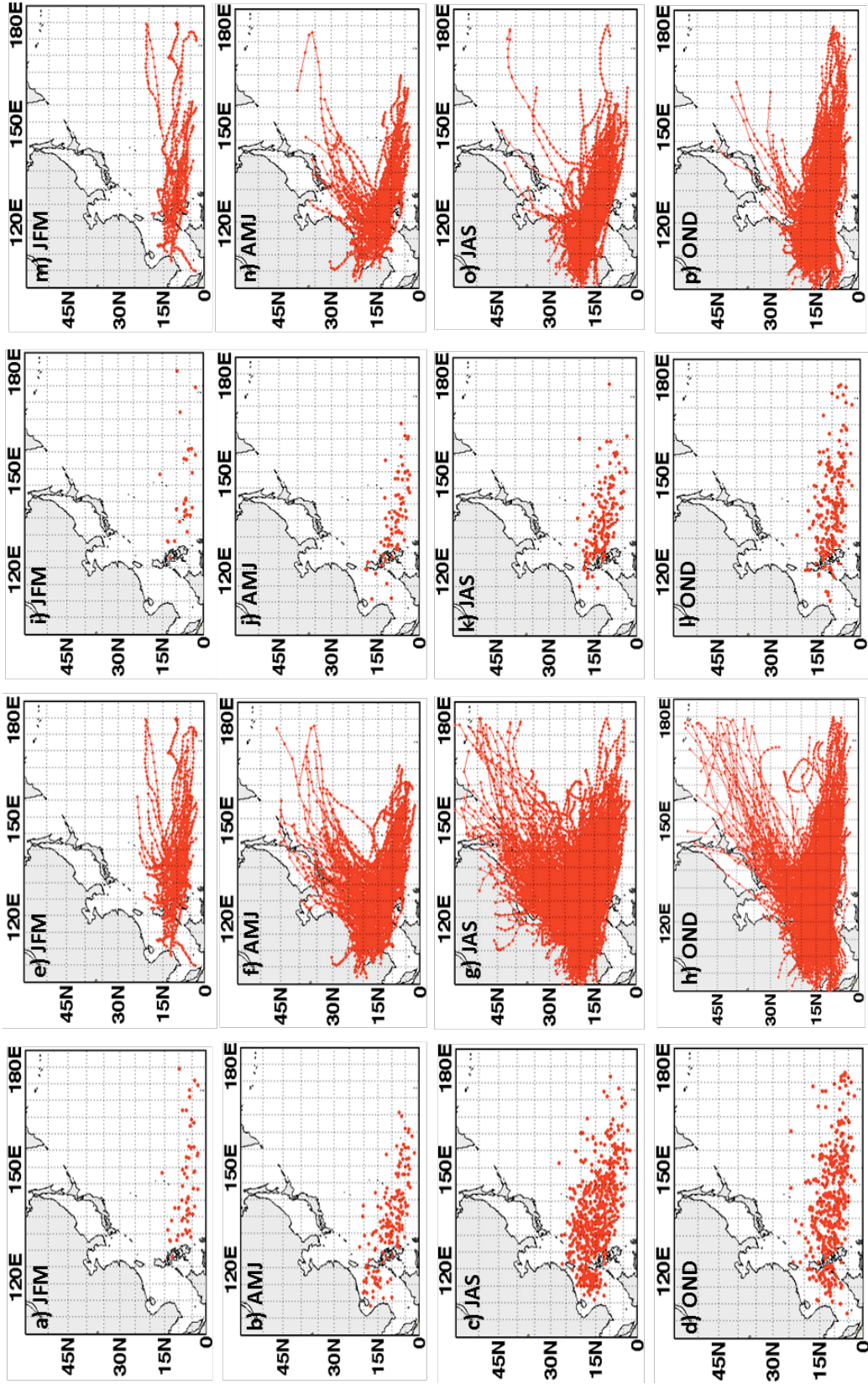
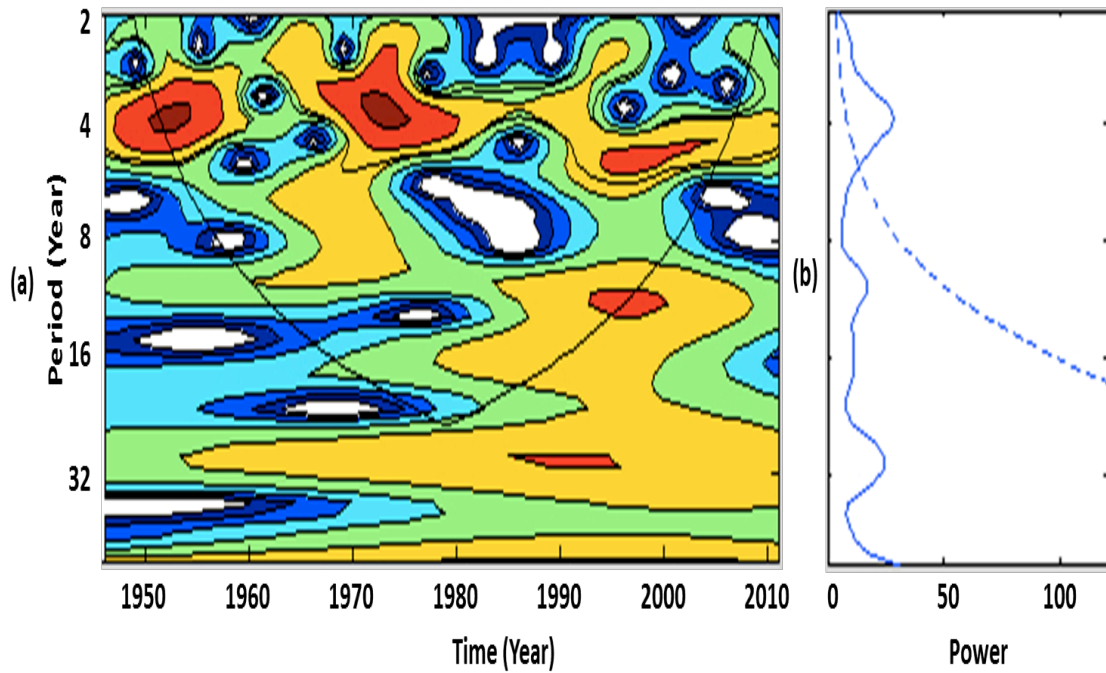


Fig. 11. Quarterly variations in genesis positions and tracks of all TCs (a-d) genesis locations of all TCs, (e-h) tracks of all TCs, and quarterly variations of genesis positions and tracks of landfalling TCs (i-l) genesis locations of landfalling TCs, (m-p) tracks of landfalling TCs.

### 3.10 The Role of ENSO

The TC activity in the WNP is known to have interannual variability (Landsea 2000). This variability is linked to ENSO (Chan 1985; Dong 1988; Lander 1993, 1994) and is attributed to the longitudinal shift of the Walker circulation (Chan 1985; Wu and Lau 1992). The changes in the large-scale circulation during an ENSO warm episode (El Niño) are discussed by Lander (1993, 1994). The WMO definitions for El Niño and La Niña conditions were adopted in this study. The definition of El Niño is that the three-month running mean of departures from normal sea-surface temperatures in the Niño 3.4 region is  $\geq +0.5^{\circ}\text{C}$ . La Niña is defined as when the three-month running mean of anomalies or departures from normal sea surface temperature in Niño 3.4 region is less than or equal  $-0.5^{\circ}\text{C}$ . In the present study the Philippines, situated in the WNP, is strongly affected by ENSO.

Wavelet analysis revealed that ENSO is the major global mode influencing the Philippine TC activity (Fig. 12a). With 67-year period dataset, the most significant is the ENSO signal as shown in the global wavelet spectrum (Fig. 12b). Wavelet analysis suggests that ENSO is active every 20 years, in 50s, 70, and 90s. It also shows other signals but this study only focuses on ENSO because those signals are not strong enough to exceed 95% confidence level (as shown by the dashed blue line).



**Fig. 12.** (a) Wavelet analysis of the Philippine TC time series. The black curve indicates the cone of influence, and (b) the corresponding global wavelet spectrum.

The quarterly and interannual variability of the Philippine TC activity during El Niño and La Niña episodes of ENSO is presented in Fig. 13. The yellow, red and blue bars in Fig. 13 represent the Neutral, El Niño and La Niña conditions, respectively. The standardized quarterly TC count during Neutral, El Niño and La Niña seasons is presented in Fig. 13a. Note that the TC activity in the Philippine region during the Neutral period, relative to El Niño and La Niña episodes, is always above normal from JFM to JAS. The same scenario was noted by Chan (2000). Below normal TC activity is observed in OND of Neutral years. Although below average TC activity is experienced throughout the year during El Niño years, there is a notable difference in the slightly negative TC count in JAS. Chan (2000) also

observed a below normal TC activity in the last quarter of the year during El Niño events. During La Niña events, AMJ and OND experienced above average TC activity as opposed to the below normal TC activity in JFM and JAS. Chan (2000) also found above normal number of TCs in OND during La Niña episodes. Gray (1968) suggested that the monthly and seasonal variations in TC activity are related to the monthly and seasonal large-scale circulation deviations from their climatology.

Chen et al. (1998) found a significant disparity in the genesis locations of TC formation during the El Niño and La Niña phases. Wang and Chan (2002) and Elsner and Liu (2003) recognized that there is variation in the tracks and duration of TCs in the WNP during strong ENSO events. Chan (1985, 2000) and Wang and Chan (2002) emphasized that large-scale climate factors such as ENSO alter the location of genesis and preferred track of TCs and may have a significant effect on landfalling activity. They also pointed out that the impact of ENSO on TC activity over the WNP depends on the strength of the ENSO events. The suppression of TC landfall activity is more significant in years associated with stronger El Niño events. Saunders et al. (2000) and Wu et al. (2004) suggested that ENSO has a significant impact on the TC landfalling activity in the coastal areas of East Asia. Relative to Neutral years, the number of TCs landfalling in the landmasses around the WNP is significantly reduced in SON of El Niño years (Wu et al. 2003). Wu et al. (2004) suggested that the relatively smaller number of landfalling TCs in China, Indochina, the Malaysian Peninsula, and the Philippines during the season can be partially explained by the eastward shift in mean genesis position and the break between the two cells in the subtropical ridge. In OND of La Niña years, the Philippines, south China, and

northern Vietnam experience higher numbers of landfalling TCs because of the westward shift in mean genesis position, and the strong subtropical ridge, which favors a steering flow toward the west-north-west.

The TC landfall numbers in the Philippine region are examined for different ENSO phases (Fig. 13b). TC landfalls in Neutral years are above average in the first half of the year, but below average in the second half of the year. Most seasons, except JAS, during El Niño events are below normal in terms of TC landfalls. The sharp drop in TC landfalls during OND of an El Niño episode confirms the findings of Wu et al. (2003). JFM and AMJ of a La Niña year exhibit below average TC landfall, in contrast with the above normal TC landfalls in the JAS and OND quarters. High TC landfall counts in OND also confirm the results of Wu et al. (2004).

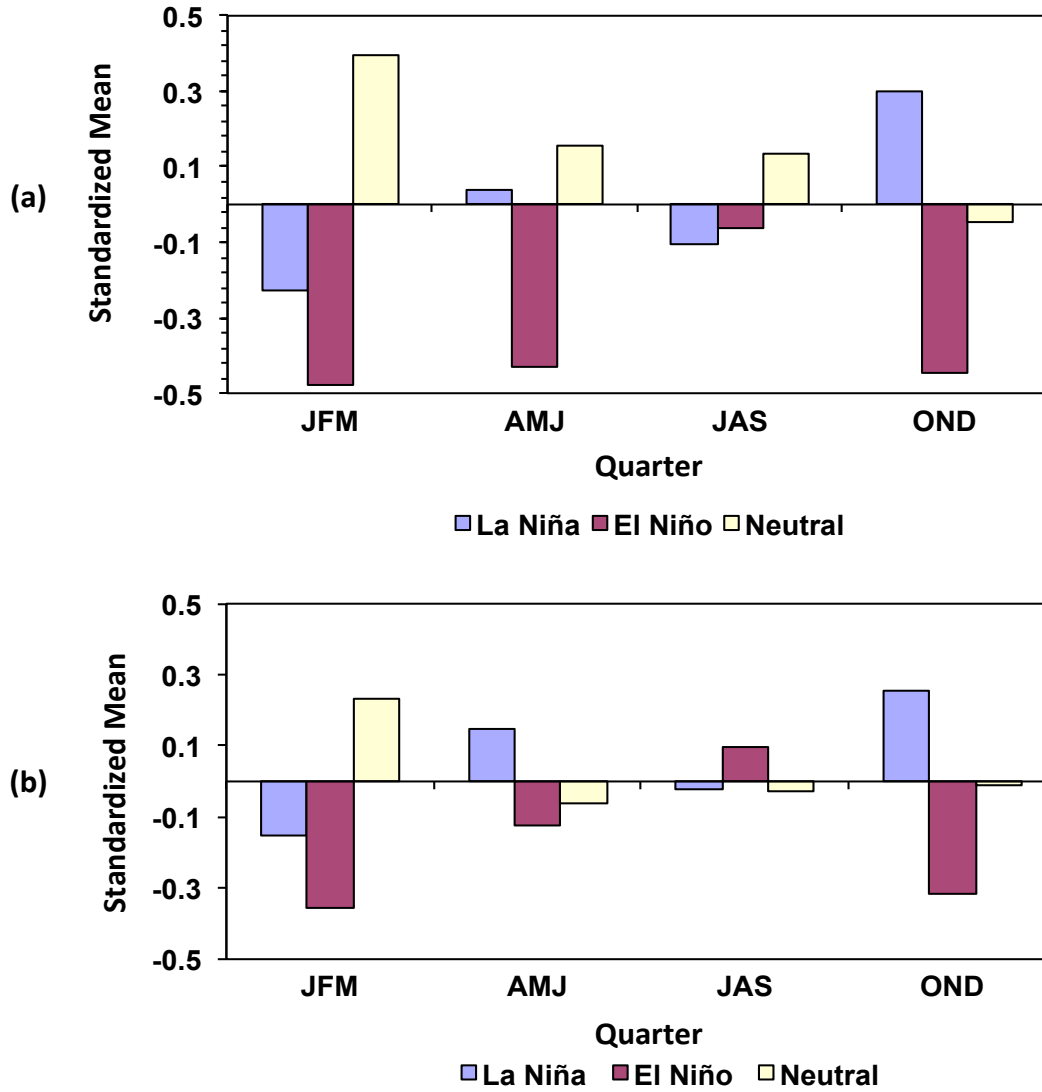


**Fig. 13.** Shows how TC-ENSO relationship varies with (a) Standardized quarterly TC total during neutral, El Niño and La Niña conditions (b) same with (a) but for standardized TC landfall count.

## Chapter 4

### Impacts of ENSO on Philippine TC Activity

#### 4.1 Introduction

This section extends the preliminary work on ENSO in chapter 3 that has identified ENSO, through wavelet analysis, as the major global climate mode causing variability in the Philippine TC activity.

Rasmussen and Carpenter (1982) presented ENSO and considered it to be the most important planetary-scale phenomenon that affects interannual variations of TC activity in the WNP (Kim et al. 2008). ENSO, a tropical air-sea coupled system, alters the thermodynamic and dynamic state of the environment that, as a result, affects the weather and climate systems (Bjerknes 1969). The El Niño phenomenon is manifested in the anomalous warming of the eastern and central tropical Pacific. La Niña refers to anomalous cooling of the tropical Pacific, or simply the opposite of El Niño. TCs form mainly in the tropics thus variation of TC activity by ENSO is most likely.

The relationship between the ENSO and TC activity in the WNP has been widely explored by several studies (Chan 1985, 2000; Dong 1988; Lander 1993,1994; Chen et al. 1998; Kimberlain 1999). Most studies were often concentrated on investigating the location of cyclogenesis (Chan 1985; Chen et al. 1998; Chia and Ropelewski 2002; Wang and Chan 2002), total number of TCs, intensity, and lifetime of TCs (Chan 1985; Dong 1988; Wu and Lau 1992; Chen et al. 1998; Camargo and Sobel 2005). The ENSO influence on the TC tracks and landfalls were also examined



(Wang and Chan 2002; Wu and Wang 2004; Wu et al. 2004; Camargo and Sobel 2005; Fudeyasu et al. 2006; Camargo et al. 2007a).

An extensive amount of literature addresses the issue of ENSO influence on WNP TC activity, but no paper has emerged studying comprehensively the local consequences of ENSO on Philippine TCs although some studies have provided hints on the influence of ENSO on the Philippines, particularly on TC activity.

The main goal of this chapter is to investigate and establish a relationship between TC activity in the Philippines and its behavioral response to various ENSO phases by examining its influence on TC properties (i.e., seasonal statistics of TC number, landfalls, intensity, TC days, season start/end dates, season length, ACE, genesis locations, and tracks). Here, the focus is to increase our understanding on the roles of ENSO on the variability of Philippine TC activity.

The irregularity in TC activity only occurs in certain months during El Niño and La Niña phases and not throughout the year. The change in the planetary-scale circulation associated with ENSO during these months explains the relationship between ENSO and TC activity (Chan 2000). It is for this reason that the approach used in this study is at intraseasonal time scale reflecting the seasonal relationship of ENSO to Philippine TCs. To explain the trends in the observational record of Philippine TCs in the context of variations in SST, a comprehensive analysis of the TC statistics is conducted.

Previous studies have shown statistically significant differences in landfall rates in the northern Philippines between El Niño and La Niña events with more intense typhoons making landfall in northern Luzon in La Niña years (Saunders et al.

2000; Elsner and Liu 2003). Moreover, the number of TCs making landfall in the Philippines is significantly less than normal in September- November of El Niño years (Elsner and Liu 2003; Wu et al. 2004).

## **4.2 Methodology**

In order to identify variations in TC activity between ENSO phases, the Philippine TC dataset was partitioned into El Niño, La Niña, and Neutral phases. Simple statistical methods are used to investigate how ENSO influences the TCs in the Philippine domain. El Niño, La Niña and Neutral years are defined according to the value of monthly SST anomalies over the Niño 3.4 region averaged over the period of interest, and in this study the periods are quarterly, LAS, and MAS. A period is classified as El Niño, La Niña, or Neutral when the averages of the Niño 3.4 SST index (Barnston et al. 1997) were at least  $0.5^{\circ}\text{C}$ ,  $-0.5^{\circ}\text{C}$ , and  $<0.5^{\circ}\text{C}$  to  $>-0.5^{\circ}\text{C}$ , respectively. For LAS, it is averaged over January-May season where it has identified 11 El Niño years, 15 La Niña years, and 36 Neutral years (Fig. 14a). For MAS, the Niño index is averaged over June-December season and has classified 17 El Niño years, 18 La Niña years, and 27 Neutral years (Fig. 14b). Table 4 shows the list of years for each ENSO phase in LAS and MAS.

Investigating TC activity by quarter and by season provides information how various ENSO phases affect early, mid, peak and late season and during less active and more active seasons. TC activity was measured by examining quarterly and seasonal number of TCs that entered the Philippine domain, number of landfalling TCs and other TC metrics. The time series of TC count, landfall, TC days and ACE

were standardized to provide a representative TC count during El Niño, La Niña, and Neutral episodes. To represent the TC intensity on seasonal and annual time scales, the accumulated cyclone energy (ACE), introduced by Bell et al. (2000), is calculated. ACE is defined as the sum of the squares of the estimated 6-hourly maximum sustained surface wind speeds for all TCs in the Philippine domain having 35 knots<sup>2</sup> intensity or greater, summed over the season or year.

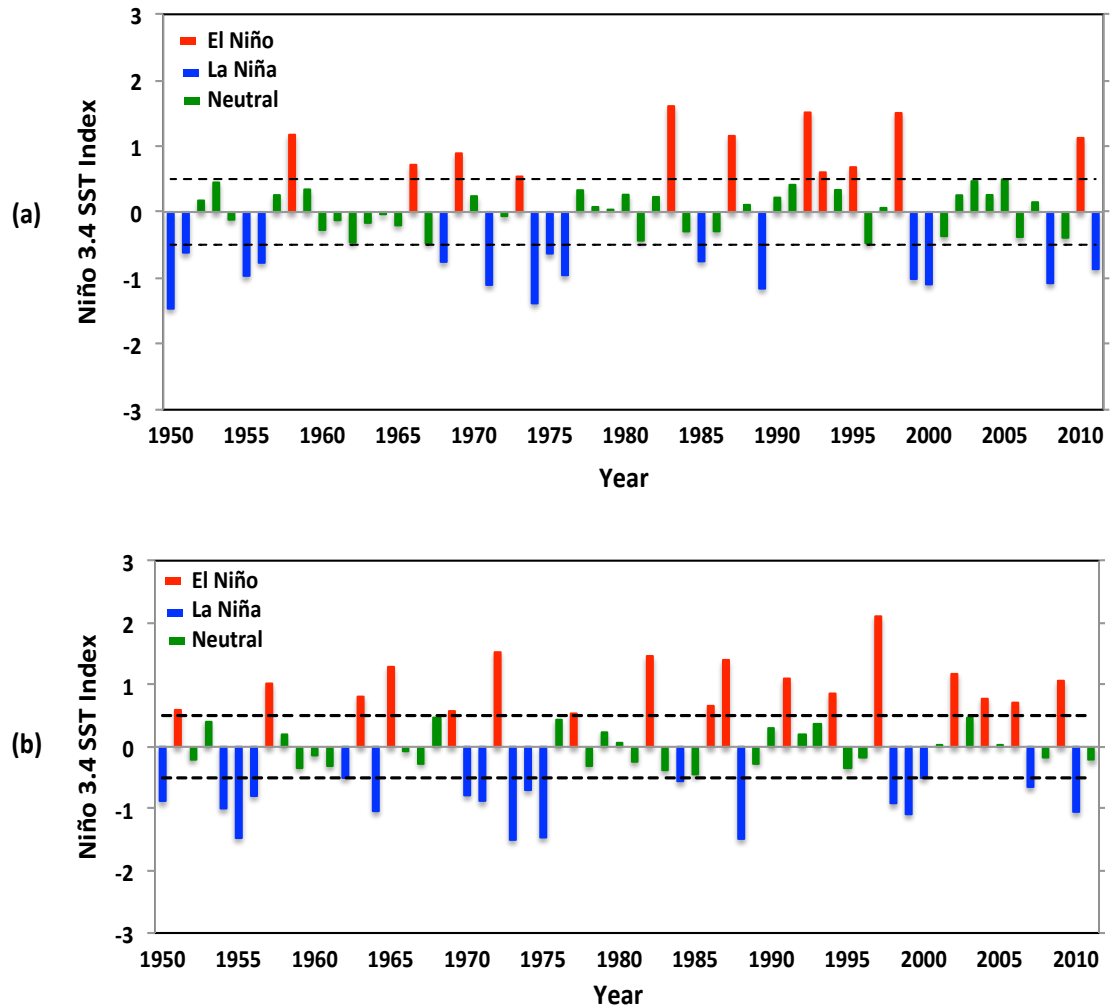


**Fig. 14.** Niño 3.4 indices (°C) for the period 1950-2011 for (a) LAS and (b) MAS, the dashed lines show the negative and positive threshold of SST index.

LAS Neutral Years		LAS El Niño Years	LAS La Niña Years	MAS Neutral Years		MAS El Niño Years	MAS La Niña Years
1952	1981	1958	1950	1952	1992	1951	1950
1953	1982	1966	1951	1953	1993	1957	1954
1954	1984	1969	1955	1958	1995	1963	1955
1957	1986	1973	1956	1959	1996	1965	1956
1959	1988	1983	1968	1960	2001	1969	1962
1960	1990	1987	1971	1961	2003	1972	1964
1961	1991	1992	1974	1966	2005	1977	1970
1962	1994	1993	1975	1967	2008	1982	1971
1963	1996	1995	1976	1968	2011	1986	1973
1964	1997	1998	1985	1976		1987	1974
1965	2001	2010	1989	1978		1991	1975
1967	2002		1999	1979		1994	1984
1970	2003		2000	1980		1997	1988
1972	2004		2008	1981		2002	1998
1977	2005		2011	1983		2004	1999
1978	2006			1985		2006	2000
1979	2007			1989		2009	2007
1980	2009			1990			2010

**Table 4.** List of years for each ENSO phase in LAS and MAS

### **4.3 ENSO Impacts on Genesis Positions, Tracks and Frequency**

A comprehensive analysis of TC data is carried out to examine the trends in the TC activity in the context of variations related with ENSO using the following metrics:

#### **4.3.1 Genesis Positions**

The Philippine domain is part of WNP where TC genesis most frequently occurs in the monsoon trough (McBride 1996; Chen et al. 2004; Lander 1994). The monsoon trough is marked by moist, southwest monsoon flows to the south and easterly trades to the north of the trough. Tropical disturbances are often found in the trough where there is a weak cyclonic rotation. As the cyclonic spin in the trough increases, the system tends to intensify into tropical storm or typhoon (Sadler 1967).

The impact of ENSO on the mean TC genesis location has been well studied, a displacement to the southeast (northwest) in El Niño (La Niña) years (Chan 1985; Dong 1988; Chen et al. 1998; Wang and Chan 2002; Chia and Ropelewski 2002), associated with the eastward extension of the monsoon trough and westerlies and the reduction of vertical wind shear near the date line, all of which increase the chance of genesis east of the climatological mean genesis point (Lander 1994, 1996; Clark and Chu, 2002; Wang and Chan, 2002). The preferred genesis region systematically shifts in response to changes in large-scale environments associated with both phases.

Fig. 15 shows the genesis locations of Philippine TCs during LAS and MAS

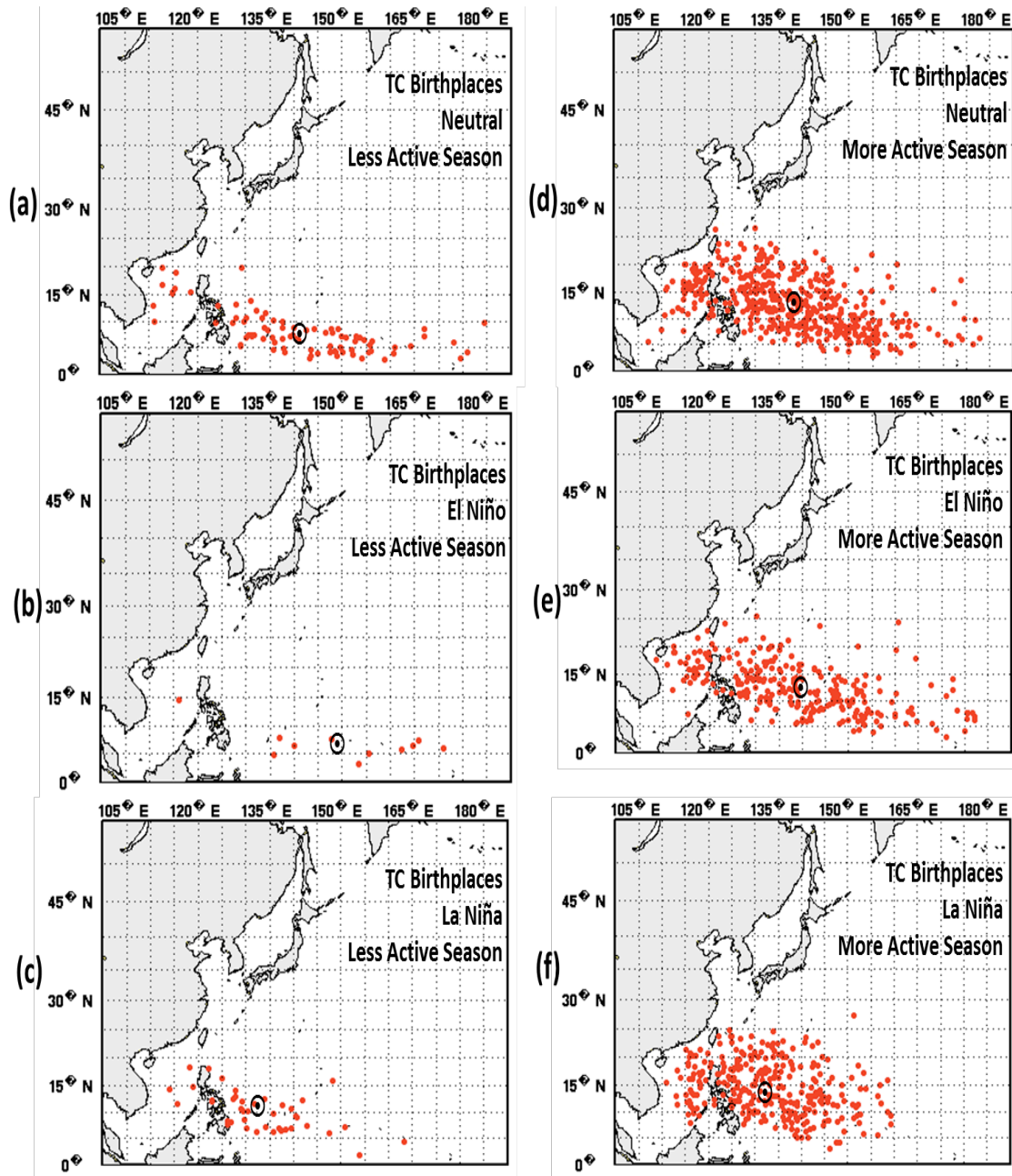
for each ENSO phase. In the LAS, the number of cyclogenesis is fewer and mostly developed in lower latitudes with only a few TCs formed in the South China Sea (Fig. 15a). Smaller numbers of TCs occur in El Niño years compared to Neutral and La Niña years. Most TC birthplaces are confined in lower latitudes, with only one TC formed in the South China Sea, and the mean birthplace location is displaced to the Southeast (Fig. 15b). Relative to La Niña years in LAS, the locations of TC genesis tend to form at lower latitudes and farther eastward. During La Niña years, majority of TCs formed west of 155°E and the mean birthplace location is displaced to Northwest (Fig. 15c). TC birthplaces in El Niño years occupy a wider longitudinal range as opposed with La Niña years, they can go as far east as 170.9°E and even farther east to 180°E in Neutral years.

There is a strong concentration of TCs in the MAS compared with the LAS. High TC activity during MAS mainly results from the frequent occurrence of favorable thermodynamic and dynamic conditions for TC development (Gray 1979). TC genesis points occupy a much broader latitudinal and longitudinal extent and noticeably more TCs are seen in the South China Sea. The spatial distribution of TC birthplaces in Neutral and El Niño years are nearly identical except for a narrower latitudinal range in the El Niño phase. The mean genesis point relative to Neutral years, as previously observed in LAS, is also displaced to the Southeast during the El Niño years and to the Northwest in La Niña years. TC formation during La Niña years can only be seen west of 160°E but can reach near the date line in Neutral and El Niño years. Most TCs form in lower latitudes during El Niño years compared to La Niña years and this is particularly clear in the Southwest displacement of the mean genesis

location. Compared to LAS, birthplace points confined west of 160°E are more pronounced in MAS (Fig. 15d-f).

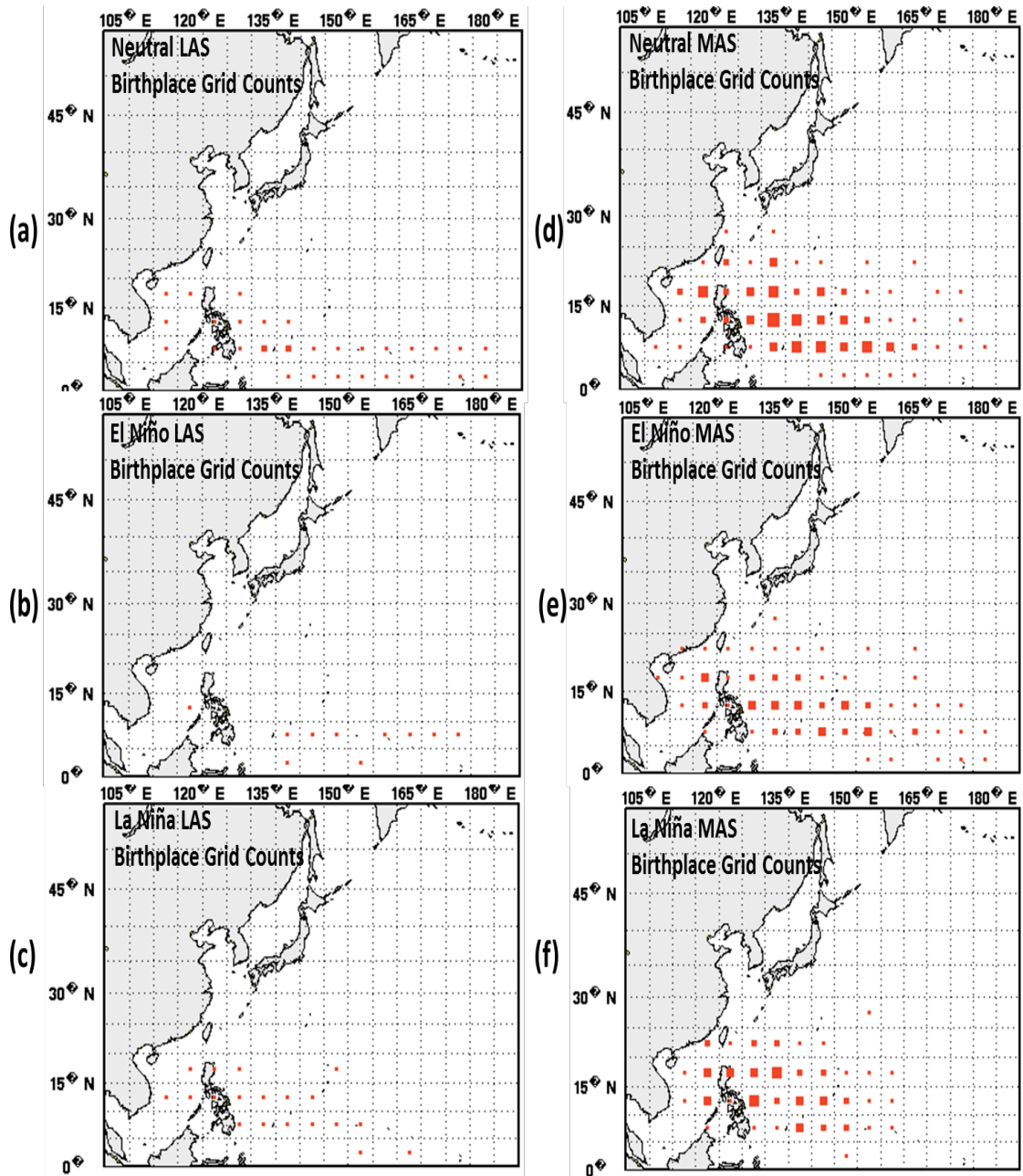
During the Neutral and El Niño phases of ENSO in both LAS and MAS, TC birthplaces could reach as far as the dateline. The pronounced change in TC activity due to ENSO is the confinement of TC birthplaces west of 155°E in LAS and 160°E in MAS during La Niña years, no TCs formed east of 160°E. The westward retreat in the genesis location during La Niña conforms to the findings of Chan (1985), Dong (1988), Lander (1994), and Dong and Holland (1994). The displacement of mean TC birthplace location is consistent with the results of Wang and Chan (2002), southeastward in the El Niño years, while they move northwestward in the La Niña years.

Fig. 16 presents the TC birthplace density per 5° x 5° grid box. In all ENSO phases, TCs are less dense and confined in lower latitudes in LAS whereas in MAS, birthplaces are denser and occupy a wider latitudinal scope reaching as far north as 30°N. The MAS is marked by an increased number of birthplaces over the South China Sea in all ENSO phases (Fig. 16d-f). Narrower grid density mostly in lower latitudes is apparent in El Niño years while broader latitudinal range in La Niña years.



**Fig. 15.** TC genesis locations during (a)-(c) LAS, and (d)-(f) MAS for each ENSO phase. The black double circles are the mean genesis locations.





**Fig. 16.** TC birthplace cumulative density per  $5^{\circ} \times 5^{\circ}$  grid box during (a)-(c) LAS, and (d)-(f) MAS for each ENSO phase.

### 4.3.2 Tracks

Fig. 17 displays all TC tracks by quarters and their division by category for El Niño, La Niña, and Neutral years. Like the genesis points, the quarterly TC tracks during Neutral and El Niño years are almost identical (Fig. 17a-h). The slight difference can only be seen in JFM when tracks are mainly straight-moving and occupy lower latitudes during El Niño years (Fig. 17e). The confinement of genesis locations west of 155-160°E in La Niña years leads to shorter straight-moving tracks but the recurving tracks can go farther Northeast and occupy higher latitudes (Fig. 17i-l).

The same scenario is seen in the TC tracks partitioned into LAS and MAS (Fig. 18). The straight-moving tracks in both seasons during La Niña years are shorter compared with straight-moving tracks in Neutral and El Niño years (Fig. 18c&f). In LAS, tracks for all ENSO phases occupy lower latitudes (Fig. 18a-c) except that in El Niño years, most TCs follow a straight track (Fig. 18b). For TCs in MAS, tracks are almost the same during Neutral and El Niño years while shorter straight-moving tracks are observed during La Niña years.

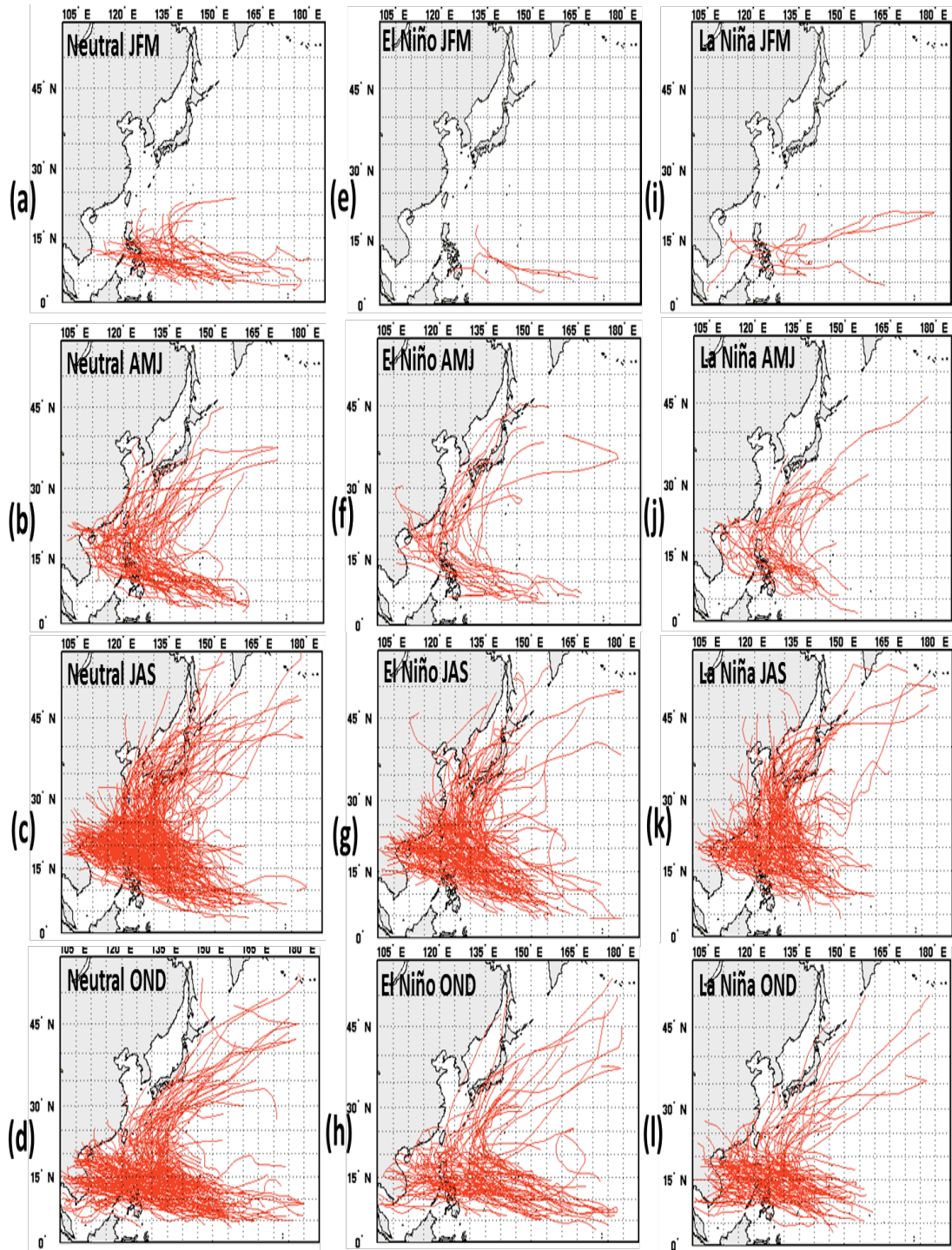


**Fig. 17.** Tracks of TCs formed in (a-d) Neutral, (e-h) El Niño, and (i-l) La Niña years during JFM, AMJ, JAS, and OND.

The cumulative track density per  $5^{\circ} \times 5^{\circ}$  grid box illustrates the region of higher concentration of TC passages and also suggest the prevailing track type during a specific ENSO phase (Fig. 19). In LAS, all ENSO phases, especially the Neutral phase, show high density of TC passages in the lower latitudes as opposed to the MAS where high density of TC passages are found in higher latitudes and tracks can reach as far as  $55^{\circ}\text{N}$ . In LAS during Neutral years, a higher density of TC passages is found east of the Philippines (Fig. 19a). In MAS, high-density TC passages are found north of  $5^{\circ}\text{N}$  in Neutral years and occupies a broader longitudinal range, and north of  $10^{\circ}\text{N}$  in El Niño and La Niña years and occupies a narrower longitudinal range relative to Neutral years (Fig. 19d-f). The absence of TC passages east of  $160^{\circ}$  in La Niña years versus El Niño years is noticeable in Fig. 19f, consistent with previous studies by Saunders et al. (2000) and Elsner and Liu (2003). More recurving tracks are evident in MAS during El Niño years than La Niña and Neutral years that conform to the findings of Wang and Chan (2002), Lyon and Camargo (2008) and Camargo et al. (2007b) that there are more recurving TC in El Niño years than La Niña years in OND. Here, we see that the identified changes in tracks are consistent with the change in mean genesis location. The Philippines is usually affected by many low-latitude, westward-moving TCs each year. Most TCs over the WNP tend to form farther east of these areas and move northward instead of westward during the El Niño phase of ENSO.

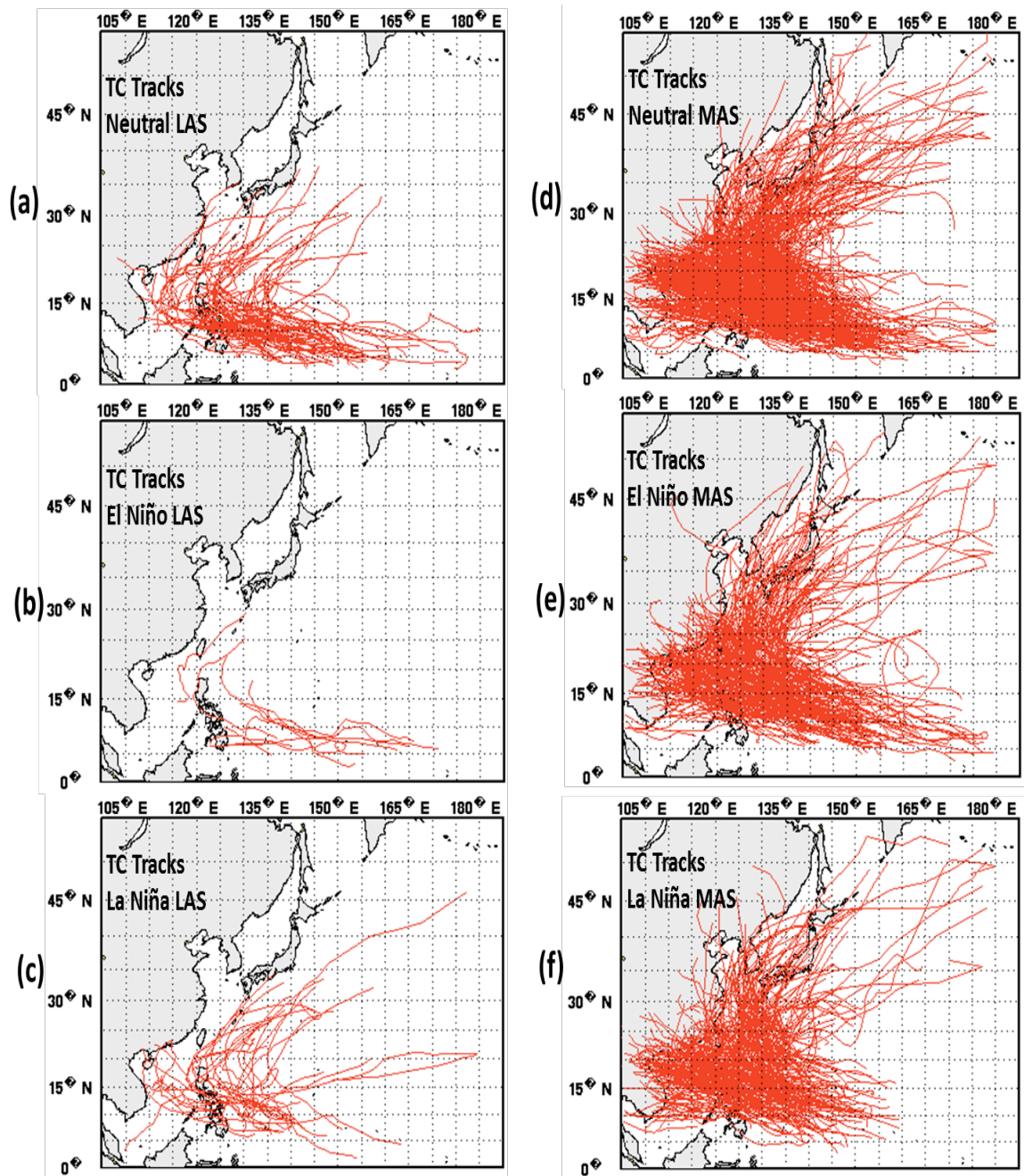


**Fig. 18.** Tracks of TCs formed in (a)-(d) Neutral, (e)-(h) El Niño, and (i-l) La Niña years during LAS and MAS.

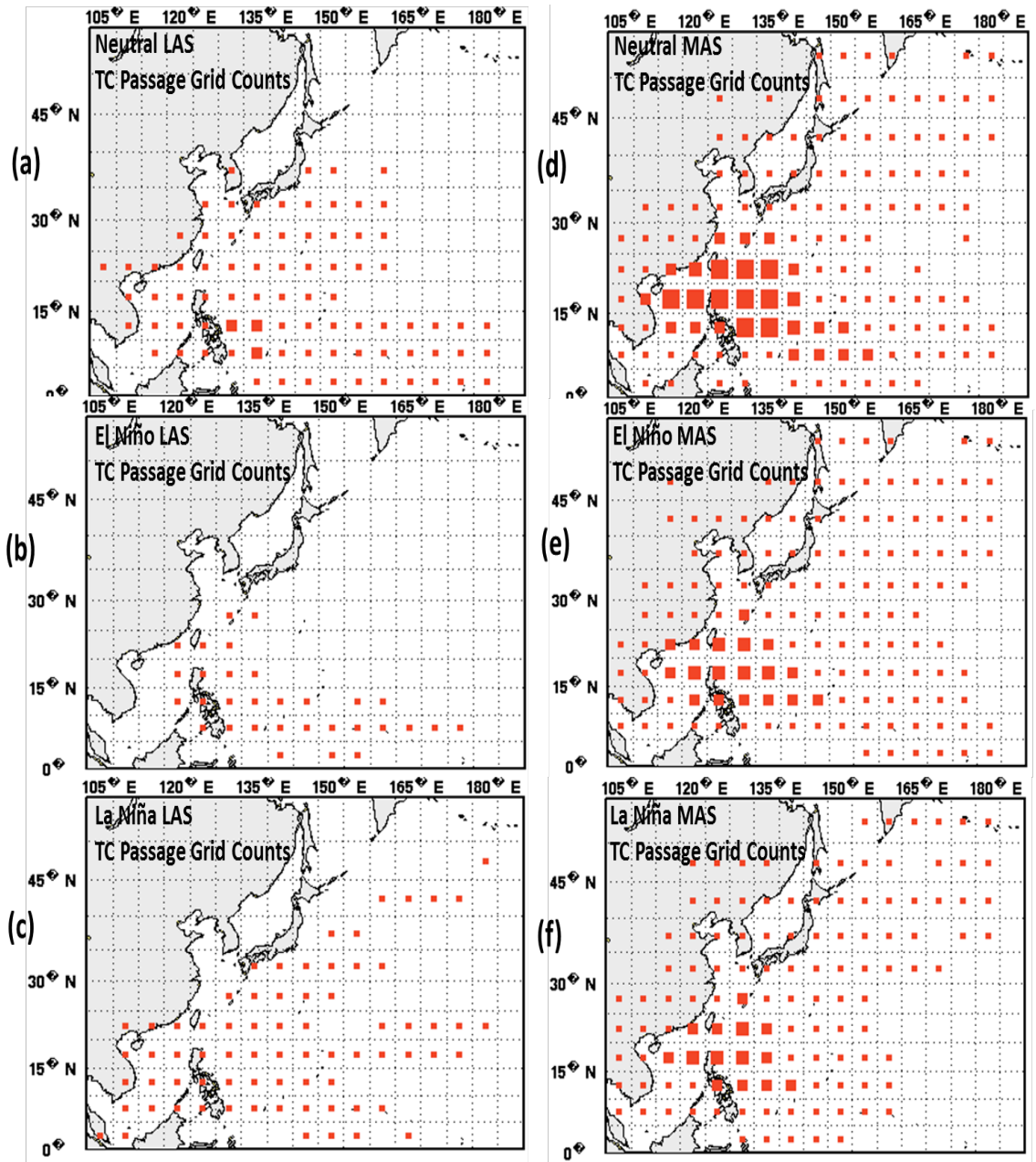


**Fig. 19.** Cumulative TC track density per  $5^\circ \times 5^\circ$  grid box during (a)-(c) LAS, and (d)-(f) MAS for each ENSO phase.

### 4.3.3 Frequency

The standardized TC mean and standardized landfall mean in LAS and MAS during various ENSO phases are presented in Fig. 20 (a,b). Above-average number of TCs and landfalls are observed in both seasons during Neutral conditions. Conversely, below-average TC frequency is common in LAS and MAS during El Niño years. This suggests that an El Niño phase tends to be followed by an overall reduction in TC frequency and is related to the longitudinal shift of the Walker circulation (Chan 1985; Dong 1988; Wu and Lau 1992; Chan 2000). In La Niña years, the TC frequency in LAS is above-average but a different condition is demonstrated in MAS, La Niña years have below-average TC frequency. La Niña years observed considerably above-average number of landfalls for both LAS and MAS, a result consistent with Chan (2000). The genesis locations being closer to the Philippines during La Niña conditions, mostly west of 160°E, significantly contribute to increasing the number of landfalling TCs. For El Niño years, TC landfall over the Philippine domain varies inversely to that of La Niña years.

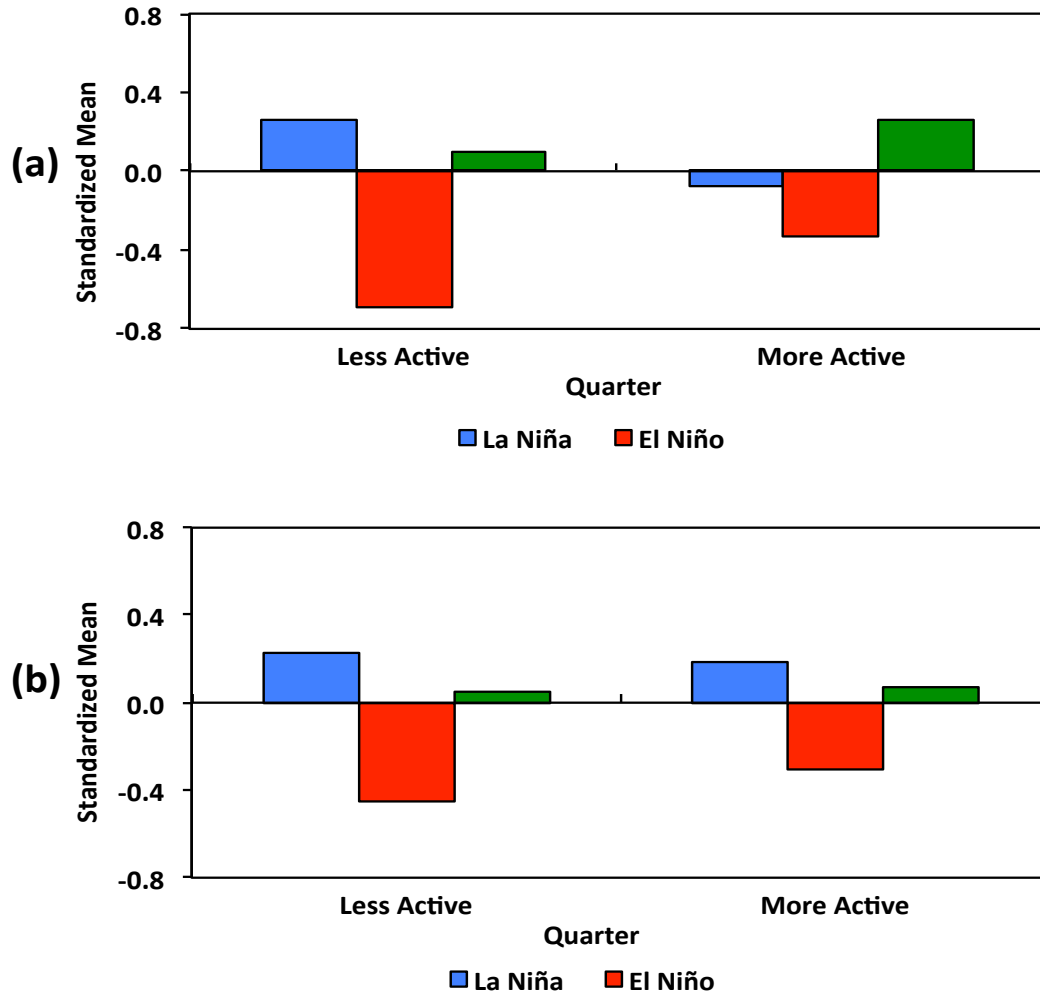


**Fig. 20.** Influence of ENSO to LAS and MAS TCs and landfalls (a) Standardized TC seasonal mean in LAS and MAS during ENSO conditions, (b) same with (a) but for standardized TC seasonal landfall mean.



## **4.4 Impacts on Other TC Properties**

In this section, we explore the relationship of ENSO to other TC properties particularly the intensity, TC days, season ACE, season start/end date, and season length.

### **4.4.1 Intensity**

The characteristic of the distribution of the three intensity categories (TD, TS, and TY) for various ENSO phases in quarterly timescales is presented in Fig. 21. The influence of ENSO on Philippine TCs depends largely on season and on the specific TC intensity.

Fig. 21a presents the quarterly standardized mean of TCs with TD intensity during different ENSO conditions. In Neutral years, TCs of TD intensity are above-average in JFM and JAS, normal in AMJ, and below-average in OND. Looking at the distribution in La Niña years, there is a tendency toward more TDs in JAS and OND but the opposite is observed in AMJ and JAS. Below-average TDs are experienced during El Niño years in almost all quarters particularly in JFM, with significantly fewer TDs, except for AMJ with above-average TDs.

How ENSO influences TCs of TS intensity is given in Fig. 21b. TSs in the Neutral phase remained relatively constant to above-average especially in JFM and AMJ. Conversely, a sustained decline in TSs occurs in all quarters during El Niño years. Throughout the first half of the year, La Niña years observed below-average

numbers of TSs but a huge tendency toward a larger number of TSs in remaining quarters of the year. Camargo and Sobel (2005) confirmed this result as more TCs of TS intensity are observed in La Niña years.

Fig. 21c demonstrates the quarterly standardized distribution of TCs of TY intensity. It exhibits a tendency to be above-average year round in Neutral years, which is also true for TSs. Examination of La Niña years reveals that substantially below-average TYs are common in JFM and JAS while above-average in AMJ and OND. El Niño conditions are characterized by lesser TYs in most quarters and only favorable to greater and more intense TCs in JAS, the peak of TC activity.

Quarterly statistics have shown the significant differences in the frequency of landfalling TCs based on intensity classification during various ENSO phases (Fig. 22). More TCs of TD intensity are making landfall in the Philippines during AMJ and JAS in El Niño years while below-average landfalling TDs are observed in JFM and OND. Less intense TCs like TDs during La Niña years are only prevalent in JFM and below-average from April to December especially in JAS. In Neutral years, above-average landfalling TDs are seen in all quarters except in AMJ.

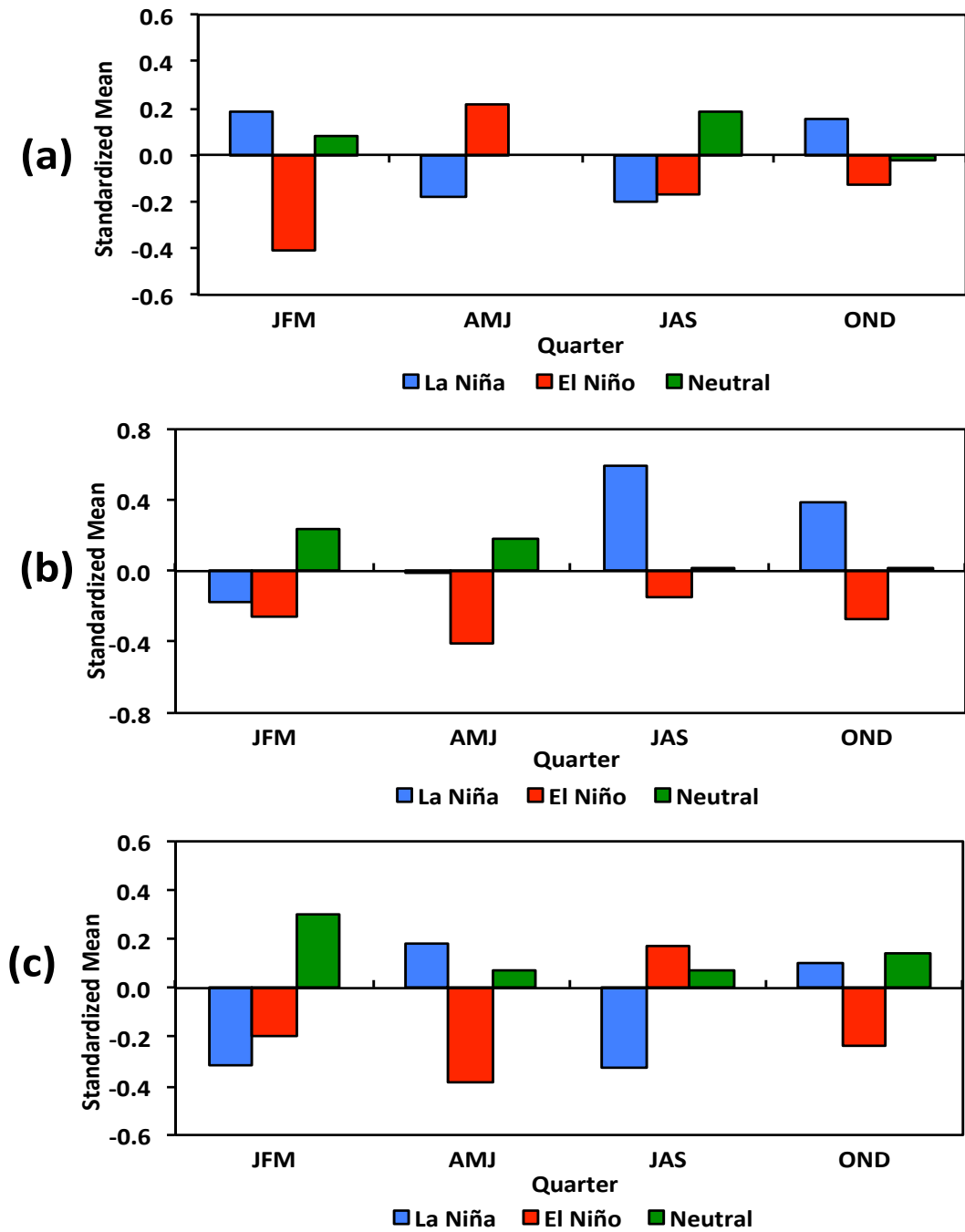


**Fig. 21.** Standardized quarterly TC mean by intensity classification during various ENSO conditions (a) tropical depression (TD), (b) tropical storm (TS), and (c) typhoon.

Neutral years have a tendency for a larger population of TS group in landfalling TCs that appeared from JFM to JAS. In contrast, an opposite tendency is observed in La Niña years, with fewer landfalling TSs from JFM to JAS and more landfalling TSs in OND. El Niño years lead to below-average TSs year round particularly in AMJ.

The influence of ENSO to landfalling TCs with TY intensity is above-average for El Niño years during JFM and JAS while below-average in AMJ and OND. Above-average landfalling TYs is observed almost year round except in JFM in La Niña phases. This is also observed in the results of Saunders et al. (2000) and Elsner and Liu (2003). In contrast, a reverse scenario occurs in Neutral years where there is below-average landfalling TYs during JFM and above-average during the rest of the year.

What is asserted in previous studies that TCs are more intense in El Niño years and weaker in La Niña years (Pudov and Petrichenko 1998, 2001; Chia and Ropelewski 2002) is not the case for Philippine TCs. It depends mainly on the seasons to identify, which ENSO phase is prevailing during a particular intensity category. Intense TCs of TY intensity are prevalent year round in Neutral years, but landfalling TYs are more common in La Niña except in JFM where El Niño years have above-average landfalling TYs in that particular season. Examining the impacts by season substantiates this, as ENSO does not prevail the entire calendar year.

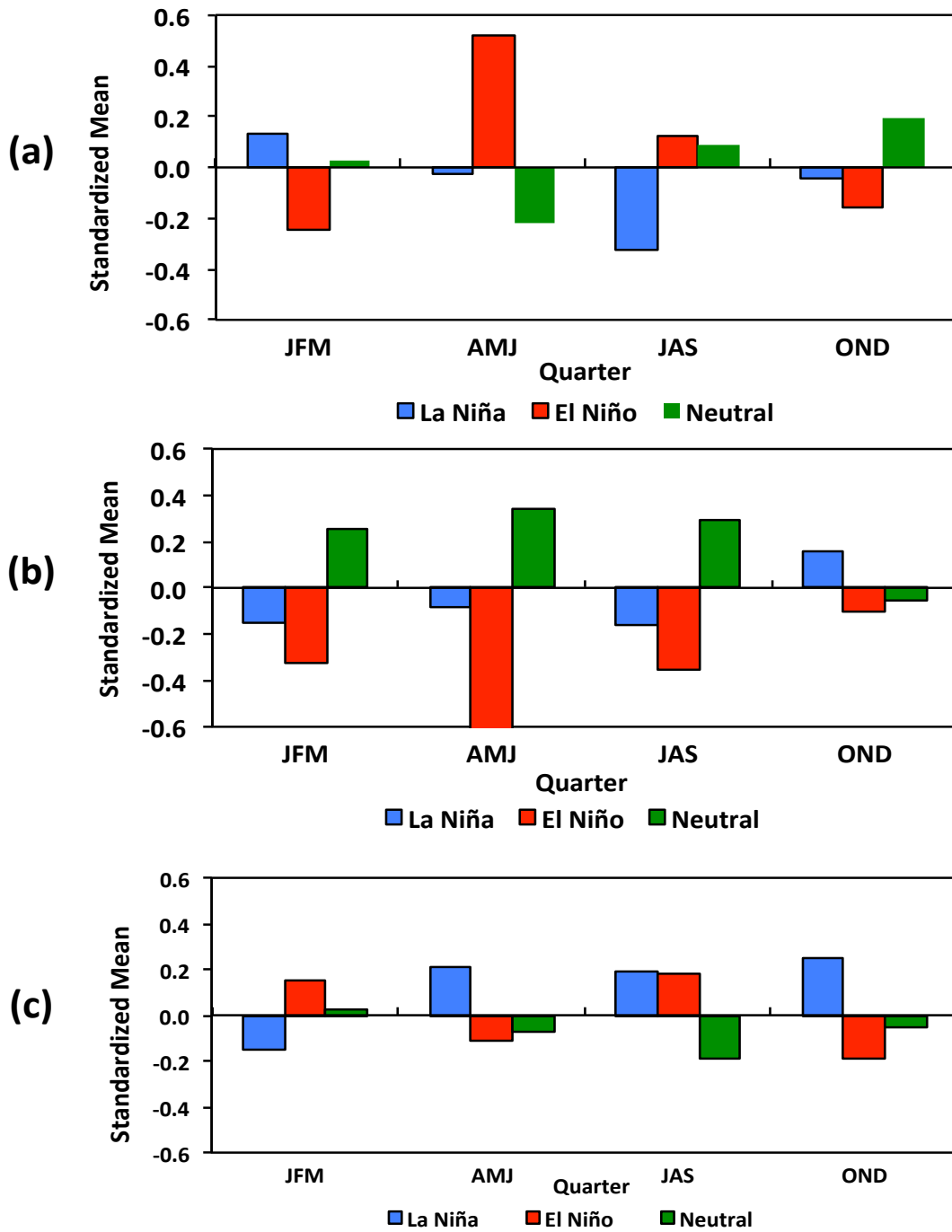


Fig. 22. Standardized quarterly TC landfall mean by intensity classification in LAS and MAS during various ENSO conditions (a) tropical depression (TD), (b) tropical storm (TS), and (c) typhoon.

#### 4.4.2 TC Days

We now consider the trend in TC days in various ENSO phases during LAS and MAS. The number of TC days during which TCs of different intensities (TD, TS, and TY) when inside the Philippine domain were counted. A day with two TCs counts as two TC days, and so on.

Fig. 23 shows the distributions of standardized mean of TC days for all ENSO phases in LAS and MAS. There are normally above-average TC days in both seasons in Neutral years especially in MAS. In La Niña years, there are more TC days in LAS and shifted toward fewer TC days in MAS. La Niña years have greater numbers of TCs than Neutral and El Niño years during LAS. TCs in La Niña years developed closer to the Philippine archipelago and although they have shorter durations, the higher number of TCs in LAS resulted to above-average number of TC days. In MAS, aside from TCs having shorter durations due to formation being confined near the Philippines, the TC number is fewer that also contributed to the below-average number of TC days.

In contrast, in El Niño years, significantly below-average TC days is observed in LAS while slightly above-average in MAS, as revealed in the standardized mean of TC days. These results conform to the studies of Pudov and Petrichenko (1998, 2001), Wang and Chan (2002), Chia and Ropelewski (2002), Chan and Liu (2004) and Camargo and Sobel (2005), which suggest that TCs are stronger and longer-lived in the seasons during which El Niño events develop. Despite having a below-average number of TCs in MAS during El Niño years compared with Neutral years, longer-

lived TCs in MAS during El Niño years considerably contribute to the number of TC days. The cyclogenesis found further east relative to La Niña years allow TCs to maintain a longer life span while tracking westward, resulting in longer durations. In LAS, there are more TCs in La Niña years than El Niño years, leading to a greater number of TC days. Wang and Chan observed the same result in 2002. The shift in number of TC days with ENSO in LAS reflects more (fewer) TCs in La Niña (El Niño) years, while in the MAS, it is due to TCs shorter (longer) lifetime in La Niña (El Niño) years.

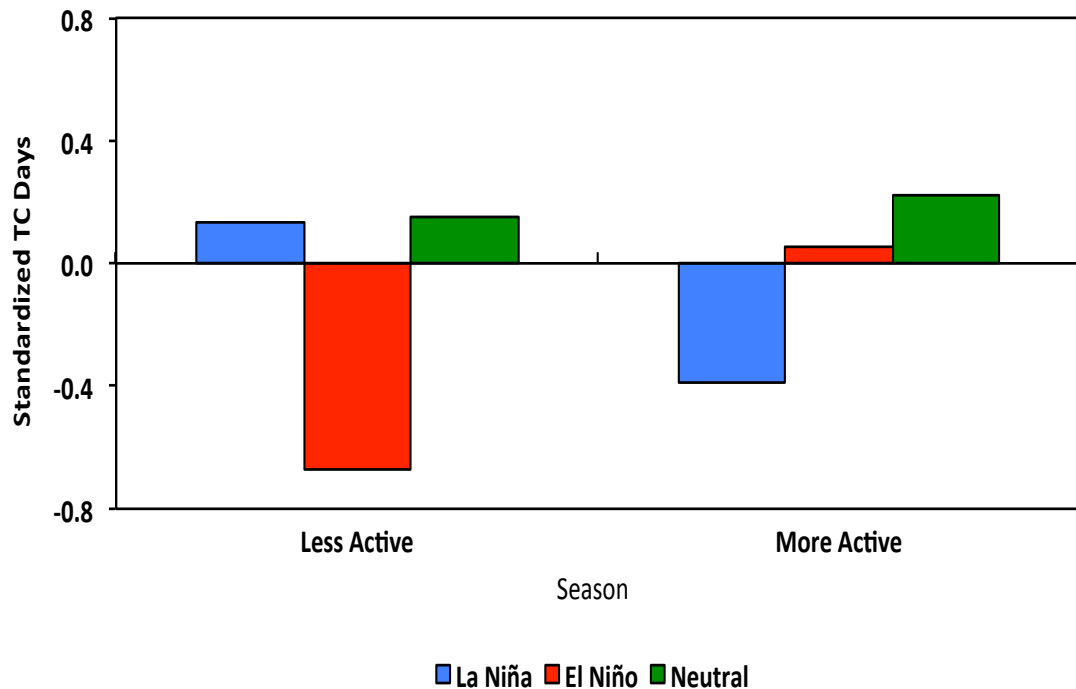


**Fig. 23.** Standardized seasonal number of TC days in LAS and MAS in various ENSO conditions.

### 4.4.3 Season ACE

The influence of ENSO on the seasonal accumulated cyclone energy (ACE; Bell et al. 2000) of TCs affecting the Philippines has been examined in this study. ACE considers the number, lifetime, and intensities of TCs occurring in a domain over a given period of time. ACE is defined as the sum of the squares of the estimated 6-hourly maximum sustained surface wind speed (knot<sup>2</sup>) for all TCs in the Philippine domain having 35 knots intensity or greater summed over all 6-hourly periods. ACE is defined as:

$$ACE = 10^{-4} \sum v_{\max}^2$$

where  $V_{\max}$  is estimated sustained wind speed in knots.

The time series of LAS ACE per year is shown in Fig. 24a. There are years when there is no value for LAS ACE; because LAS TCs during those years have intensities below 35 knots, or no TCs have occurred in LAS that year. This happened once in a La Niña LAS out of 15 years and 6 times in an El Niño LAS of 11 years. The year with the lowest LAS ACE on record is a La Niña year (1974), and the highest LAS ACE value occurred in 2004, a Neutral year. Out of 11 years with LAS El Niño, there are 8 ACE values below the median, with 7 of them below the 25<sup>th</sup> percentile, and 2 of these years are above the 75<sup>th</sup> percentile of the climatology. In contrast, 6 of the 15 La Niña years have LAS ACE values below the median, with 3 of them below the 25<sup>th</sup> percentile, and 5 La Niña years are with LAS ACE above the 75<sup>th</sup> percentile of the entire 62-year data record.



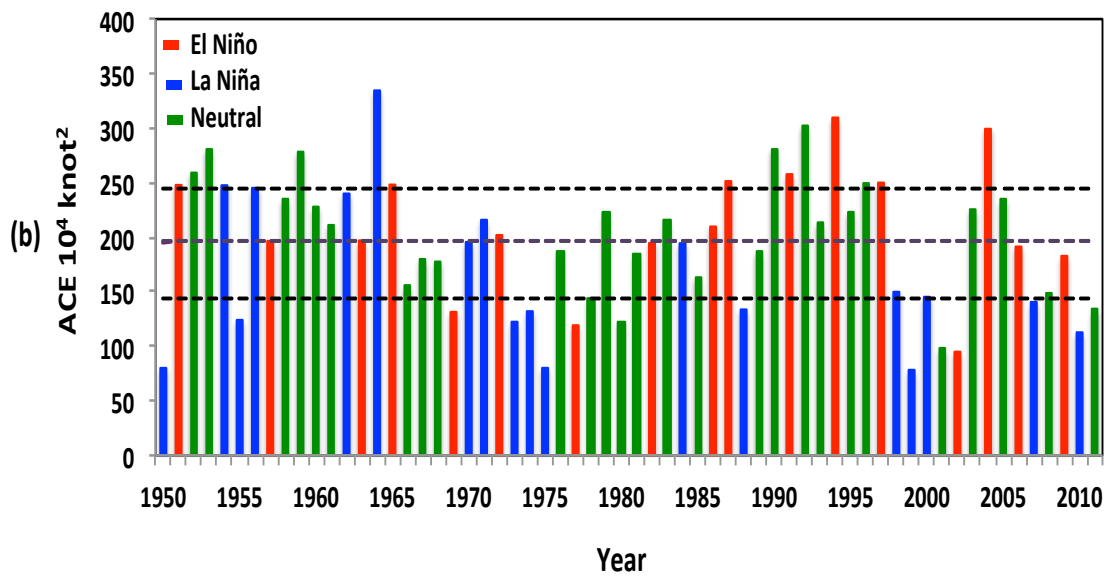
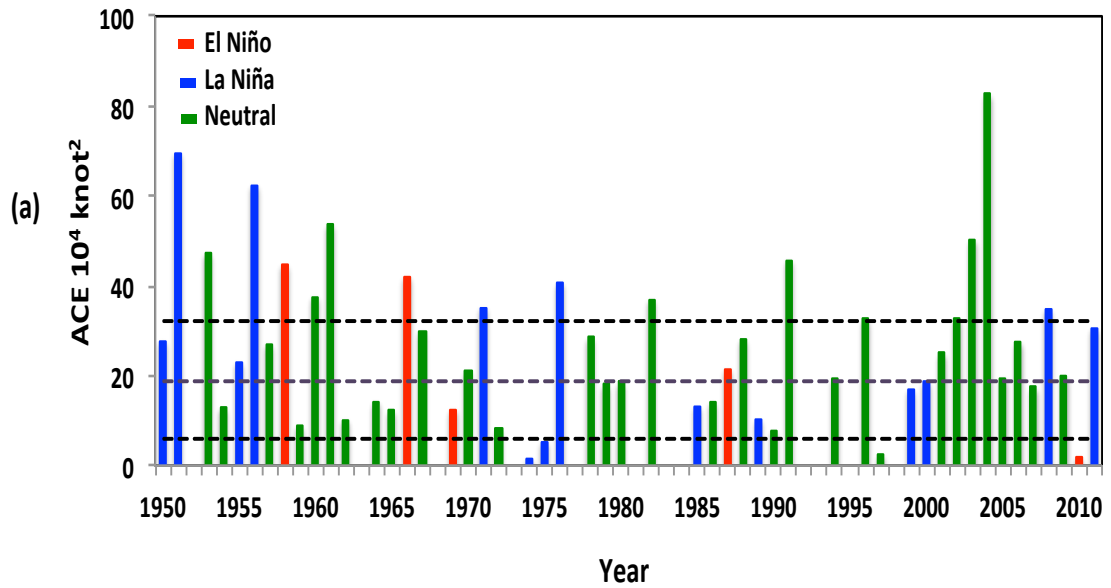
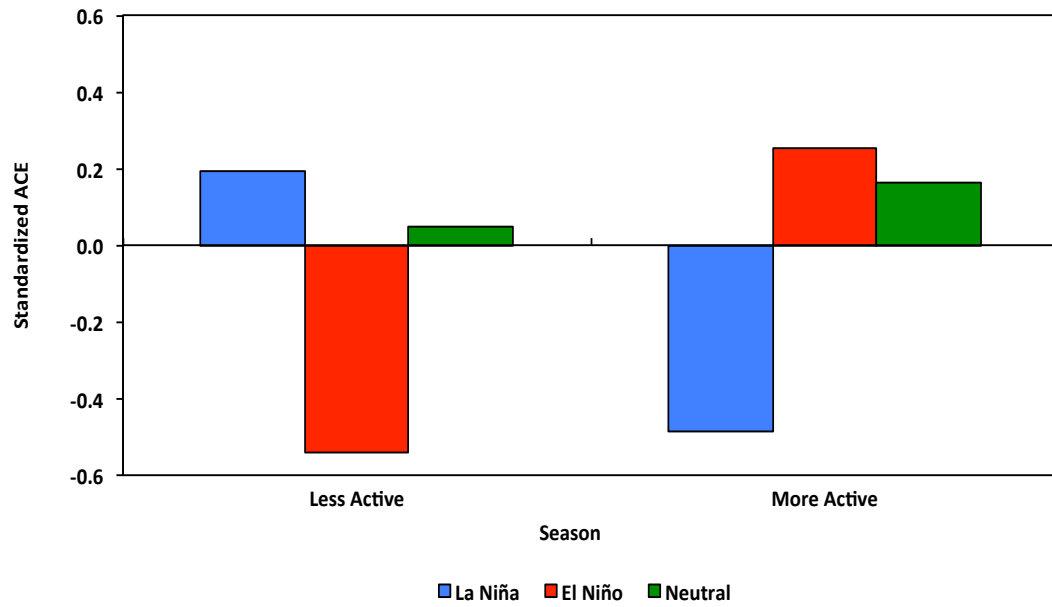


Fig. 24. Climatological ACE per year for (a) LAS and (b) MAS. The dashed lines denote the 25<sup>th</sup>, median, and 75<sup>th</sup> percentiles.

Fig. 24b presents the characteristics of the MAS ACE distribution including the 25<sup>th</sup>, median, and 75<sup>th</sup> percentiles, and the yearly MAS ACE values during various ENSO phases. The lowest MAS ACE has occurred in a La Niña year (1999) and the year with the highest MAS ACE value is also a La Niña year (1964). There are 17 years with MAS El Niño and 6 of which are below the median where 3 of them below the 25<sup>th</sup> percentile, and 7 years with MAS ACE values above the 75<sup>th</sup> percentile. While 13 of 18 La Niña years have below the median MAS ACE values, with 9 of them below the 25<sup>th</sup> percentile, and 3 of these years are above the 75<sup>th</sup> percentile.

Fig. 25 shows impact of ENSO on the seasonal ACE of TCs occurring in the Philippine domain. It shows the inverse difference of El Niño and La Niña phases in terms of ACE between LAS and MAS. Neutral phase has above-average ACE for both seasons. The standardized mean of LAS ACE suggests that during El Niño (La Niña) phase, the LAS ACE values are shifted toward below (above) average. The El Niño LAS ACE is distinct from both the La Niña and Neutral phases of ENSO. The below-average ACE in LAS El Niño is mainly due to the weaker intensity and lesser number of TCs in an El Niño year as there are years when no TCs have occurred in the Philippine domain and if there are, intensities are below 35 knots. An opposite scenario occurs in MAS. The standardized mean of MAS ACE implies that in the El Niño (La Niña) phase, the MAS ACE tend to be above (below) average. There is a lower number of TCs in the MAS El Niño phase compared with Neutral and La Niña phases. The increase in MAS ACE in El Niño years is mainly due to longer durations of individual TCs. These long-lived TCs were developed in the region of the WNP where SSTs are warmer, thus enabling the TCs to receive more energy input from the

ocean relative to weak TCs formed over the cooler ocean region (Camargo and Sobel 2005).



**Fig. 25.** Standardized seasonal ACE in LAS and MAS during various ENSO conditions.

#### 4.4.4 Season Start/End Date and Length

This section examines the effect of ENSO on the LAS and MAS TCs particularly the variation it causes on start and end dates and season length, in a manner similar on how these metrics were investigated in chapter 3. The characteristics of LAS and MAS in various ENSO phases are shown in Figs. 26 and 27, and are summarized and presented in Table 5 and 6.

In Neutral years, the LAS TCs begin in the Philippine domain as early as January 2<sup>nd</sup> and occur as late as May 31<sup>st</sup>. On the other hand, TCs leave the Philippine domain as early as January 15 and extend as late as June 6<sup>th</sup>. During El Niño (La Niña) years, the earliest a LAS TC begins to occur in the Philippine is on January 11<sup>th</sup> (January 2<sup>nd</sup>) and the latest is May 31<sup>st</sup> (May 12<sup>th</sup>) while LAS TCs can leave the domain as early as January 16 (January 11<sup>th</sup>) and the latest on June 8<sup>th</sup> (June 6<sup>th</sup>).

In the MAS, the earliest season start date during Neutral years is June 1<sup>st</sup> and the latest start date is July 19<sup>th</sup>. TCs exit the Philippine domain as early as November 23<sup>rd</sup>, and as late as January 2<sup>nd</sup>. In El Niño (La Niña) years, TCs occur in the domain as early as June 1<sup>st</sup> (June 4<sup>th</sup>) and as late as July 8<sup>th</sup> (July 30<sup>th</sup>). During El Niño (La Niña) years, TCs leave the domain as early as September 10<sup>th</sup> (October 28<sup>th</sup>) and as late as January 3<sup>rd</sup> (January 5<sup>th</sup>).

In Neutral years, the mean start date of LAS is March 6 and June 18 for MAS. Relative to Neutral years, the mean start date of LAS during El Niño years is later while earlier in La Niña years. An opposite trend is seen in MAS start date. El Niño years have earlier start date and a later one in La Niña years. The LAS in Neutral years

on average ends on May 12 while MAS normally ends on December 16. Compared with Neutral years, the mean LAS end date is earlier in La Niña years and much earlier in El Niño years. The same scenario is observed in MAS.

The average LAS length in Neutral years is 67 days and 181 days for MAS. In El Niño, both LAS and MAS have shorter season lengths compared with Neutral years. This is not the tendency in La Niña years where LAS length is longer and MAS length is much shorter.

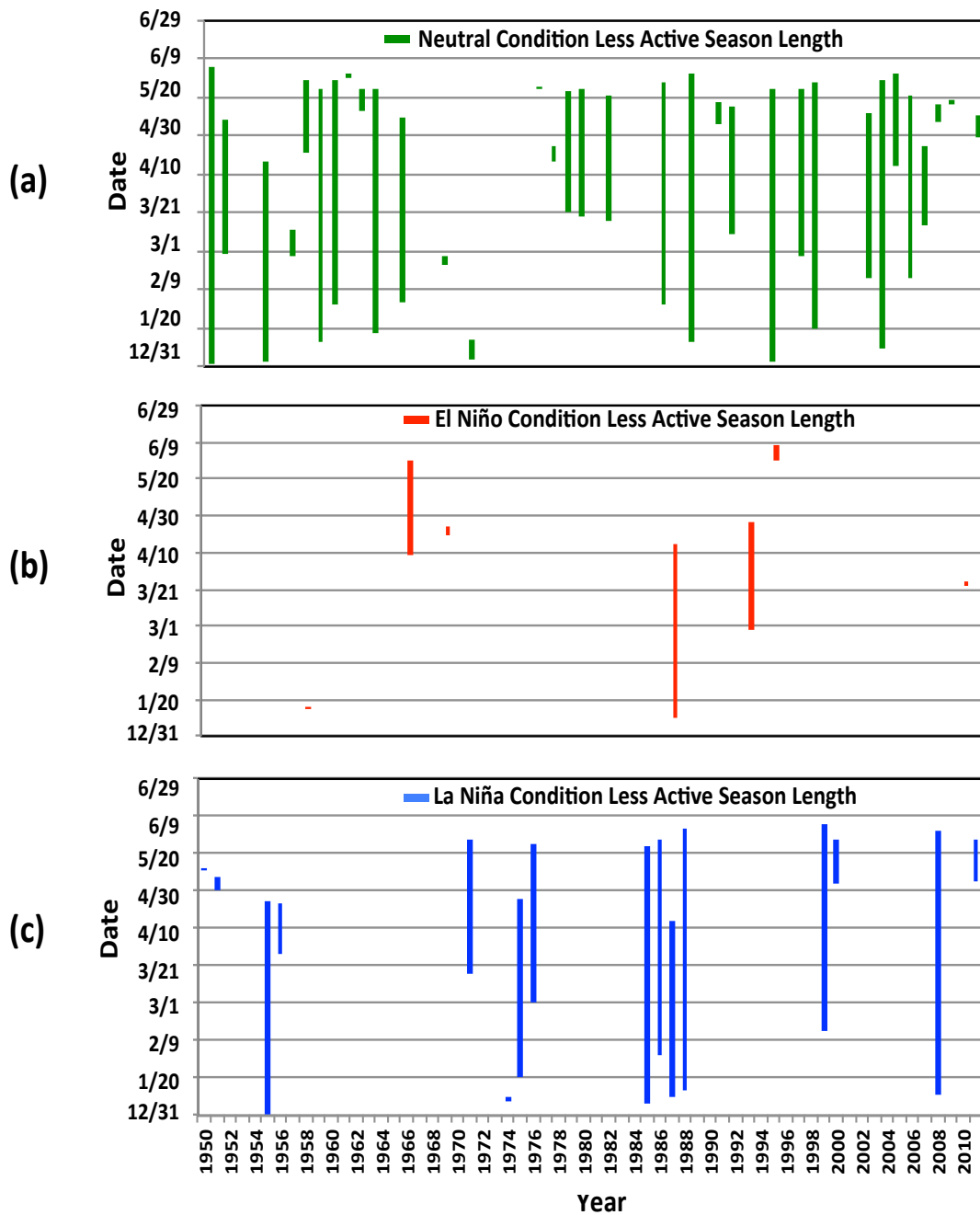


**Fig. 26.** The LAS start and end dates denoted by the lower and upper tip of the bar, respectively during (a) Neutral, (b) El Niño, and (c) La Niña phases of ENSO. The length of the bar also denotes the season length.

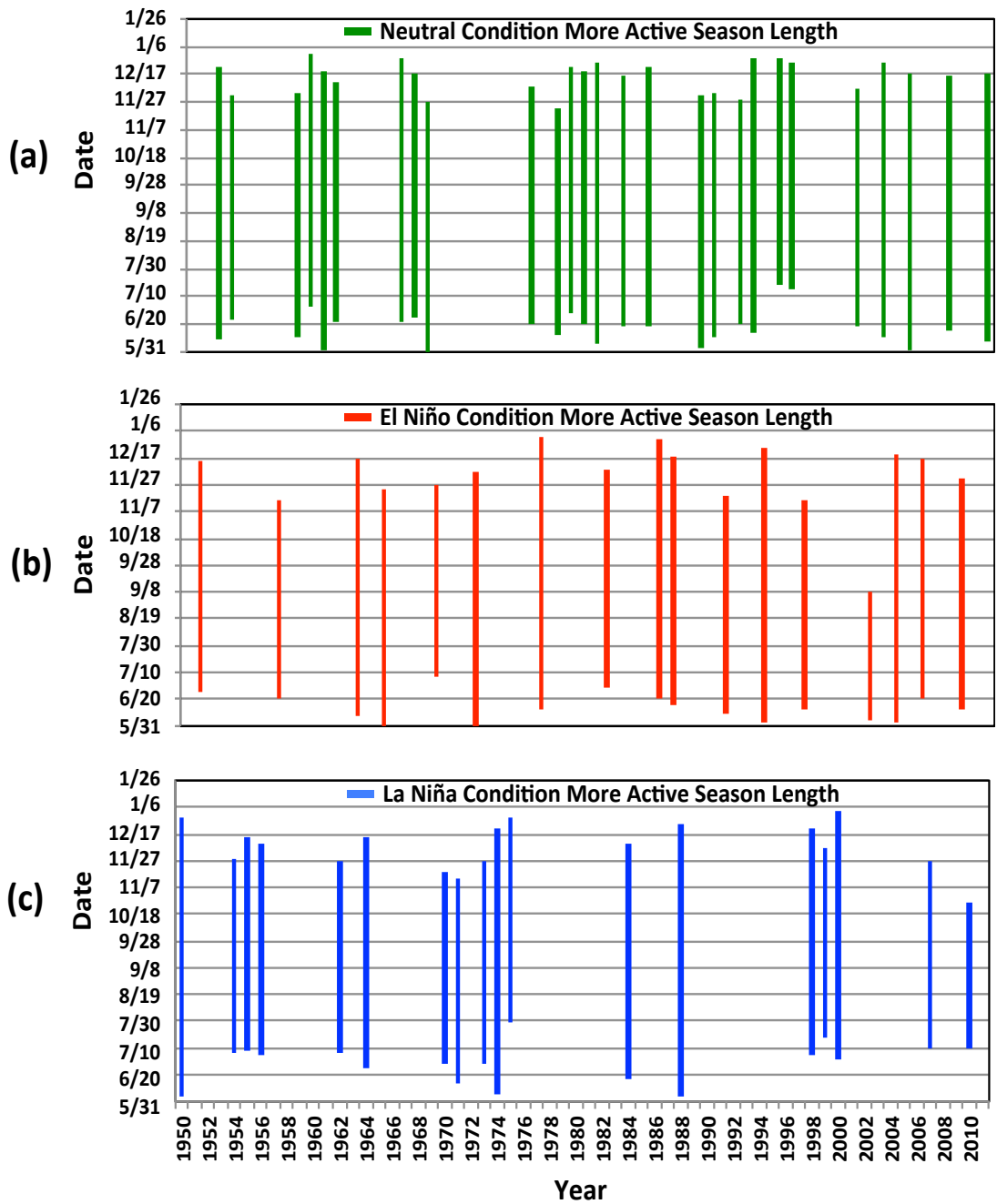


Fig. 27. Same as Fig. 26, but for MAS.

LAS	Neutral	El Niño	La Niña
<b>Start Date:</b>			
Earliest	1/2	1/11	1/2
Latest	5/31	5/31	5/12
Mean	3/6	3/16 (later)	2/24 (earlier)
<b>End Date:</b>			
Earliest	1/15	1/16	1/11
Latest	6/6	6/8	6/6
Mean	5/12	4/17 (much earlier)	5/9 (earlier)
<b>Season Length:</b>			
Minimum	1 day	1 day	1 day
Maximum	155 days	94 days	141 days
Mean	67 days	32 days (shorter)	74 days (longer)

**Table 5.** Comparison of season start and end dates and season length of El Niño and La Niña phases with Neutral phase during LAS.

MAS	Neutral	El Niño	La Niña
<b>Start Date:</b>			
Earliest	6/1	6/1	6/4
Latest	7/19	7/8	7/30
Mean	6/18	6/14 (earlier)	6/30 (later)
<b>End Date:</b>			
Earliest	11/23	9/10	10/28
Latest	1/2	1/3	1/5
Mean	12/16	12/4 (much earlier)	12/8 (earlier)
<b>Season Length:</b>			
Minimum	162 days	96 days	109 days
Maximum	203 days	206 days	209 days
Mean	181 days	173 days (shorter)	162 days (much shorter)

**Table 6.** Same as Table 3, but for MAS.



## **4.5 ENSO Influence on Large-scale Environmental Variables**

The physical mechanisms responsible for the variations in the behavior of Philippine TCs in LAS and MAS between ENSO phases are discussed in this section. Large-scale environmental conditions conducive to the development and intensification of TCs during El Niño and La Niña years differ from those of Neutral years. The climatological settings in which Philippine TCs are formed are quite different during the respective ENSO phases in both the LAS and MAS. The mean variables related to the Philippine TC activity during the specific ENSO phase in LAS and MAS were analyzed which include:

### **4.5.1 SST**

The SST in the WNP differs in both LAS and MAS during various ENSO phases. The SST plays a significant role in accounting for the difference in the seasonal number of TCs in the Philippine domain. The SST and the position of the monsoon trough influence the seasonal distribution of TC genesis location and frequency (McBride 1996).

The WNP is warmest in MAS especially in the June-November period when SST values of 29-30° are usually observed (Vincent and Schrage 1995). The SSTs in MAS are greater than the SSTs in LAS. The region of warmest SSTs in LAS is confined to a narrower region (Fig. 28a-c) while the latitudinal and longitudinal extent of the warmest SST is broader in MAS in all ENSO phases (Fig. 28d-f).

The regions of warmest SSTs occupy a wider longitudinal range in LAS El

Niño years (Fig. 28a). Reverse situations occur in La Niña years of LAS, highest SST values are only found west of date line (Fig. 28b).

In Neutral years of MAS, areas with the highest SST values are observed over the central equatorial Pacific and some patches of warm SSTs occur in the eastern equatorial Pacific (Fig. 28d). Similar SST characteristics are observed in El Niño years of MAS but regions with the highest values of SSTs extend continuously to the eastern equatorial Pacific reaching the Central American coast (Fig. 28f). This observation does not hold true in La Niña years of MAS, where warmest SSTs are only confined in a narrower longitudinal range just east of 160°W (Fig. 28e).

Fig. 29a compares the SST in LAS during Neutral years with El Niño years. Warmer SSTs over the entire WNP and cooler SSTs in the central and eastern equatorial Pacific are observed in Neutral years relative to El Niño years. The SST difference between Neutral and El Niño years in LAS over the WNP is not as big as in MAS (Fig. 29d) but the same trend as that of LAS is also experienced in MAS but much cooler SSTs occur over the central and equatorial Pacific.

Most of the WNP has cooler SSTs but warmer SSTs over the central and eastern equatorial Pacific during Neutral years when compared with La Niña years in LAS (Fig. 29b). The reverse occurs in La Niña years. This is also true in MAS (Fig. 29e). The reversed scenarios of Fig. 29a&b are seen in Fig. 17d&e.

Comparing the SSTs during El Niño and La Niña years of LAS and MAS (Fig. 29c,f), SSTs just east of the Philippines are cooler and SSTs east of 150°-160°E are warmer during El Niño years. On the other hand, the opposite scenario occurs in La Niña years. Fig. 29c and Fig. 29f suggest a southeast-northwest SST difference

between El Niño and La Niña years. Cooler SSTs over the WNP during El Niño years of LAS have caused reduction in the number of TCs in the region, especially in the South China Sea.

The significant change in SST distribution during La Niña years for both the LAS and MAS impacts the location and movement of TCs over the Philippine domain. No TCs formed east of 165°E in LAS and east of 160°E in MAS.

Many authors have concluded that the locations of TC genesis over the WNP tend to shift southeastward during El Niño years (Chen et al. 1998; Chia and Ropelewski 2002; Wang and Chan 2002). This is not the case for Philippine TCs. Relative to Neutral years TC birthplaces are almost the same in El Niño years. The substantial change is observed in La Niña years when there is an absence of TC formation east of 160°-165°E.

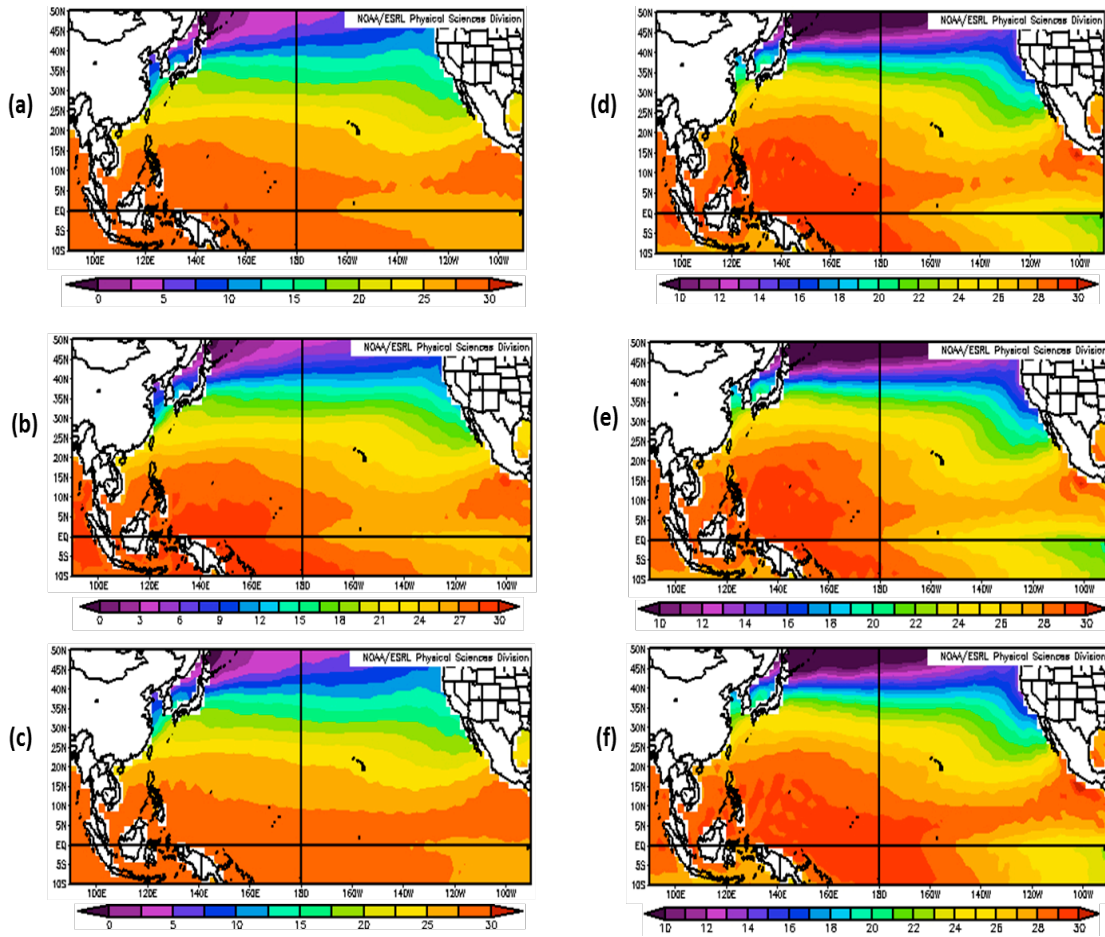


**Fig. 28.** Composite mean of surface SST during (a) LAS Neutral, (b) LAS La Niña, (c) LAS El Niño, (d) MAS Neutral, (e) MAS La Niña, and (f) MAS El Niño.

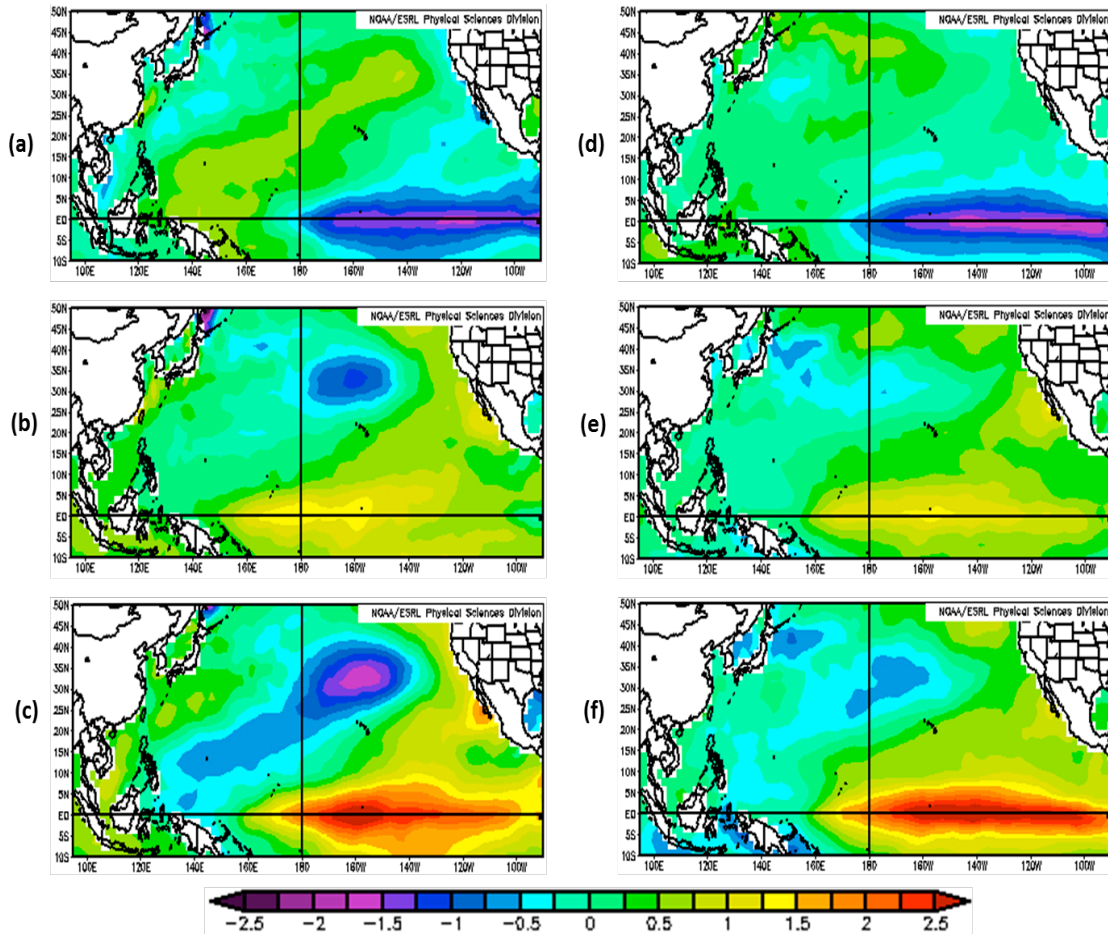


**Fig. 29.** SST differences (a) LAS Neutral minus LAS El Niño, (b) LAS Neutral minus LAS La Niña, (c) LAS El Niño minus LAS La Niña, (d) MAS Neutral minus MAS El Niño, (e) MAS Neutral minus MAS La Niña, and (f) MAS El Niño minus MAS La Niña.

#### 4.5.2 Vorticity

The Southeast Asian monsoon trough is a favorable region of TC genesis and associated with large cyclonic low-level vortices (McBride 1996; Briegel and Frank 1997). Flow intensification on either side of this monsoon trough increases the low-

level vorticity and enhances TC genesis (Frank 1987). The variation in the location and intensity of the monsoon trough impacts the genesis location and frequencies of TCs over the WNP (Lighthill et al. 1994), which can be taken as characteristic of El Niña and La Niña phases (Camargo et al. 2007a). Lyon and Camargo (2008) identified that the changes in Philippine TC activity in terms of the frequency of TCs being formed at a more eastward location and the recurving tracks east of the Philippines are related with the changes in vorticity and moisture flux in the monsoon trough region. In this section, the low-level vorticity has been investigated during various ENSO phases with respect to its influence on the Philippine TC activity.

Fig. 30 shows the low-level vorticity composite mean in LAS and MAS during different ENSO phases. In LAS, the area coverage of positive low-level vorticity values in El Niño years is wider than in Neutral and La Niña years (Fig. 30c). It extends from the lower latitudes of the entire WNP crossing the date line and reaching the western American coast. In La Niña years, the spatial extent of positive low-level vorticity is narrower than that of Neutral and El Niño phases (Fig. 30b). The same situation is observed in MAS although the area coverage of positive low-level vorticity is wider in LAS than in MAS.

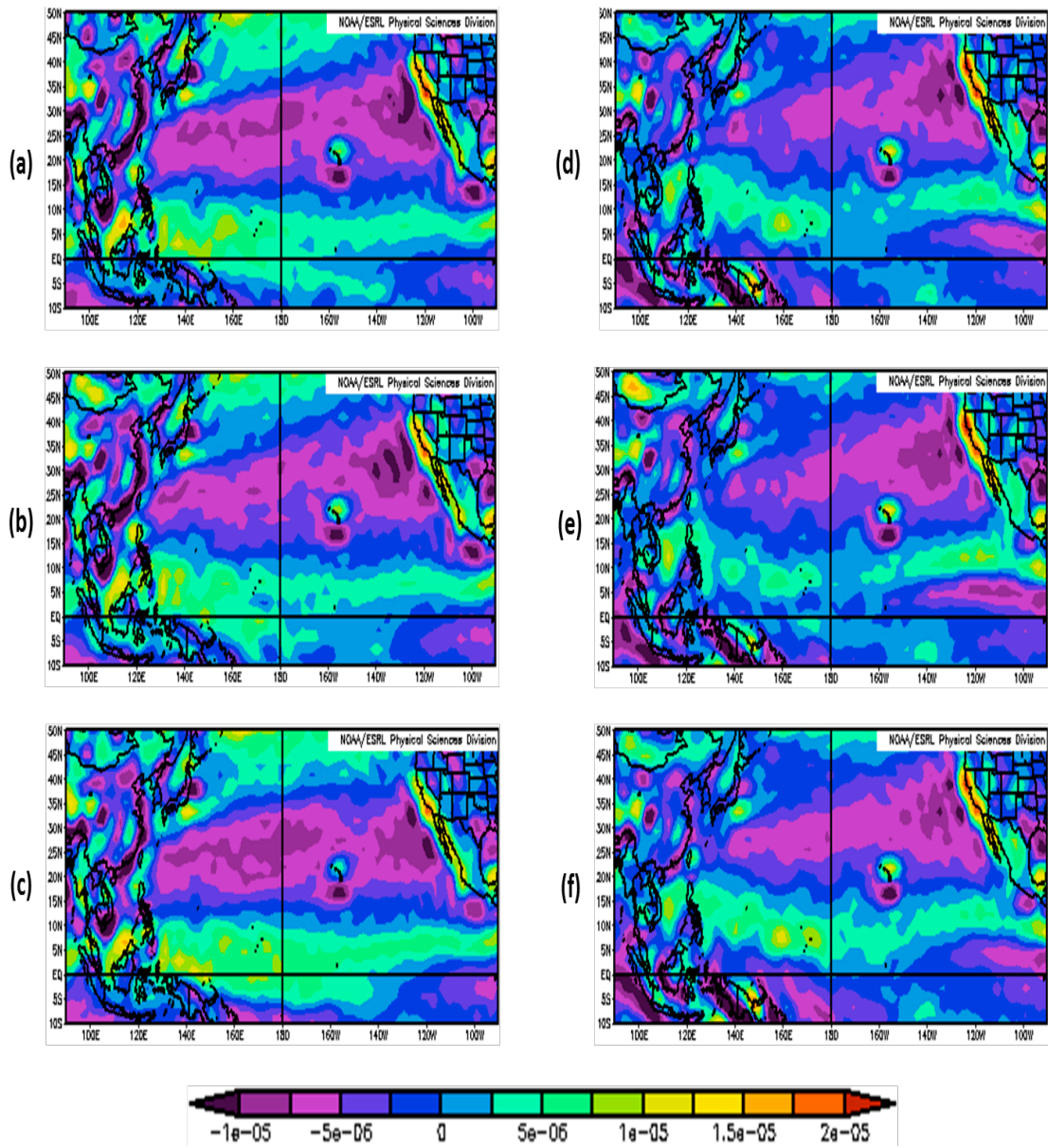


Fig. 30. Same as Fig. 28, but for vorticity at .995 sigma level.

The differences in low-level vorticity values between different ENSO phases are shown in Fig. 31. The low-level vorticity in LAS during Neutral years relative to El Niño years is stronger in the region east of the Philippines while weaker vorticity is

seen from central equatorial Pacific up to about 135°W (Fig. 31a). The vorticity during Neutral years is stronger than in La Niña years in most parts of the northern Pacific (Fig. 31b). Weaker vorticity is experienced in El Niño years compared with La Niña years in the region east of the Philippines while stronger vorticity is observed in central and eastern Pacific with highest positive vorticity in the equatorial Pacific (Fig. 31c). In MAS, vorticity in Neutral years is stronger in small region of WNP relative to El Niño years, while most of the eastern Pacific exhibits stronger vorticity in El Niño years than in Neutral years (Fig. 31d). Neutral years experience higher vorticity values in almost the entire northern Pacific in contrast with La Niña years in MAS but stronger vorticity is prevalent in equatorial WNP west of dateline in La Niña years (Fig. 31e). The vorticity in El Niño years is stronger than in La Niña years in almost all parts of the Northern Pacific but weaker vorticity relative with La Niña years is seen in equatorial WNP (Fig. 31f).

The region that exhibits higher values of vorticity during an individual ENSO phase is consistent with the cyclogenesis locations. TC genesis during La Niña years is closer to the Philippines, just east of the country, where highest vorticity values are also seen in that region. In Neutral and El Niño years, stronger values of vorticity are found to extend eastward where cyclogenesis during these ENSO phases are also prevalent in that region of the WNP.



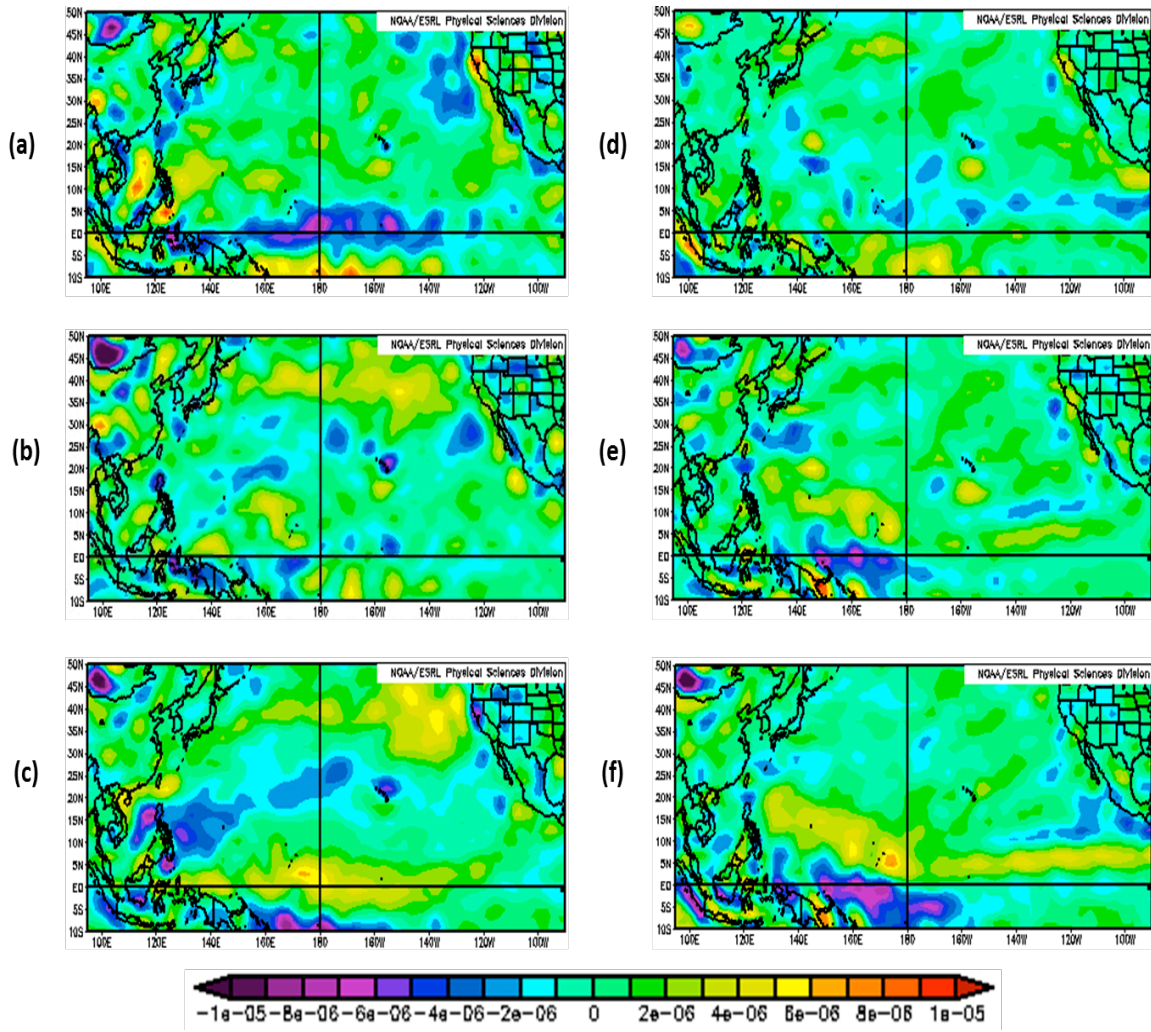
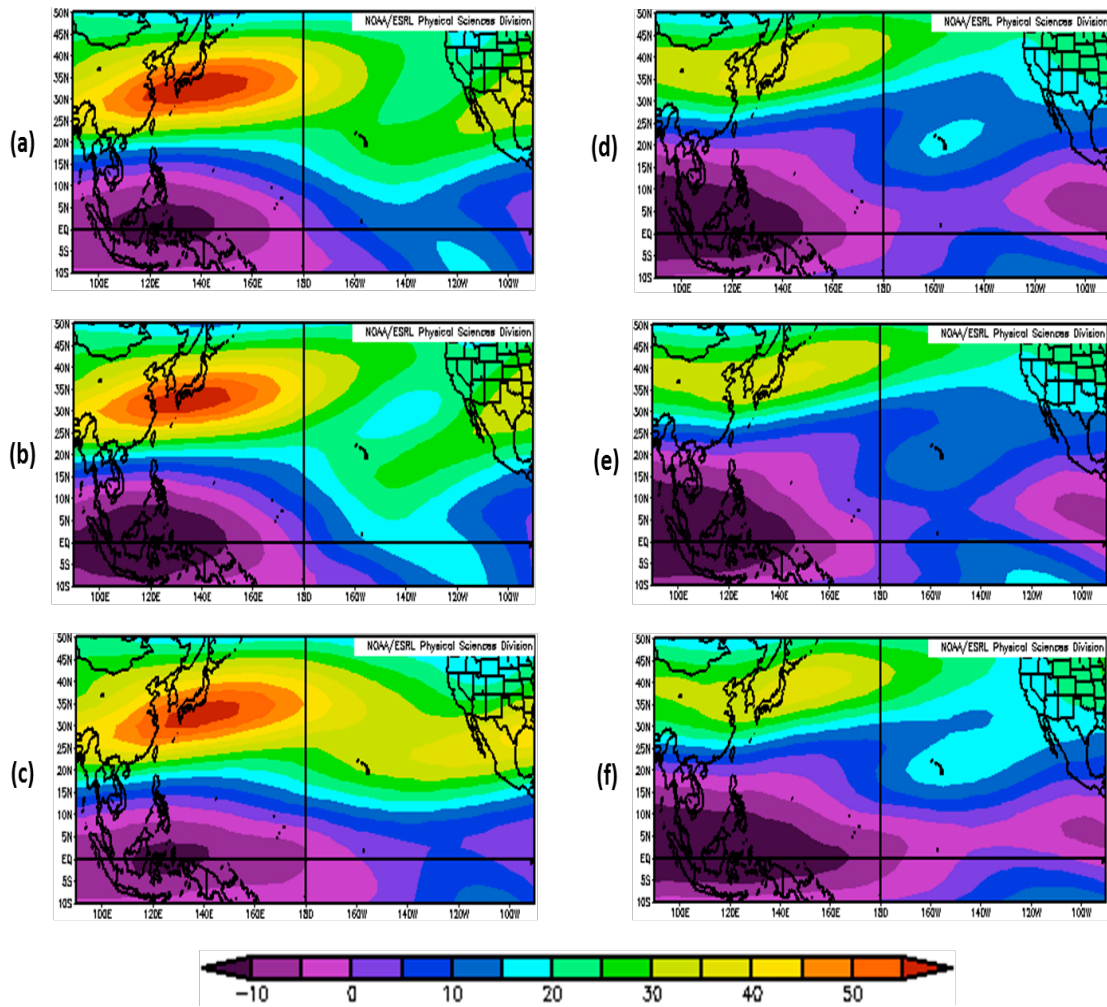


Fig. 31. Same as Fig. 29, but for vorticity differences.

### 4.5.3 Zonal Wind

Zonal vertical wind shear is another important dynamic parameter that controls cyclogenesis and modulates the seasonal TC activity (Gray 1977). Environmental vertical wind shear is the magnitude of the vector difference of winds between the 200 and 850 pressure levels. Cyclogenesis is favored in regions of weak 850-200mb vertical wind shear (Tuleya and Kurihara 1981). With strong vertical shear, the organized deep convection around the TC low-level center is being disrupted that prevents intensification, the TC also loses its upper level outflow channel and the TC quickly dissipates (Gray 1968). This study uses the zonal wind at 200 mb as a proxy for the zonal vertical wind shear.

Fig. 32 shows the zonal wind at 200 mb in various ENSO phases during LAS and MAS. In Fig. 32a-c, we can see that the mean negative 200-mb zonal wind values occupy a wider area in El Niño years than in Neutral and La Niña years, although La Niña phase has a wider region of smallest value of 200-mb zonal winds. How the 200-mb zonal wind behaves in MAS in different ENSO phases is shown in Fig. 32d-f. A much wider section of negative 200-mb zonal winds are observed during MAS compared to the LAS. A substantial reduction in 200-mb zonal wind is demonstrated in MAS. El Niño years in MAS have a broader area of negative 200-mb zonal winds continuously extending up to the Central American coast. The 200-mb zonal wind in La Niña years is very similar to that of Neutral years.



**Fig. 32.** Same as Fig. 28, but for zonal wind at 200 mb.

Fig. 33 shows the difference in composite mean of 200-mb zonal winds between ENSO phases. The difference of 200-mb zonal wind in LAS between Neutral and El Niño years is given in Fig. 33a. In LAS, comparing Neutral years with El Niño years, the 200-mb zonal wind is weaker near the Philippines while stronger in central and eastern equatorial Pacific. The reverse situations occur in El Niño years of LAS. The pattern is generally opposite that of Neutral years minus La Niña years of LAS

(Fig. 33b). Fig. 33c suggests that the 200-mb zonal wind around the vicinity of the Philippines is weaker in La Niña years while a significant increase in central and eastern equatorial Pacific and an opposite scenario in El Niño years. Basically the same trend is observed in MAS except that MAS has a smaller magnitude difference of 200-mb zonal wind between ENSO phases (Fig. 33d-f).

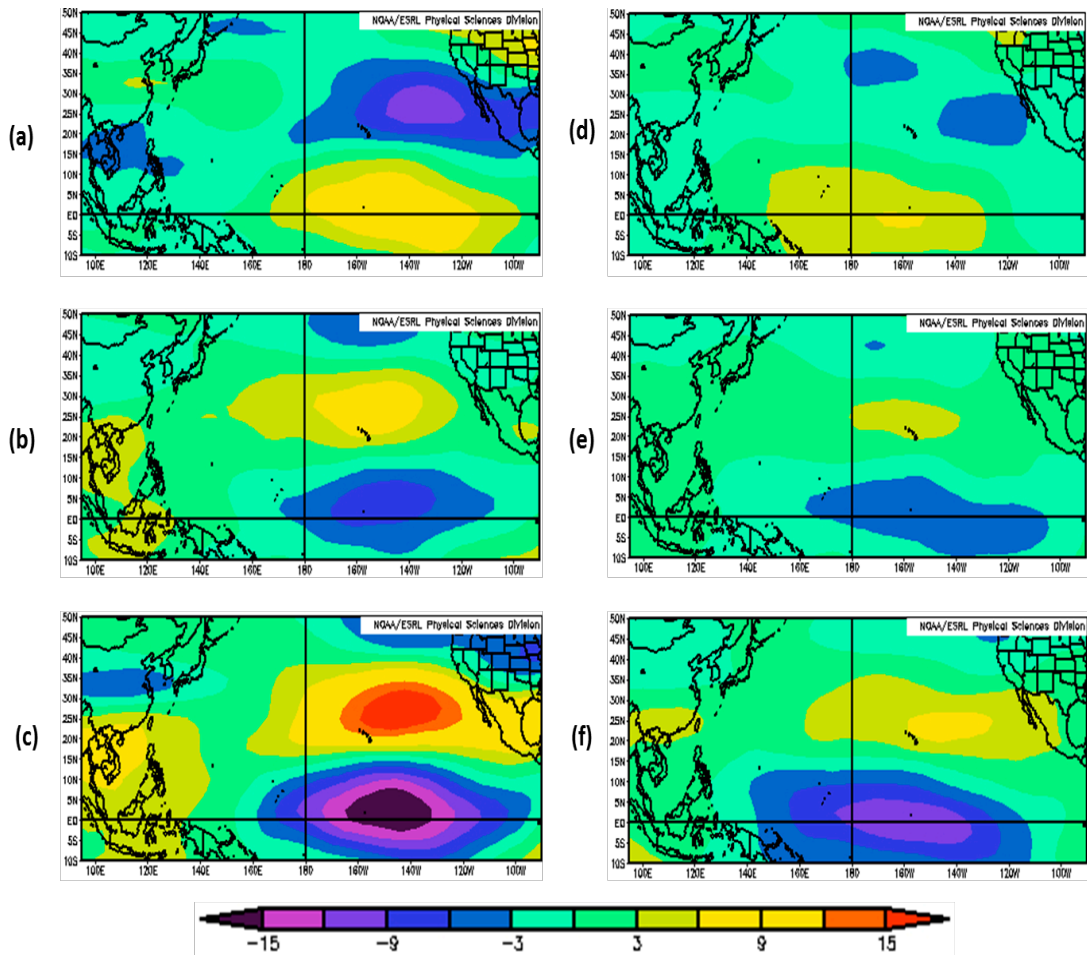


Fig. 33. Same as Fig. 29, but for zonal wind differences.

#### 4.5.4 Divergence

The upper level divergence is associated with low-level convergence or surface low-pressure area development. Surface low-pressure areas require divergence aloft to continue deepening. The development of TCs can be initially traced to divergence aloft which is the ultimate result of heating of the air columns over the warmer ocean surface.

The divergence composite mean at .2101 sigma level during different ENSO phases in LAS and MAS are given in Fig. 34a-f. The area of positive divergence in WNP during LAS in La Niña years resembles that of Neutral years although a narrower region of positive divergence is seen in La Niña years, just west of the dateline (Fig. 34a&b). El Niño years exhibit weaker positive divergence in the WNP (Fig. 34c). Divergence in MAS in all ENSO phases is stronger compared with LAS. Again in MAS, Neutral and La Niña years have similar area patterns of positive divergence (Fig. 34d&e) while El Niño years demonstrate a broader region of positive divergence extending eastward beyond the dateline (Fig. 34f). Neutral and El Niño years have a slightly increased magnitude of divergence than in La Niña years over the WNP in MAS.

The divergence difference between ENSO phases in LAS and MAS is shown in Fig. 35. The Neutral years relative with El Niño years during LAS have higher divergence in the WNP but weaker divergence in central and eastern equatorial Pacific (Fig. 35a). The Neutral years divergence is stronger than in La Niña years in most parts of western and eastern Pacific in LAS (Fig. 35b). Comparing the divergence in LAS during El Niño and La Niña years, higher divergence over the WNP prevails

during La Niña years but stronger divergence over the central and eastern equatorial Pacific in El Niño years of LAS (Fig. 35c).

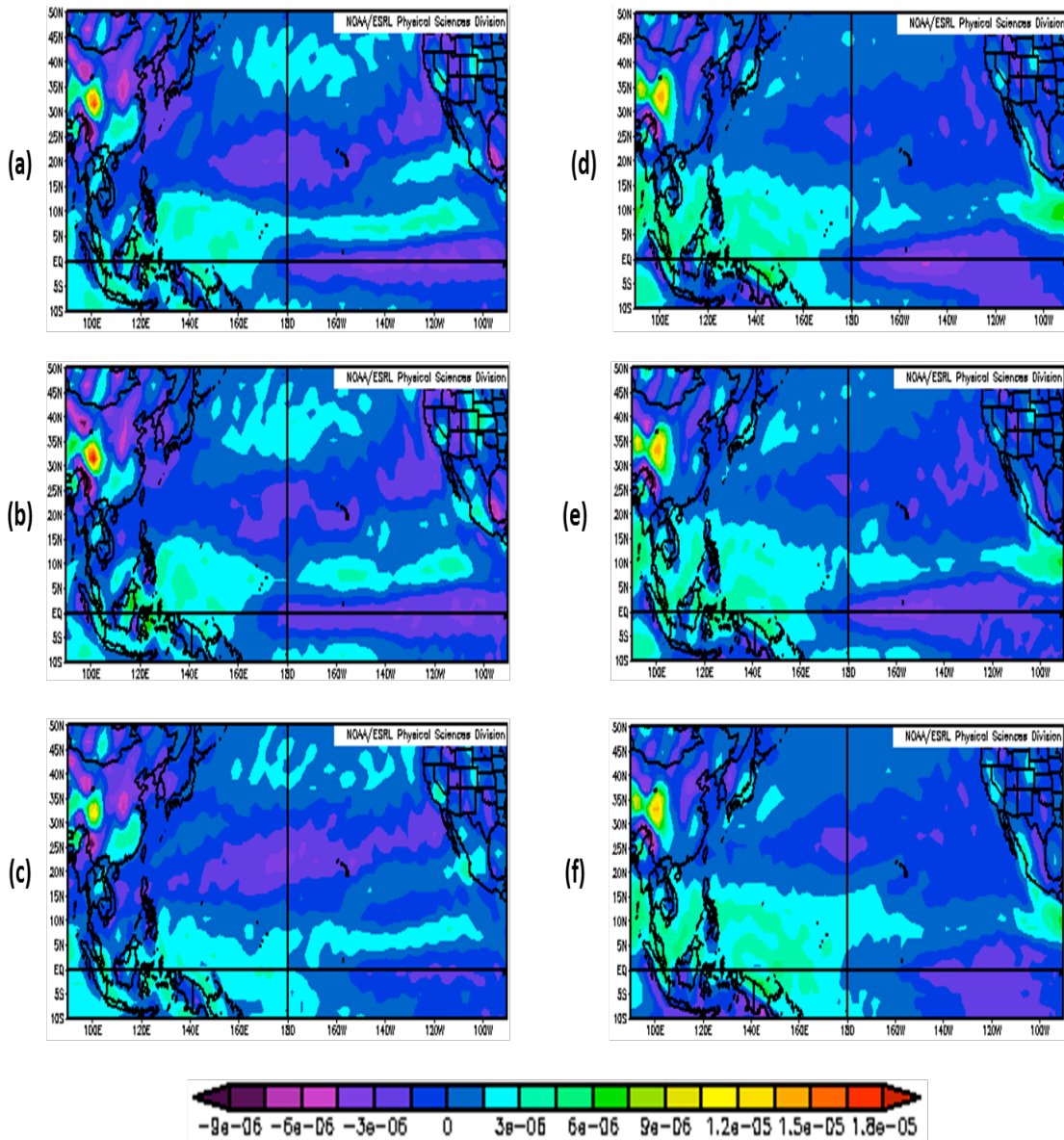


**Fig. 34.** Same as Fig. 28, but for divergence at .2101 sigma level.

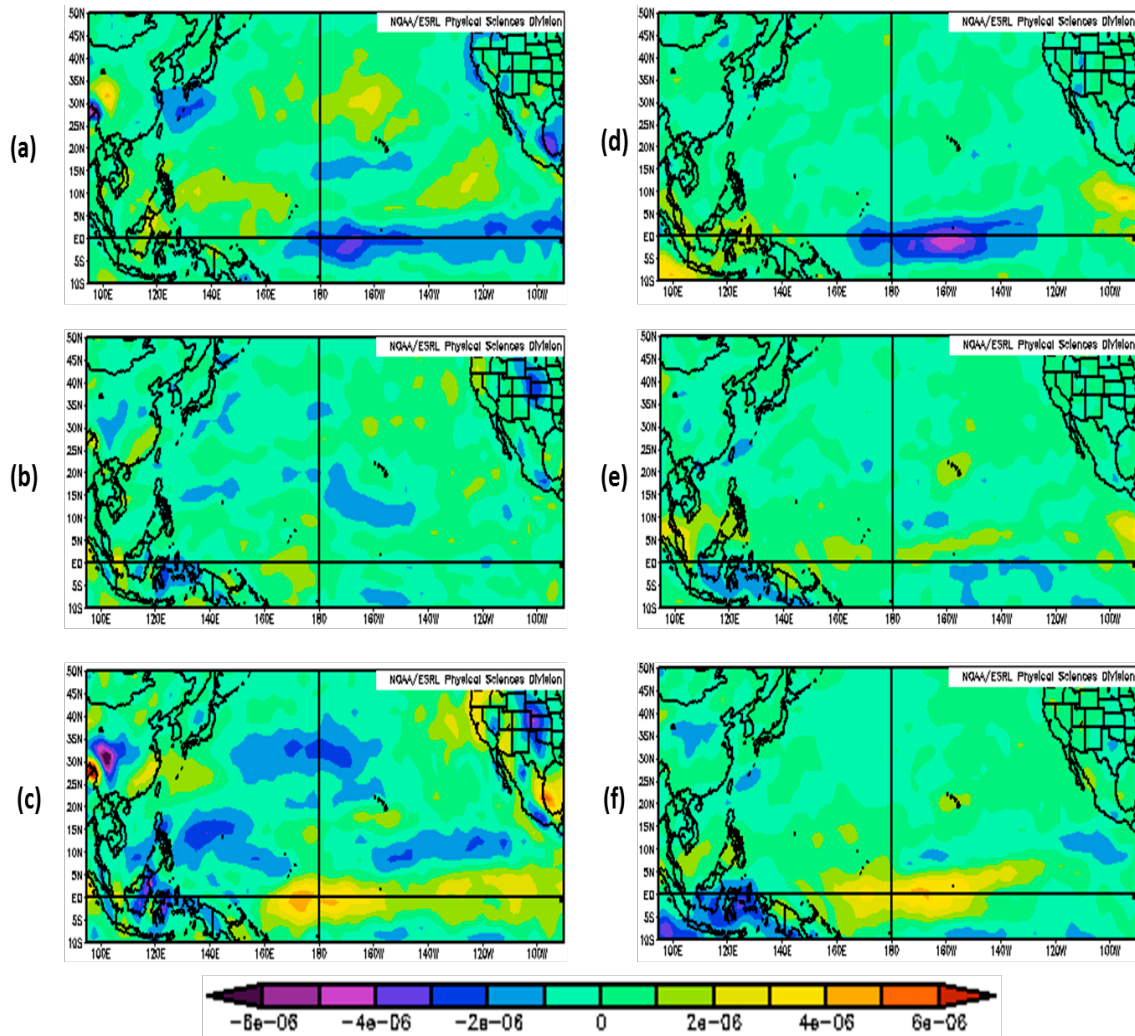


**Fig. 35.** Same as Fig. 29, but for divergence differences.

Fig. 35d-f show the difference in divergence during MAS. The Divergence composite mean is stronger over the WNP in Neutral years and even stronger in magnitude in El Niño years over the central equatorial Pacific (Fig. 35d). Neutral and El Niño years in contrast with La Niña years have stronger divergence in most parts of the Pacific (Fig. 35e&f).

## 4.6 Summary and Conclusions

This section examines the impact of ENSO in the Philippine TC activity. The genesis of TCs is significantly lower in LAS than in MAS. A substantial reduction of TC frequency in LAS occurs in El Niño years and most TCs developed in the lower latitudes and notably only one TC formed over the South China Sea during 1945-2011 period. El Niño years in MAS have occupied a broader region of cyclogenesis, very similar with Neutral years. On the other hand, the majority of TCs in La Niña years formed west of 155°E and occupied a narrower region of formation. For both LAS and MAS, the mean genesis position during El Niño (La Niña) years is displaced to the southeast (northwest). The confinement of cyclogenesis in the southeastern portion of WNP in El Niño years is attributed to the displacement of the Southeast Asian monsoon, being shifted farther east of the Pacific.

Since both Neutral and El Niño phases of ENSO have relatively the same spread and coverage of cyclogenesis positions, they also have similar track characteristics. The tracks types of Neutral and El Niño years are almost identical. Most TCs in LAS in El Niño years traversed the lower latitudes. The TCs with straight-moving tracks in La Niña years are shorter compared with those in Neutral and El Niño years. Additionally, more recurving tracks occur in El Niño years than in La Niña and Neutral years in MAS. The observed change in tracks is consistent and relative with the change in mean genesis location.



During the Neutral phase of ENSO, the first three quarters of the year demonstrated above-average TC frequency whereas that trend is not seen in the last quarter, with below-average TC frequency. Below-average TC frequency is observed all year round during El Niño years. The eastward displacement of the mean cyclogenesis that caused some TCs to decay or dissipate prior to entering the domain and the recurving tracks of some TCs have contributed to the reduced TC frequency in El Niño years. In La Niña years, above-average numbers of TCs and landfall are experienced in AMJ and OND, in contrast, below-average in JFM and JAS for all TCs and landfall frequencies. Gray (1968) suggests that the monthly and seasonal variations in TC activity are related to the monthly and seasonal large-scale circulation deviations from their climatology. The number of landfalling TCs in Neutral years is above-average in the first half of the year while below-average the rest of the year. During El Niño, landfalling TCs are below-average in all seasons except JAS.

Both LAS and MAS have above-average TCs and landfalls in Neutral years whereas an opposite trend is observed in El Niño years. The overall reduction of TC frequency in El Niño years is related to the longitudinal shift of the Walker circulation. Above-average TC number is seen in LAS during La Niña while below-average in MAS. The locations of cyclogenesis being closer to the Philippines have caused above-average number of landfall in La Niña years.

The effect of ENSO on the Philippine TC intensity depends mainly on the seasons, that identifies the specific ENSO phase that is prevalent during a particular intensity category. What was observed by other studies that TCs are more intense in El Niño years and weaker in La Niña years does not hold true with the Philippine TCs.

Intense TCs of TY intensity prevail year round in Neutral years but landfalling TYs are more common in La Niña years except in JFM where El Niño years have above-average landfalling TYs in that particular season. Examining the impacts by season substantiates this, as ENSO does not prevail the entire calendar year.

In LAS, there are more TCs in La Niña years than in El Niño years leading to a larger number of TC days. The shift in number of TC days with ENSO in LAS is because of more (fewer) TCs occur in La Niña (El Niño) years while in MAS is due to TCs shorter (longer) lifetime in La Niña (El Niño) years. The cyclogenesis found farther east in El Niño years allow TCs to maintain a longer duration while tracking westward, thus increased numbers of TC days.

The standardized mean of LAS ACE suggests that during El Niño (La Niña) phase, the LAS ACE values are shifted toward below (above) average. The below-average ACE in LAS El Niño is mainly due to the weaker intensity and lesser number of TCs in an El Niño year as there are years when no TCs have occurred in the Philippine domain and if there are, intensities are below 35 knots. An opposite scenario is observed in MAS. The standardized mean of MAS ACE implies that in El Niño (La Niña) phases, the MAS ACE tends to be above (below) average. There are lower numbers of TCs in MAS El Niño phase compared with Neutral and La Niña phases. The higher MAS ACE in El Niño years is mainly due to longer lifetime of individual TCs.

In Neutral years, the mean start date of LAS is March 6 and June 18 for MAS. Relative to Neutral years, the mean start date of LAS during El Niño years is later, and earlier in La Niña years. An opposite trend is seen in MAS start dates. El Niño years

have earlier start dates and La Niña years have a later ones. The LAS in Neutral years on average ends on May 12 while MAS normally ends on December 16. Compared with Neutral years, the mean LAS end date is earlier in La Niña years and much earlier in El Niño years. The same scenario is observed in MAS.

The average LAS length in Neutral years is 67 days and 181 days for MAS. In El Niño, both LAS and MAS have shorter season length compared with Neutral years. This is not the tendency in La Niña years where LAS length is longer and the season length is much shorter in MAS.

The changes in the physical properties of Philippine TC activity during ENSO phases can be explained by examining the large-scale environmental factors associated with TC development and intensification.

The large-scale parameters discussed above are consistent with their trend in individual ENSO phases during LAS and MAS. A broader area of increased magnitude is observed in MAS. Neutral and El Niño years have a more confined area of stronger magnitude in LAS but have been seen to extend more eastward passing the dateline and even reaching the Central American coast in MAS. El Niño years have seen to have an increased magnitude in all large-scale parameters in central and eastern equatorial Pacific. These situations result in more TCs forming in the southeastern region of the WNP in Neutral and El Niño years both in LAS and MAS.

A narrower region of stronger magnitude is seen in La Niña years both in LAS and MAS, mostly just confined west of the dateline. All the parameters are found to have an increased magnitude just east of the Philippines in La Niña years. This trend explains why during La Niña years in both LAS and MAS the locations of

cyclogenesis are usually found closer to the Philippines compared with Neutral and El Niño years. Chan (2005) mentioned that when La Niña event has fully developed, easterly anomalies near the dateline reduce the cyclonic shear that makes the conditions in the southeastern region of the WNP become unfavorable to cyclogenesis thus TCs can only form further west of the dateline. At the same time, the subtropical high tends to be enhanced that caused a northward displacement of the monsoon trough. As a result, more TCs form in the northwestward quadrant of WNP.

The studies of Gray (1968, 1979, 1985) and Briegel and Frank (1997) summarized that the monsoon trough provides an environment that satisfies all of the criteria for cyclogenesis. The changes in the atmospheric circulation associated with ENSO causes a shift in the location of the monsoon trough and a change in the location and intensity of the subtropical high, which then modify the TC formation locations, intensity and movement (Pao et al. 2004).

While ENSO seems to affect the Philippine TC activity especially in the locations of cyclogenesis during La Niña events, the entire variability in the Philippine TC activity cannot be solely attributed to ENSO. There are other factors, that need to be identified and examined, that also affect the behavior of Philippine TCs. The impacts of ENSO on Philippine TC activity are summarized in Table 7.

Characteristic	LAS El Niño	LAS La Niña	MAS El Niño	MAS La Niña
TC Mean	Below Average	<b>Above Average</b>	Below Average	<b>Below Average</b>
Landfall Mean	Below Average	<b>Above Average</b>	Below Average	<b>Above Average</b>
TC Days	Below Average	<b>Above Average</b>	Above Average	<b>Below Average</b>
ACE	Below Average	<b>Above Average</b>	Above Average	<b>Below Average</b>
Mean Season Start Date	Later	<b>Earlier</b>	Earlier	<b>Later</b>
Mean Season End Date	Much earlier	<b>Earlier</b>	Much Earlier	<b>Earlier</b>
Mean Season Length	Shorter	<b>Longer</b>	Shorter	<b>Much Shorter</b>
Quiescent Periods	Longer	<b>Shorter</b>	Shorter	<b>Longer</b>
Mean Genesis Location	Displacement to the Southeast	<b>Displacement to the Northwest</b>	Displacement to the Southeast	<b>Displacement to the Northwest</b>
Tract Type	Tracks identical to Neutral years  Most TCs in lower latitudes	<b>Shorter tracks</b>	Tracks identical to Neutral years	<b>Shorter tracks</b>

**Table 7.** Summary of ENSO impacts on Philippine TC activity.

## Chapter 5

### Cluster Analysis of Philippine Tropical Cyclones

#### 5.1 Introduction

Several recent studies used numerical clustering to classify TC tracks into a number of patterns over various ocean basins. Elsner and Liu (2003) used the tropical cyclone track data for the entire WNP and showed that K-means clustering (MacQueen 1967) could be applied to TCs using the positions at maximum and final hurricane intensities. The same method was applied to North Atlantic TCs (Elsner 2003) and  $k$  that refers to the *a priori* specification of the number of clusters was set to a value of three. Blender et al. (1997) also used K-means cluster analysis to extratropical cyclone tracks in the North Atlantic. However, K-means method cannot accommodate tracks of different lengths. In order to overcome this limitation, the probabilistic clustering technique based on a mixture of polynomial regression models (Gaffney 2004) was employed. The regression Finite-Mixture Model (FMM) is described in detail in Gaffney et al. (2007) and was applied to Atlantic extratropical cyclones to fit the geographical “shape” of the trajectories. Track patterns classified using this model exhibit the various TC characteristics and the physical relationship with large-scale environments. The model has been applied to TC tracks in WNP (Camargo et al. 2007b,c), eastern North Pacific (Camargo et al. 2008), Fiji (Chand and Walsh 2009, 2010), Southern Hemisphere (Ramsay et al. 2011) and North Atlantic (Kossin et al. 2010). The study of Kossin et al. (2010) recognized four as the optimum

number of clusters. Zhang et al. (2012) applied an FMM-based clustering algorithm to cluster post-landfall tracks of TCs making landfall over China that revealed three clusters. A probabilistic clustering method based on regression mixture models has been applied to group TCs over southwestern Indian Ocean resulting in track shape groups (Ash and Matyas 2012). Unlike K-means, the regression mixture model allows clustering of TC tracks with varying shapes and lengths. Nakamura et al. (2009) resolved the issue by using the first and second moments of TC tracks to approximate the shape and lengths of tracks. The mass moments were then applied to K-means that demonstrated reliable clustering results for the North Atlantic tropical cyclone tracks, producing an optimum of six clusters.

The Fuzzy c-means is another cluster method applied to tropical cyclone tracks of Korean peninsula landfalling TCs (Choi et al. 2008) that shown four optimal clusters. Kim et al. (2011) also used the same method to the TCs over the WNP and identified seven clusters as the favorable number. Unlike K-means clustering that produce direct partitions; the Fuzzy c-means cluster technique does not immediately assign a data object to a cluster but preserving the ambiguity of the data. The method has been known to produce more natural classification results. In 1995, Harr and Elsberry used fuzzy cluster analysis and empirical orthogonal functions to identify recurrent large-scale circulation patterns associated with TC characteristics. Tracks were classified into four types, straight-mover, recurve-south, recurve-north, and South China Sea, and tracks not fitting into these four types were discarded.

Elsner et al. (2000) performed K-means clustering on the North Atlantic TC locations at 85 knots. The clustering yielded six dissipation clusters that show where the hurricane was last at an intensity of 85 knots. Colbert and Soden (2012) focus on TCs that formed in the main development region (MDR) of the North Atlantic basin. The classification method used to classify the track types is based on defined threat regions that yield similar results as that of Nakamura et al (2009) and Kossin et al. (2010). Six clusters were identified in this study. McCloskey et al. (2013) used K-means clustering techniques to group TC tracks into coherent clusters and analyzed in regards to NAO, AMM, ENSO and MJO.

Given that most of the previous studies have ventured on the cluster analysis of TCs over western and eastern North Pacific and North Atlantic, no attempts have been made to classify attributes of Philippine TCs. Here, K-means method has been used to analyze not only the TC tracks but also the genesis and decay locations. Major difference in clustering the tracks lies in the track being represented by single point based on average position of genesis, maximum intensity and decay. All the TCs included in the Philippine domain dataset were used in the study, a total of 1,161 TCs during the period 1950-2012.

This study has great importance due to its capabilities in unraveling the hidden useful information and patterns of the Philippine TCs. The specific goals of this study are (1) to examine the spatial and temporal behavior of TCs by looking at monthly patterns of genesis and decay locations and tracks, and (2) identify the seasonal cycle of each cluster.



## 5.2 Methodology

Information on the location, maximum winds and central pressure is obtained every six hours from JTWC best-track data. This study focuses on TCs that existed over the Philippine domain and data from 1950-2011 were used to apply cluster analysis on the locations of TC genesis and decay and on the TC tracks. The latitude-longitude of the TCs considered is inside the domain during at least part of their lifetimes. All TCs regardless of intensity classification (e.g., TD, TS, and TY) are included in the cluster analysis, allowing a larger sample and more thorough statistical results.

To interpret clustering results, composite analyses of SST were performed using the monthly NOAA ERSST V3 product (Smith et al. 2008). Vorticity, SLP and RH composites were plotted using the NCEP-NCAR reanalysis fields (Kalnay et al. 1996).

In clustering the genesis locations, two variables are used, the latitude and longitude. The genesis location is defined as the first reported location of the TC. Similarly, in classifying the decay locations, the latitude and longitude of the decay point were employed. Decay location is defined as the last reported position of the TC. Each TC track is represented by the average location of TC genesis, maximum intensity, and decay. The latitude and longitude of the average location are the variables used to cluster the tracks, thus a single point represents a single TC track.

### 5.2.1 K-means Cluster Algorithm

Cluster analysis is a convenient method for identifying homogenous groups of objects called clusters. Objects or observations in a specific cluster share many characteristics, but are dissimilar to objects not belonging to that cluster. There are a number of techniques available for clustering but in this study, the K-means (MacQueen 1967) cluster algorithm is used to obtain and describe classification of TC genesis locations, tracks, and decay locations.

K-means cluster algorithm is one of the most popular and widely used clustering techniques. It is a simple method that follows a partitioning procedure. This algorithm is not based on distance measures from one observation to another observation, but uses the within-cluster variation as a measure to form homogenous clusters. For a given number,  $k$ , of clusters, this method minimizes the sum,  $S$ , of the squared distances within the clusters. Specifically, the procedure aims at segmenting the data in such a way that the within-cluster variation is minimized. The objective function  $S$  is defined as:

$$S = \sum_{j=1}^K \sum_{n \in S_j} |X_n - \mu_j|^2$$

where  $|x_n - \mu_j|^2$  is a chosen distance measure between a data point  $x_n$  and the cluster center  $\mu_j$ , is an indicator of the distance of the  $n$  data points from their respective cluster centers.

The clustering process starts by randomly assigning objects to a number of clusters  $k$ , where  $k$  is a user pre-specified parameter, also corresponds to the number of centroids. The objects are then successively reassigned to other clusters to minimize

the within-cluster variations, which is basically the distance from each observation to the center of associated cluster. If the reallocation of an object to another cluster decreases the within-cluster variation, this object is reassigned to that cluster. The process is repeated until no change at all in cluster membership.

K-means provides a mathematically transparent and simple algorithm, the primary reason why this method was chosen. It has many advantages over other methods. The computational space requirements for K-means are modest because only the data points and centroids are stored. In particular, the time requirements are basically linear in the number of data points. With K-means, cluster affiliation can change in the course of the clustering process. Consequently, K-means does not build a hierarchy, that is why the approach is also labeled as non-hierarchical. Generally, K-means is superior to other clustering methods as it is, first, less affected by outliers and the presence of irrelevant clustering variables and second, by making the multiple passes through the data, the final solution optimizes within-homogeneity and between-clusters heterogeneity. Furthermore, K-means can be applied to very large data set, as the procedure is less computationally demanding (Aldenderfer and Blashfield 1984; Hair et al. 1992).

One problem associated with the application of K-means relates to the fact that one has to pre-specify the number of clusters  $k$  to retain from the data. This makes K-means less attractive to some and hinders its routine application in practice. A solution advocated by many experts is to apply a single linkage procedure to determine the number of clusters and K-means afterwards (Hair et al. 1992; Milligan 1980; Punji and Stewart 1983). Researchers have shown that this procedure increases validity of

solutions (Milligan 1980; Punji and Stewart 1983). The only cost is the extra time and effort required on the researchers' part, a cost worth bearing.

The MATLAB statistical toolbox containing functions for K-means clustering was used to perform cluster analyses on 1161 TCs.

In an attempt to exhaust the optimal number of clusters  $k$  in K-means, the pre-determined value for  $k$  was sequentially set to 3, 4, 5, 6, and 7 as candidates for the number of clusters to see how much the cluster membership differ from one cluster to another cluster as the number of clusters increases. The corresponding mean silhouette coefficient value for different values of  $k$  has also been considered.

## **5.2.2 Determining the Number of Clusters**

Two of the most difficult tasks in cluster analysis are deciding on the appropriate number of clusters and deciding how to tell a bad cluster from a good one. The K-means clustering result depends mainly on the appropriate choice of cluster number that should be given in advance before carrying out the cluster algorithm process. In this study, the cluster number is determined objectively by the mean silhouette coefficient value and total sum of point-to-centroid distances, and subjectively, by looking at the meteorological and oceanic variables in deciding for the number of genesis clusters.

### **5.2.2.1 Silhouette Coefficient**

Kaufman and Rousseeuw (1990) define a set of values called silhouettes that provide a graphical aid to the interpretation and validation of clusters of data. The silhouette is a measure of how cohesive each cluster is and how well the clusters are separated. It is also a gauge of the clustering solution's overall goodness-of-fit. The silhouette coefficient values can be used to compare the clustering solutions quantitatively. It is based on the average distance between the objects and can vary between -1 to +1. For each datum  $i$ , let  $a(i)$  be the average dissimilarity of  $i$  with all other data within the same cluster. Any measure of dissimilarity can be used but distance measures are the most common.  $a(i)$  is interpreted as how well  $i$  is assigned to its cluster (the smaller the value, the better the assignment). The average dissimilarity

of point  $i$  to a cluster  $c$  is defined as the average of the distance from  $i$  to points in  $c$ . Let  $b(i)$  be the lowest average dissimilarity of  $i$  to any other cluster, which  $i$  is not a member. The cluster with this lowest average dissimilarity is said to be the "neighboring cluster" of  $i$  because it is the next best fit cluster for point  $i$ . For  $i$  total points, a silhouette  $s(i)$  is defined as,

$$s(i) = \frac{b(i) - a(i)}{\max\{a(i), b(i)\}}$$

which can be written as:

$$s(i) = \begin{cases} 1 - a(i) / b(i), & \text{if } a(i) < b(i) \\ 0, & \text{if } a(i) = b(i) \\ b(i) / a(i) - 1 & \text{if } a(i) > b(i) \end{cases}$$

From the above definition it is clear that

$$-1 \leq s(i) \leq 1$$

For  $s(i)$  to be close to 1 we require  $a(i) \ll b(i)$ . As  $a(i)$  is a measure of how dissimilar  $i$  is to its own cluster, a small value means it is well matched. Furthermore, a large  $b(i)$  implies that  $i$  is badly matched to its neighboring cluster. Thus an  $s(i)$  close to one means that the datum is appropriately clustered. If  $s(i)$  is close to negative one, then by the same logic we see that  $i$  would be more appropriate if it was clustered in its neighboring cluster. An  $s(i)$  near zero means that the datum is on the border of two natural clusters. The average  $s(i)$  over all data of a cluster is a measure of how tightly

grouped all the data in the cluster are. Thus, the average  $s(i)$  over all data of the entire dataset is a measure of how appropriately the data has been clustered. Specifically, a silhouette value of less than 0.20 indicates a poor solution quality; a value between 0.20 and 0.50 indicates a fair solution, whereas values of more than 0.50 indicate a good solution.

The initial application of K-means clustering to TC genesis locations, tracks and decay locations, has produced negative silhouette coefficient values. To improve the cluster cohesiveness, several rounds of clustering were performed. For each clustering process, the TCs that produced negative silhouette coefficient values are removed from the dataset, until such time that negative silhouette values are completely eradicated. The process has reduced the number of TCs to 1,109, 1,128, and 1,108 for genesis, decay, and track datasets, respectively. Another useful summary statistic is the average silhouette value across all objects. This summarizes how well the current configuration fits the data. An easy way to select the appropriate number of clusters is to choose that number of clusters which maximizes the average silhouette. The sum of silhouette values and average silhouette value are presented in Table 8.

The graphs of silhouette coefficient values after applying the K-means clustering to TC genesis locations, decay locations and tracks are presented in Fig. 36.

	Genesis, $k=4$	Decay, $k=5$	Tracks, $k=6$
Sum of Positive Silhouette Value	676.0	680.6	625.5
Mean of Positive Silhouette Value	0.61	0.61	0.56
Total Sum of Point-to-Centroid Distances	40077.8	62150.1	25438.0

**Table 8.** Silhouette coefficients and total sum of point-to-centroid distances.

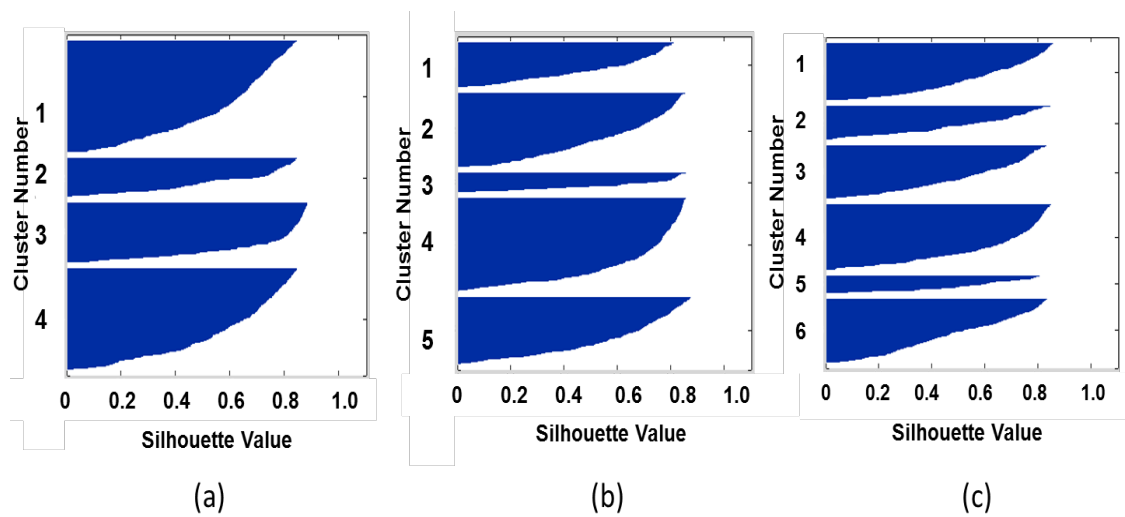


**Fig. 36.** Silhouette graphs for (a) genesis, (b) track, and (c) decay clusters.



### **5.2.2.2 Total Sum of Point-to-Centroid Distances**

One of the steps in K-means algorithm is taking each data point and calculates the Euclidean distance between it and every cluster centroid. At each iteration, the K-means technique reassigns points among clusters to decrease the sum of point-to-centroid distances, and then recomputes cluster centroids for the new cluster assignments. The total sum of distances and the number of reassignments decrease at each iteration until the algorithm reaches a minimum. When there are no more changes in cluster membership or until the centroids do not change, the total sum of the point-to-centroid distances is used in comparing the solutions. Normally, the solution with the lowest total sum of distances is chosen. Table 8 presents the total sum of point-to-centroid distances for each cluster of genesis, track, and decay.

### **5.2.2.3 Oceanic and Meteorological Variables**

There is no objectively incorrect cluster method. But as it was noted, clustering is in the eye of the beholder. In grouping the TC genesis locations, decay locations and tracks, it is important to understand the large-scale environmental conditions that affect them. Perrone and Lowe (1986) linked various thermodynamic and dynamic parameters to tropical cyclone genesis. To help decide the most appropriate number of clusters, the results are interpreted and justified from the meteorological and oceanic perspective. The large-scale environmental variables related to TC development and growth are examined including SST, vorticity, SLP, and RH.

The NCEP/NCAR reanalysis of SST climatology is given in Fig. 37a. Warm SSTs are necessary for TC initiation and development. TC formation requires a sea surface temperature of at least 26.5°C (Gray 1993; Wendland 1977; Emmanuel 1999). TC movement and tracks are largely influenced by large-scale circulation parameters such as vorticity (Wu and Wang 2004; Holland 1995), SLP (Wu and Emmanuel 1993; Wang and Holland 1996; Corbosiero and Molinari 2003) and RH (Carlson 1971). The composites of these parameters are provided in Fig. 37(b-d). TC tracks are also influenced by the steering flow (Chan 1985, 2005; Holland 1983, 1993). The interaction between the steering flow and TC dynamics was also investigated but the constructed composites are not shown.

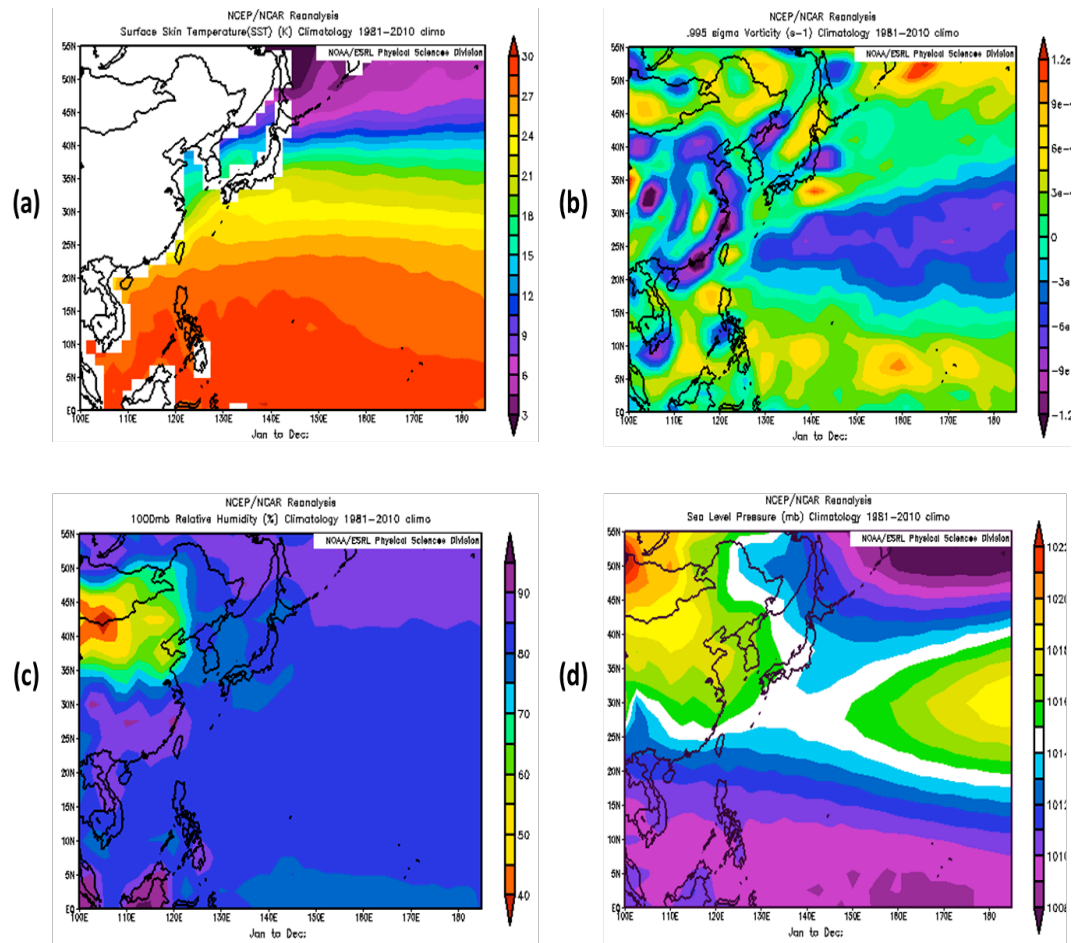


**Fig. 37.** Key variables conducive to TC development and were used to subjectively decide on the most appropriate number of clusters. (a) SST, (b) vorticity, (c) relative humidity (RH), and (d) sea level pressure (SLP).

## 5.3 Results

This section separately describes the clusters produced after employing the K-means to Philippine TCs and discusses the seasonality and the monthly spatial and temporal distribution of each cluster.

### 5.3.1 The Optimal Cluster Number

The most appropriate number of clusters is determined using silhouette coefficients and the total sum of point-to-cluster distances as an objective measures, while the meteorological reasons serve as subjective measures. The final selection of the number of clusters  $k$  is then made based on the relationship between the clusters and the large-scale environmental variables especially in the genesis clustering.

K-means cluster analysis of the TC genesis led to a classification of four distinctly different groups. The sum of silhouette values equals to 676.03 and the mean silhouette value is 0.6096. The composites of large-scale fields also support the choice of four. The meteorological features of one TC region are different from the other so settling for a fewer number of clusters would mean generalizing the TC region of genesis and losing the distinct characteristics of other genesis regions. Clustering of TC decay locations demonstrated five optimum number of clusters. The sum of silhouette values is 680.57 with 0.6126 as the mean silhouette value. Track clustering yielded six as the best possible number of clusters. The silhouette coefficient values for tracks clustering also give acceptable values, 625.49 for the sum of silhouette values and 0.56 for the mean silhouette value. All the silhouette values indicate good

solutions. Fig. 38 presents the optimal number of clusters for genesis locations, decay locations and tracks. The various clusters generated differ in the physical and geometrical properties of their TCs as shown by the geographical positions.

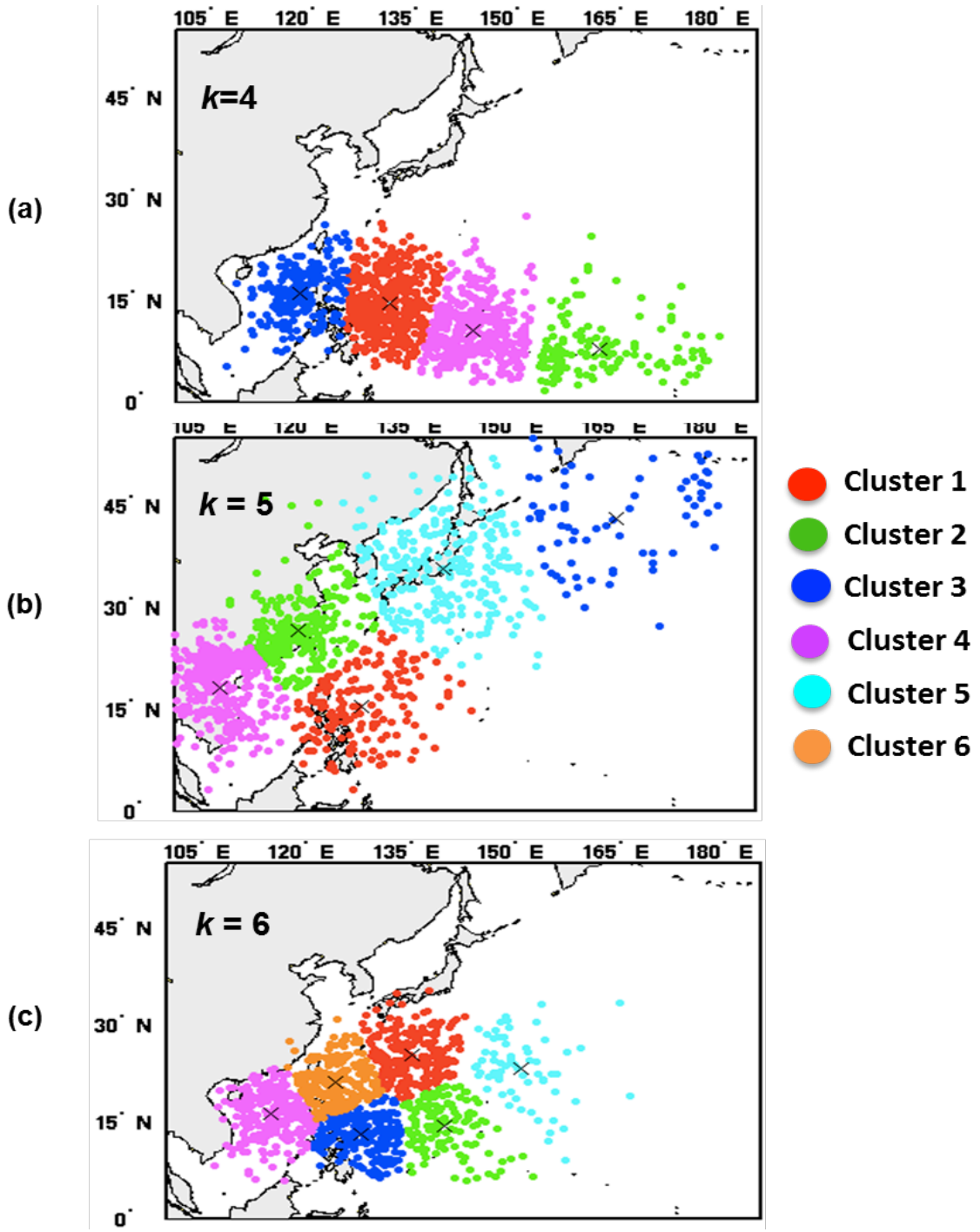


**Fig. 38.** K-means clusters of (a) genesis, (b) decay, and (c) track. The black asterisks are the centroid of each cluster.

### 5.3.2 Clustering of Genesis Locations

The locations of genesis of TCs that exist in the Philippine domain take place in a broad region west of the date line and are distributed within the confines of 2.5°N to 27.5°N latitudes and 107°E to 179.5°E. K-means clustering has been performed to 1,109 TC locations and the resultant mean silhouette value suggests four as the optimal cluster number of TC genesis locations. Fig. 38a shows the genesis locations of all TCs color-coded by cluster number and the black asterisks are the cluster centroids. Fig. 39 illustrates the cumulative density (number of TC genesis per 5° latitude by 5° longitude grid box) of genesis locations that shows the preferred area of TC formation. The cluster analysis of TC genesis locations captures the longitudinal separation of TC formation region. Clusters are arranged starting from the region west of the dateline to the South China Sea. The formation region near the Marshall Islands represents cluster 2, the smallest cluster with only 136 TCs accounting for 12% of the entire count. The genesis locations in cluster 2 have the widest spread compared with other clusters and are located farther east and closer to equator. TCs that developed near Northern Marianas Islands and over the central part of Micronesia belong to cluster 4 with 363 TCs (33%). The biggest cluster is the formation region over the Philippine Sea (cluster 1) that comprises 398 TCs (36%), and cluster 3 represents the cyclogenesis over the South China Sea accounting for 212 TCs (19%).

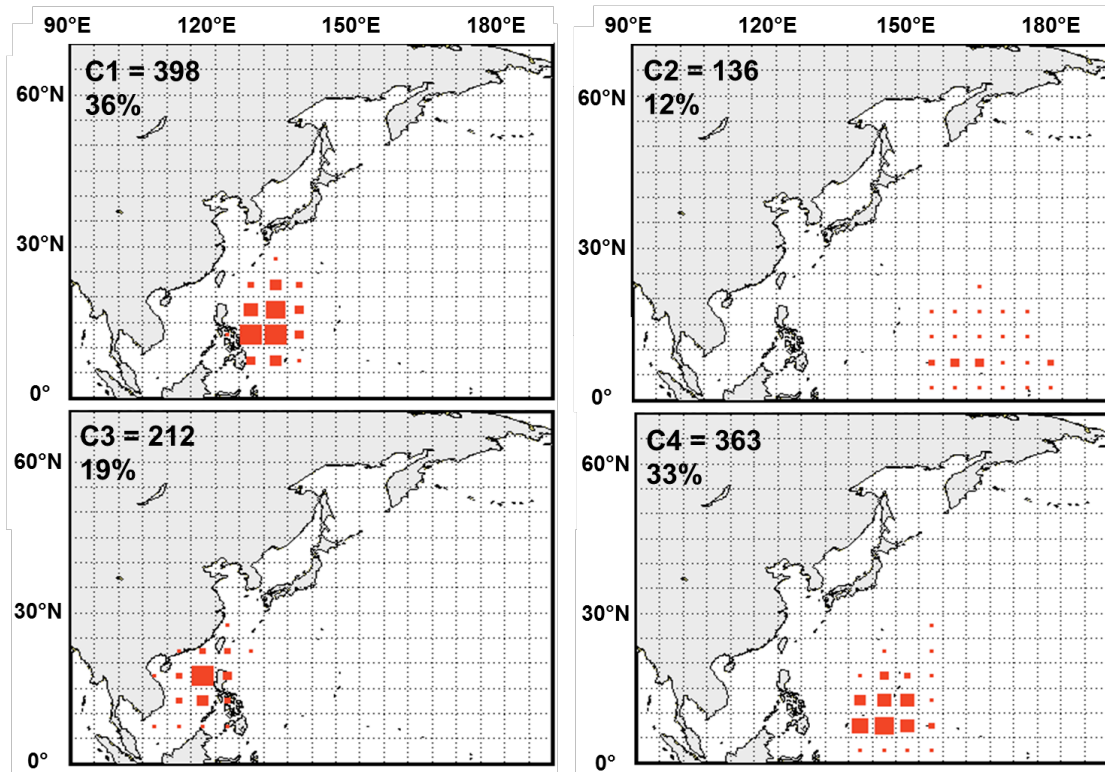
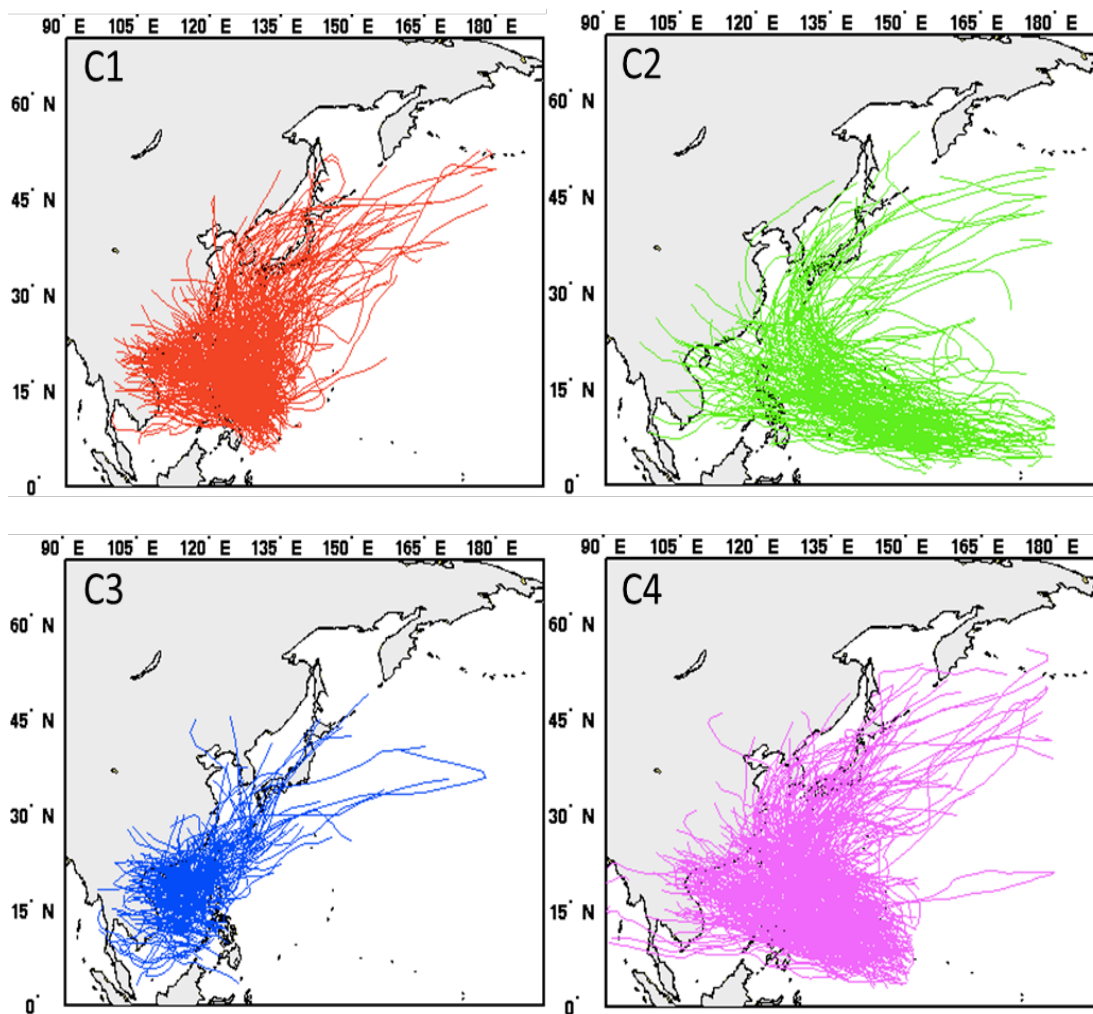


Fig. 39. Cumulative density per 5°latitude by 5°longitude grid box of genesis locations.

The genesis location provides a perception on the possible track type of a particular TC, as the genesis location greatly influences the movement and therefore the track and the decay point of the TC. The corresponding TC tracks of each four genesis clusters are shown in Fig. 40. The tracks of TCs that formed in clusters 2 and 4 (east of 135°E) are consisting of recurving and long straight tracks. The straight-moving TCs here are those that head off to Southeast Asia and the recurving TCs are those that veered northeastward and decayed over the open sea. Cyclogenesises in cluster 1 mainly consist of short straight tracks that head to Southeast Asia and slightly



recurving tracks that dissipate over the sea while genesis cluster 3 is comprised of short tracks heading to Southeast Asian coast and the long straight tracks have general movement of northeastward.



**Fig. 40.** Corresponding TC tracks of each genesis cluster.

### 5.3.3 Genesis Seasonality

Fig. 41 shows the number of TCs per calendar month for each cluster. Here we can see that the seasonal evolution of TC genesis is distinctly different from cluster to cluster. The TC geneses in cluster 1 continuously increase starting from April and peaks in August then decrease significantly in September and continue to diminish until December. Cluster 2 has a flatter seasonal cycle compared with other clusters. It has lower frequency as only 136 TCs are classified under this cluster and October is the peak of TC genesis. Cluster 3 has similarity with cluster 1 but nearly no TC in January and no TC occurrence in February and March. The TC formation in cluster 3 peaks in August and September is the next most active month. Cluster 4 shows smooth evolution of TC activity from January to June and shows a bimodal distribution with one maximum in July and another in September. The biggest group in genesis clustering is cluster 1 that accounts for TC formation over the Philippine Sea. The environmental condition in this cluster is the most conducive for TC development. This is attributed to warmer SSTs and weaker wind shears that enhance the formation of TCs. The differences in seasonality between clusters can be attributed to the changes in large-scale environmental factors associated with TC formation (Ramsay et al. 2011).

The seasonal cycle of each genesis cluster is summarized in the box plots (Fig. 42) showing the months that are considered outliers. The box plots also demonstrate the season's length, mean, median, and the upper and lower quartile of each genesis

cluster. Clusters 1 and 3 have nine-month season from April to December but TCs in January to March for cluster 1 and January for cluster 3 are considered outliers. Cluster 2 has a year-round season while cluster 4 has ten-month season and TCs in January and February are outliers. The seasonal cycle of all TCs is exactly the same that of cluster 4 having January and February as the outliers and has a 10-month season from March to December.

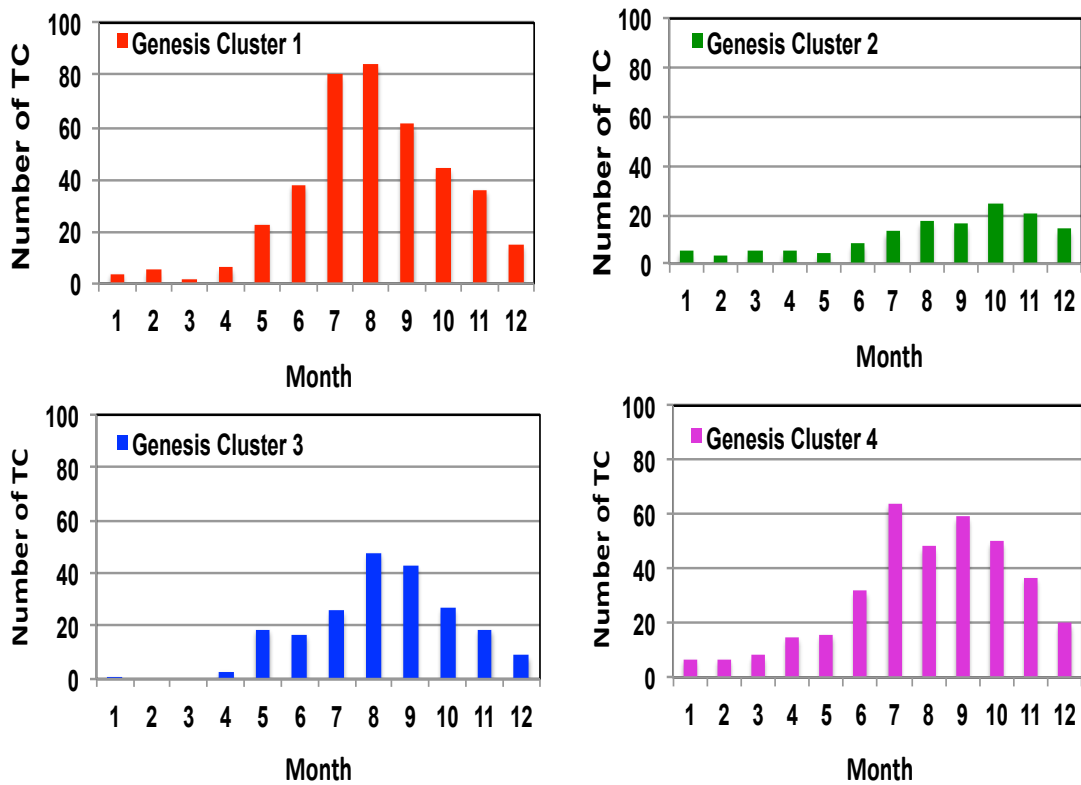


**Fig. 41.** Number of TCs per calendar month for each genesis cluster.

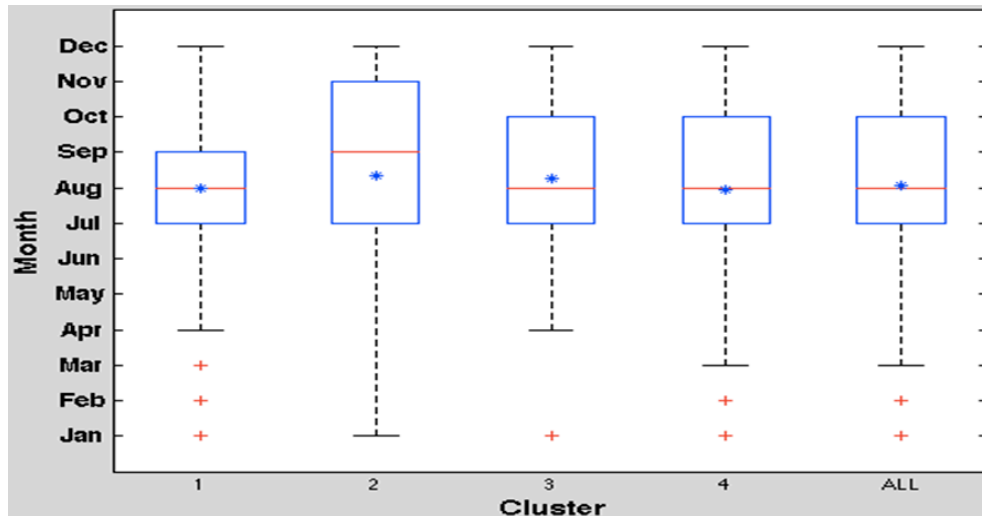


Fig. 42. Boxplots for each genesis cluster.

### 5.3.4 Clustering of Decay Locations

The TC landfall is contingent upon the TC track. The main impact of a TC is felt at landfall, the location where a TC crosses the coastline (Powell 2005). During each TC season, TC landfalls cause a great amount of social and economic damage due to the accompanying strong wind gust, heavy rainfall, and storm surge. A TC with landfall in a populous area will have a greater associated cost than one with landfall in an uninhabited area. The path or track of the TC determines the eventual cost.

In the preceding section, the TC genesis locations are clustered and the tracks of TCs from each cluster are plotted. This demonstrates the potential in predicting the possible decay point as a function of genesis location. Here, K-means cluster analysis is employed to classify the 1,128 TC decay locations. A five-cluster solution was chosen to best describe the locations of TC decay over the Philippine domain. Fig. 38b

is a map showing decay points of all TCs in Philippine domain, color coded to signify groupings by cluster number and distinct features of each cluster. The number of TCs decaying in each 5° latitude x 5° longitude box for each cluster is given in Fig. 43. The cumulative density of the distribution suggests the most preferred area of TC decay.

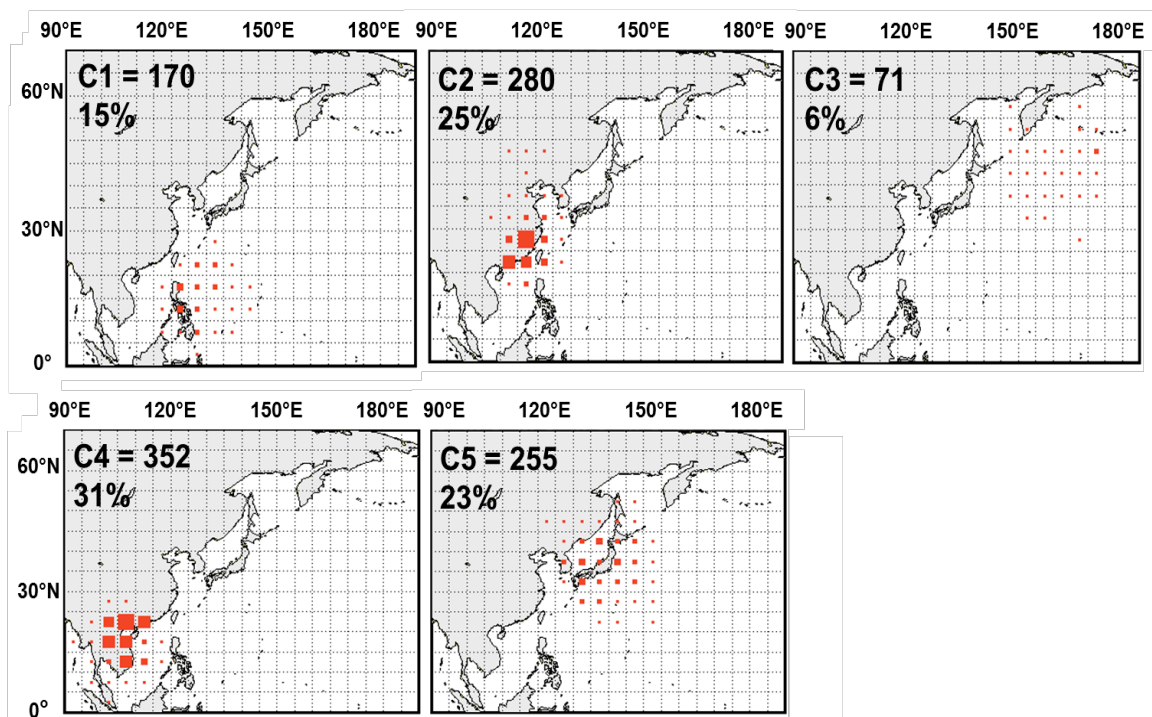


**Fig. 43.** The cumulative density of TCs decaying in each 5°latitude x 5°longitude box for each cluster and the percentage of decay per cluster.

Decay clusters also reflect the classification according to the threat region. Decay cluster 1 accounts for 170 TCs (15%) that includes TCs that pose a risk to the Philippines. Genesis cluster 4 has the largest number of cases, corresponding to TCs that made landfall over the South China and mainland Southeast Asia or Indochina that consists of 352 TCs (31%). Genesis cluster 2 represents the TC decays over Eastern China with 280 TCs (25%). TCs that dissipate over Taiwan and Japan are in cluster 5 comprising 255 TCs (23%). TCs that decay in higher latitudes of North Pacific, south of the Bering Sea, comprise cluster 3 with only 71 TCs (6%) representing the smallest cluster, the one that occurs least frequently.

The tracks of TCs from each decay cluster are shown in Fig. 44, exhibiting the region of genesis and track type for each cluster. Using the results of Decay clustering, one can easily separate straight tracks from recurving tracks. Of 1,128 Decay points, 29% of TCs have recurving tracks and these include clusters 3 and 4, TCs that pose a threat to Taiwan and Japan and the TCs that decayed south of Bering Sea. The straight-moving tracks, based from the decay classification, accounts for 71% of the entire TC counts. Clusters 1, 2, and 4 demonstrate straight tracks making landfall over Philippines, Eastern China, and Indochina, respectively. TC landfalls are dependent on TC tracks, TCs that strike in Philippines, Southeast Asia or Indochina, and Eastern China follow straight-moving tracks while those that will landfall in Taiwan and Japan and over the open seas east of Japan, follow a recurving tracks.

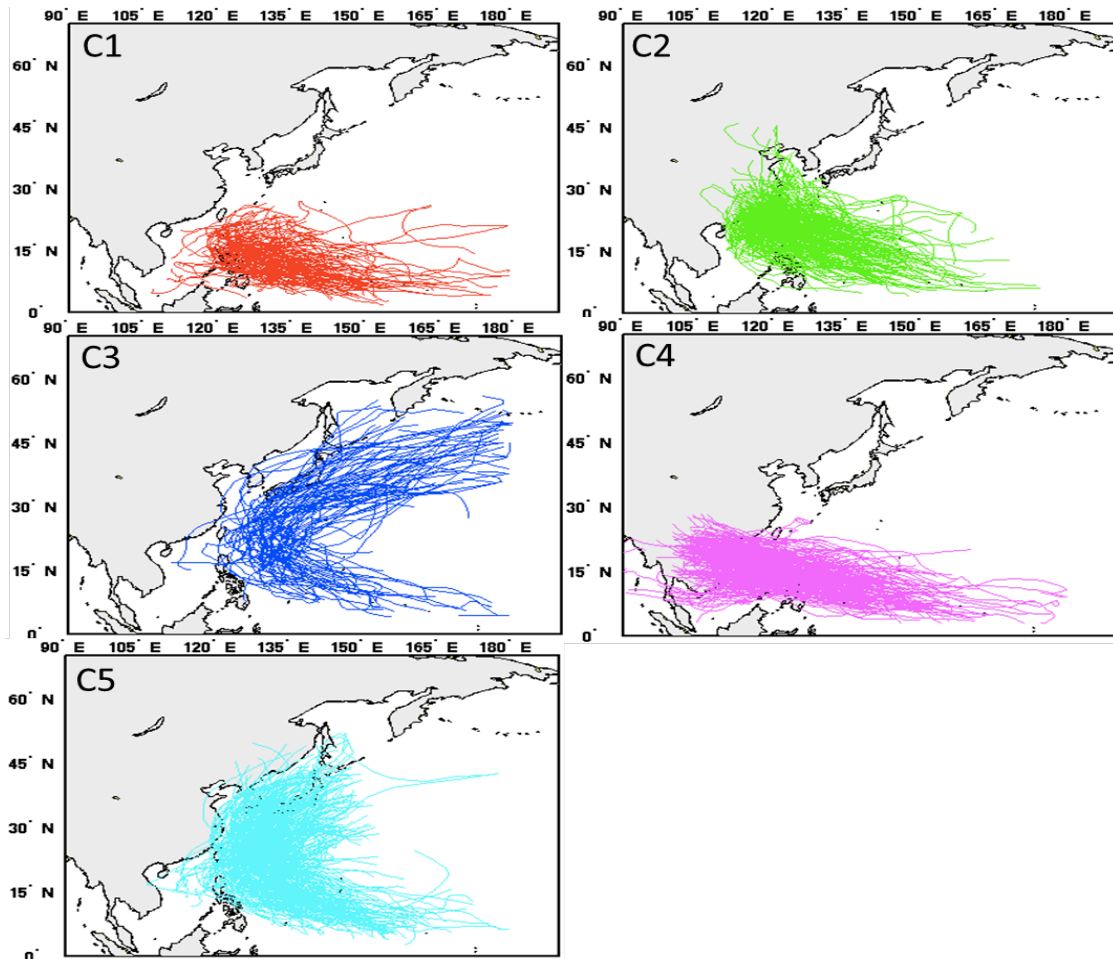


Fig. 44. Corresponding TC tracks of each decay cluster.

### 5.3.5 Decay Seasonality

The monthly frequency of each decay cluster is presented Fig. 45. Clusters 1 and 3 have flatter seasonal cycles but cluster 1 has the broadest TC seasonal distribution stretching from January to December. The TC decay is observed in cluster 3, the smallest decay, only from April through December with September as the most active month. No TC decays in cluster 2 in January and February and nearly none in

March and December. A significant increase occurs in the number of TC decays in July, then decreases continuously starting in August and persists until December. Cluster 4 has no TC incidence in February but has an almost uniform number of TC decays in January, March, April, and May then increases to October, which is also the peak of TC season, then a notable dip occurs in November and December. Cluster 5 is characterized by a smooth evolution of TC decays. No TC decays in January and February and nearly none in March. Starting May, TC decays continue to increase as the month progresses and peaks in August then decreases in September through November and almost none in December.

A succinct description of the seasonal cycle of each decay cluster is shown in Fig. 46. Cluster 1 has a year-round season while clusters 2 and 3 have nine-month season and TCs in March of cluster 2 are treated as outliers. Cluster 4 has the shortest season, only eight months and TC decays in January, March and April are considered outliers. Cluster 5 and all TCs have ten-month season.



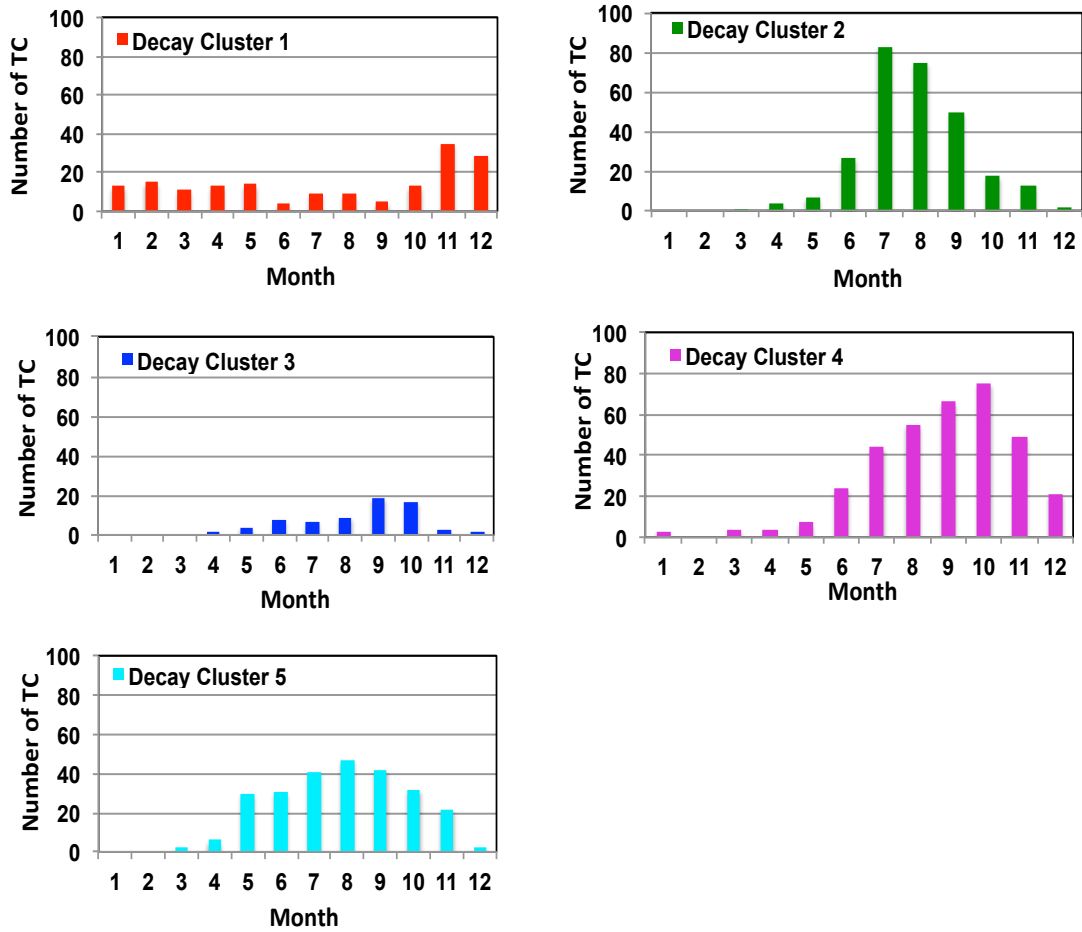


Fig. 45. Same as Fig. 41, but for each decay cluster.

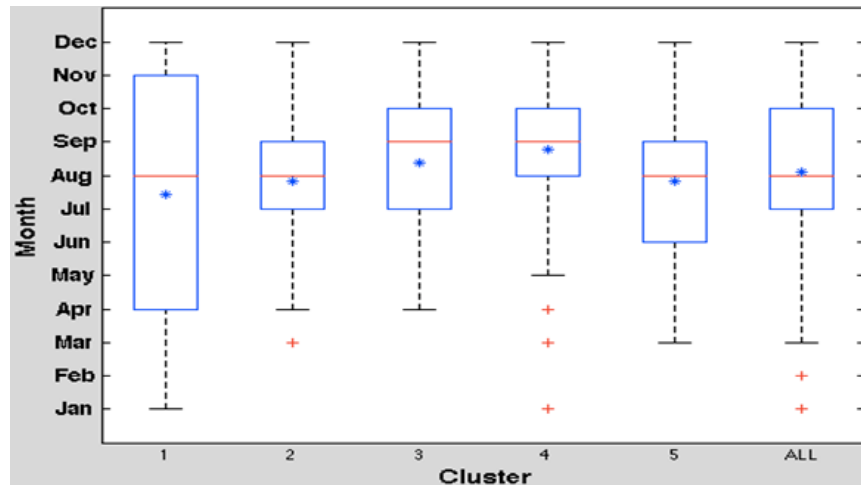


Fig. 46. Same as Fig. 42, but for decay clusters.

### **5.3.6 Clustering of Tracks**

In order to isolate potentially predictable aspects of the movement or landfall of TCs affecting the Philippines and also to mitigate the damage caused by them in advance, it is necessary to understand the characteristics of various TC tracks and the large-scale environment factors that affect them. The risk of landfall of a TC depends on its trajectory. The TC trajectory varies strongly with the season (Gray 1979; Harr and Elsberry 1991), as well as on interannual (Chan 1985) and interdecadal time scales (Ho et al. 2004).

Cluster analysis has long been used to discover hidden configurations from historical TC tracks. The quantitative characteristics of clusters in TC tracks can naturally provide valuable references for TC track and landfall prediction due to its capabilities in unraveling the hidden pattern from the best-track data. Previous researchers noted that an effective way to explain the characteristics of various TC tracks is to classify TC trajectories into definite numbers of patterns (e.g., Hodanish and Gray 1993; Harr and Elsberry 1991, 1995a, 1995b; Lander 1996; Elsner and Liu 2003; Elsner 2003; Hall and Jewson 2007; Camargo et al. 2007b, 2007c, 2008; Nakamura et al. 2009).

In this study, K-means cluster algorithm is applied to the tracks of 1,108 TCs in the Philippine domain for the same period, 1950-2011. A single point based on the average position of the genesis point, location of the TC at its maximum intensity, and decay point represents the TC track. The actual geographical position of the individual point that represents each TC track is presented in Fig. 38c; colors suggest cluster

number. The density of TC passages per  $5^\circ$  latitude by  $5^\circ$  longitude grid box is given in Fig. 47. The density and size of the red square marker indicate number of TC passages per grid box. Also shown in Fig. 47, in parenthesis is the percentage of TCs for each cluster to the total number of TCs.

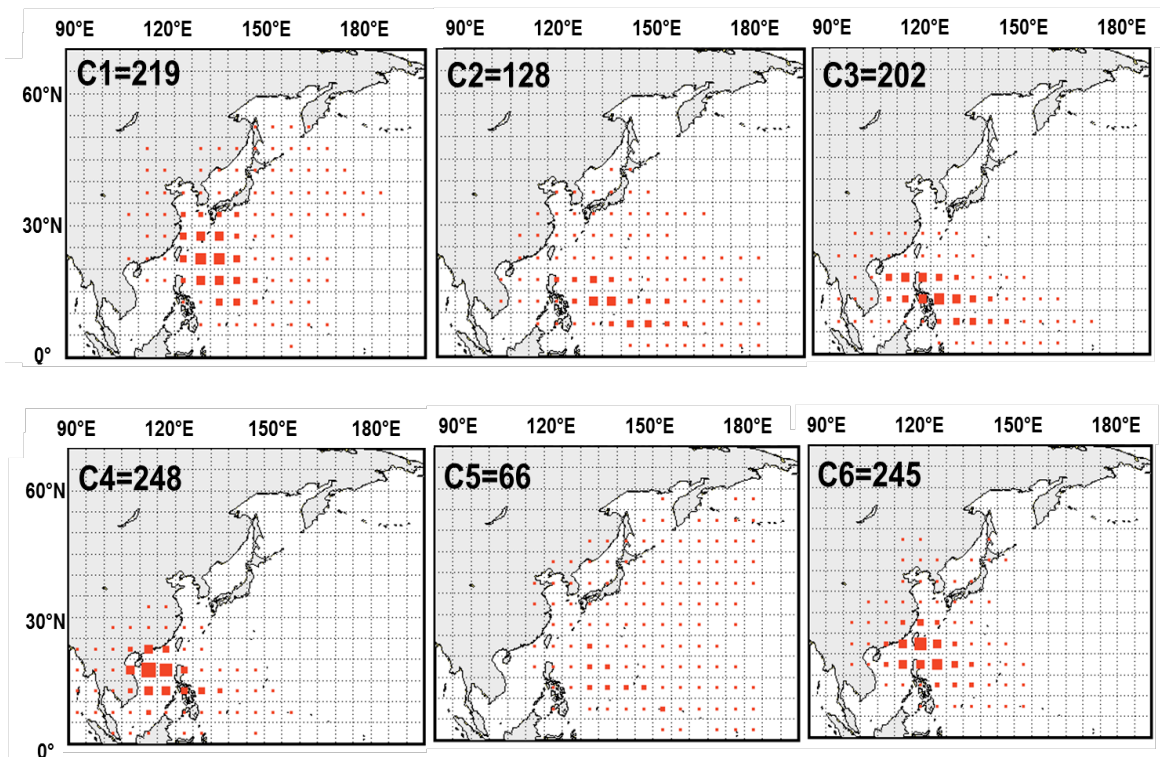


Fig. 47. Cumulative density of TC passages per  $5^\circ$  latitude by  $5^\circ$  longitude grid box.

Clustering of TC tracks produced six clusters but the two main trajectory types identified by the cluster analysis correspond to straight-movers and recurvers. The actual geographical position of the individual TC track of clusters 1-6, separated by cluster is presented in Fig. 48. The six track clusters correspond to more detailed differences between these two main types, according to location and track type. There are 3 clusters with general pattern of recurving tracks (clusters 1, 2, and 5) and also 3 clusters with straight tracks (clusters 3, 4, and 6); these clusters also share great similarity. Three straight-moving trajectory types have very small within cluster spread, geographically limited while the recurving types are more diffuse, occupying a much larger area of WNP ocean.

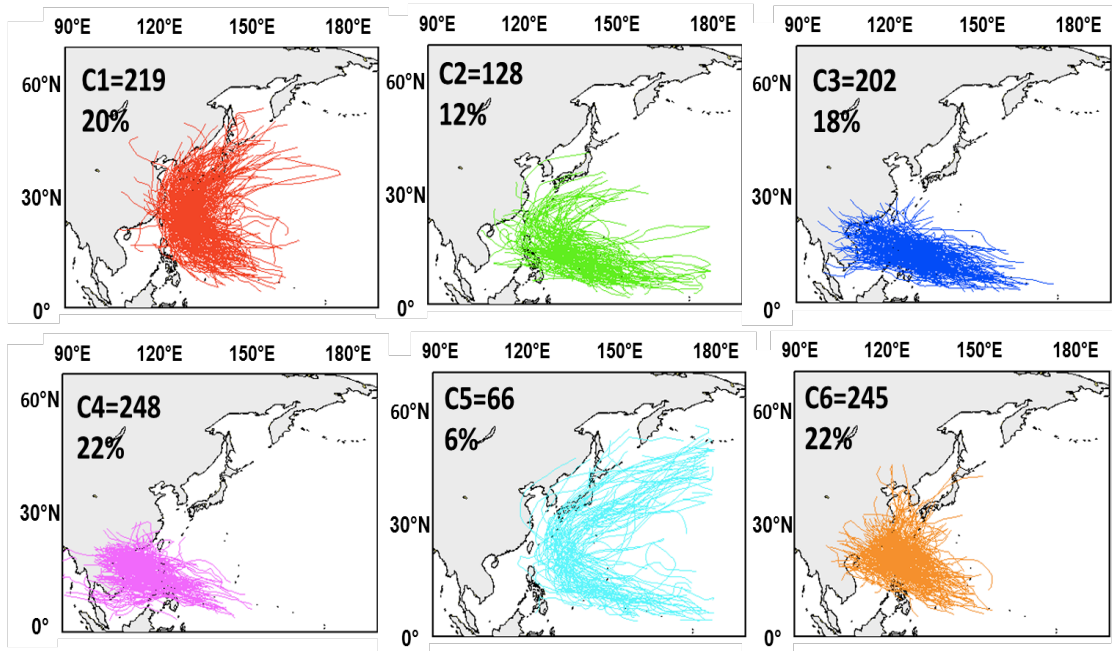


Fig. 48. Track clusters after applying K-means clustering to Philippine TC tracks.

Cluster 1 consists of 219 TCs (20%), the second largest cluster, with short recurving tracks heading to Japan and some hitting Eastern China, Taiwan, Korea, and Japan. TCs in cluster 2 are characterized by long straight tracks that move northwestward before recurving northeastward toward south of Japan. Cluster 2 consists of 128 TCs (12%). The majority of the TCs in this cluster recurved northeastward while a few crossed the Philippines and headed straight to the east coast of China. Cluster 3 consists of 202 TCs (18%) that represent west-northwestward long, straight tracks across the Philippines and the South China Sea heading to inland regions of the southeastern coast of mainland China and mainland Southeast Asia (Indochina). Cluster 4 is the most frequent trajectory type with 248 TCs (22%) and the

track type resembles that of cluster 3, also heading west-northwestward but with shorter straight tracks and making landfall over regions similar to those of cluster 3. TCs in cluster 5 stay mostly offshore and dissipate over the open sea east of Japan, posing no threat to land. The TC tracks have similarity with cluster 1 characterized by longer recurving or parabolic shape. Being the smallest cluster, cluster 5 has only 66 TCs (6%). Cluster 6 is one of the two most frequent tracks with 245 TCs (22%), comparable to clusters 3 and 4, characterized by straight-moving tracks with northwestward direction passing through the northern part of the Philippines then striking Taiwan and the east coast of mainland China. In this study, the three dominant clusters are 1, 4, and 6, each cluster accounting for at least 20% of the tracks. Clusters 2 and 3 are less often (12% and 18%, respectively), while cluster 5 is relatively rare, only 6% of the total TC count.

### **5.3.7 Tracks Seasonality**

The monthly TC distribution for each track cluster is summarized in Fig. 49, which shows the seasonality of TC activity in each track type. Clusters 1, 4, and 6 have the same shape and appearance; they have narrower seasonal distributions, and TC activity commences in April and ends in December except for cluster 1 that ends earlier in November. The peak months are August, September, and July for clusters 1, 4, and 6, respectively. Clusters 2, and 3 have flatter but broader seasonal cycles with TC occurrence year round and both clusters reach highest frequency of TC occurrence in November with a sub-peak in April and July, respectively. Cluster 5 has flatter and

narrower seasonality; TC season starts in April and run through December. October is the peak of TC activity.

Fig. 50 presents the box plots of track clusters. Clusters 1, 2, and 6 have a nine-month season but TCs in January of cluster 4 are taken as outliers. Clusters 2 and 3 have a year-round season. Cluster 5 has the shortest season with only eight months and TCs in April are treated as outliers. The box plot that represents all TCs has a ten-month season and January-February TCs are outliers.

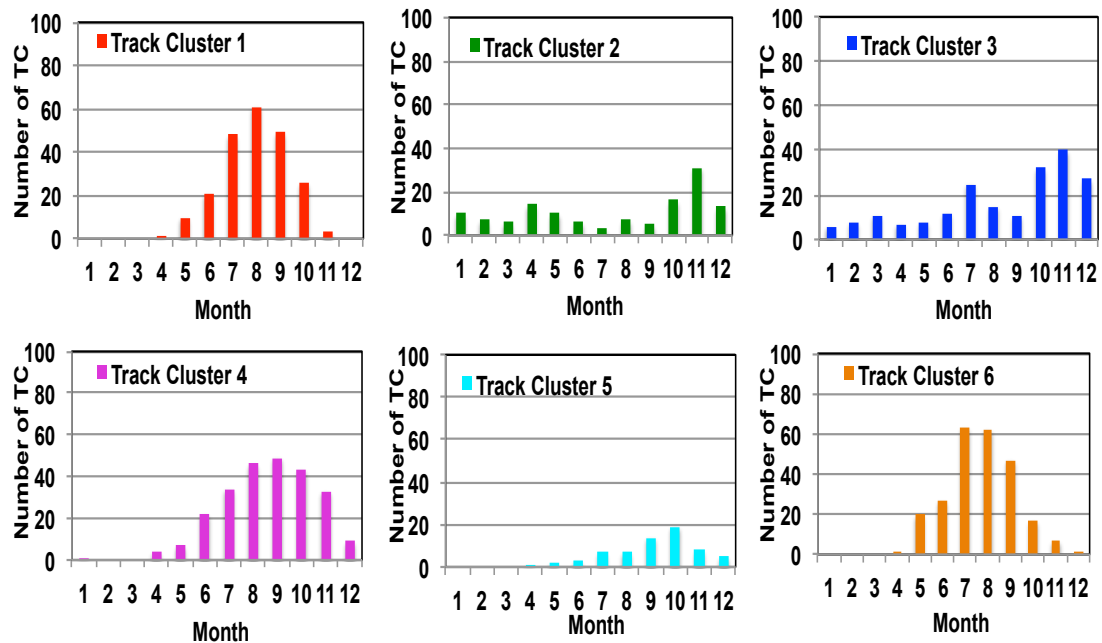


Fig. 49. Same as Fig. 45, but for each track cluster.

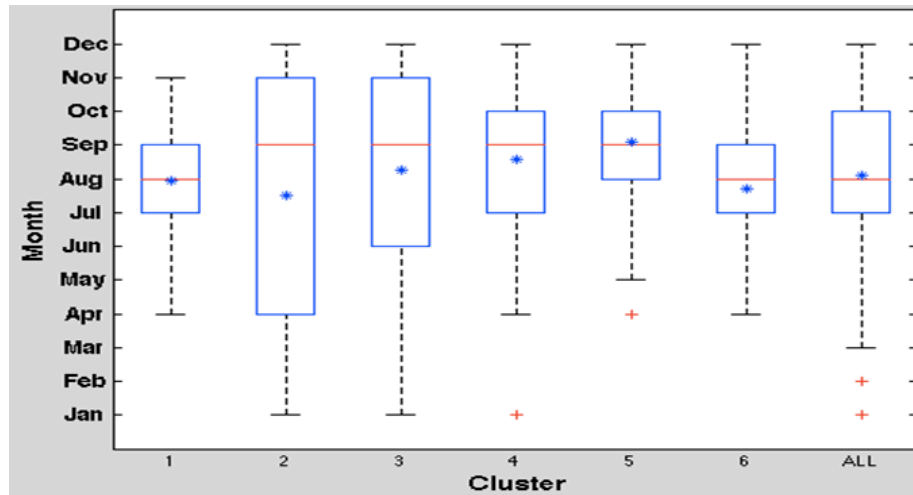
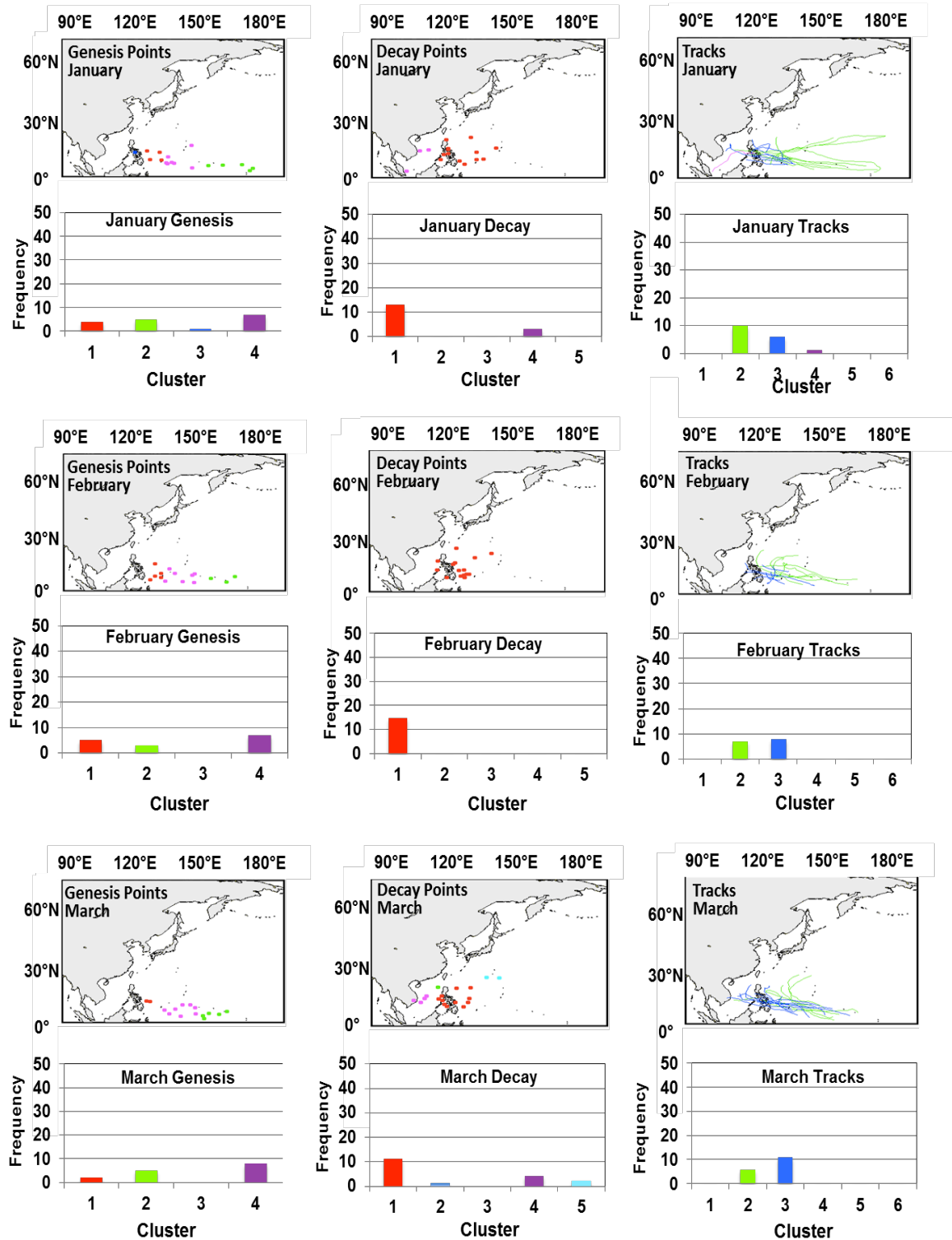


Fig. 50. Same as Fig. 46, but for each track cluster.



### **5.3.8 Monthly Analysis of TC Activity**

The key motivation in doing the monthly analysis is to obtain a description of the temporal and spatial behavior of TC activity. This section describes the monthly variations of TC activity over the Philippine domain during the period 1950-2011 by examining the features of each cluster. The plots of TC genesis locations, tracks, and decay locations provide the distinct characteristics of each cluster as time progresses. The graphs present the TC frequency of each cluster by month. Every dot and track in the figures is color coded to signify the cluster number to which it belongs. JFM comprises the quiet months and represents the calm phase of TC activity in the Philippine domain. In these months, TC formations are only found east of the Philippines (Fig. 51), over the Philippine Sea (genesis cluster 1), Northern Marianas Islands and central Micronesia (genesis cluster 4), and Marshall Islands (genesis cluster 2) and are confined to lower latitudes; at its most equatorward position in March. No TCs formed over the South China Sea (genesis cluster 3). Like the cyclogenesis, the tracks of TCs occupy the lower latitudes, reaching 23°N at most, and follow straight tracks (track clusters 3 and 4) than in February and March, some TCs veer northeastward (track cluster 2). JFM TCs are characterized by straight-moving tracks. In January and February, TCs make landfall over the Philippines including the Philippine Sea and South China Sea; decay clusters 1 and 4, respectively. TCs in March decay in clusters 1, 2, 4, and 5, posing a threat to Philippines, and Indochina. The most active decay region in JFM is cluster 1, signifying the TCs over the Philippines and Philippine Sea



**Fig. 51.** The monthly variations of TC activity over the Philippine domain during JFM by cluster

The second quarter, April-June (AMJ) is marked by an increase in the genesis numbers (Fig. 52); it has more TC birthplaces than JFM. The birthplaces extend farther north to 22°N, about 6° latitude higher than the JFM birthplaces. All genesis clusters are represented in this quarter including the South China Sea (genesis cluster 3). More than half, 52%, of the TCs in April originate from cluster 4, those that form near Northern Marianas Islands and over central Micronesia. Very few TCs belong to cluster 3, merely 10% of the total TC genesis. During the 62-year period, there is only one TC genesis in April over the South China Sea. Straight tracks are the major trajectory type, accounting for more than 50% of the TCs for the month and most April TCs, 45%, make landfall over the Philippines and Philippine Sea (decay cluster 1). In May and June, there is an increase in the number of TC formation over the South China Sea and more TCs develop in higher latitudes especially in June. TC development is also common in clusters 1 and 4, the TC formation over the Philippine Sea and near Northern Marianas Islands and central Micronesia.

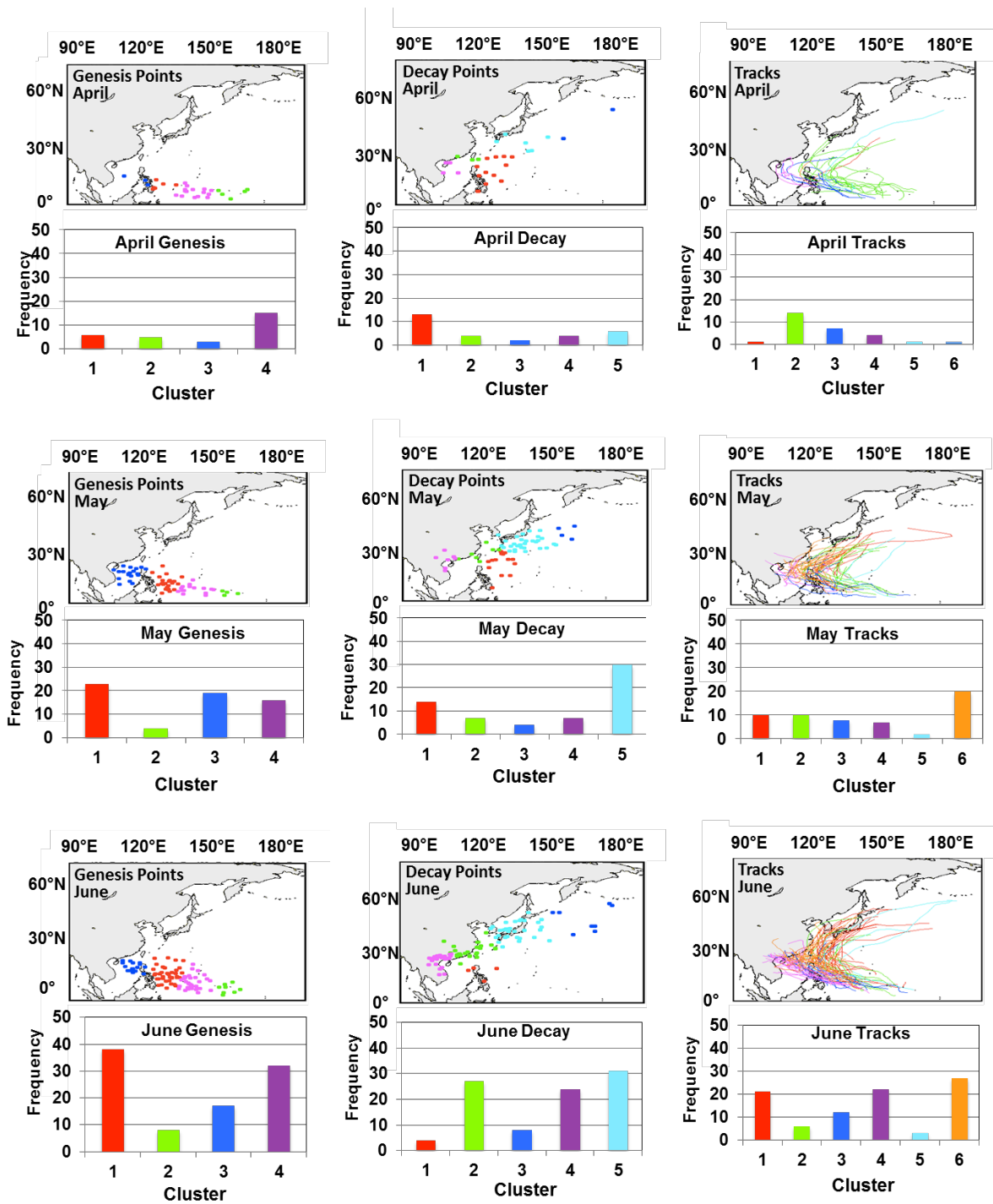


Fig. 52. Same as Fig. 51, but for AMJ.

Fig. 53 shows the variations and distinct characteristics of JAS TC activity. The frequency and areal extent of TC geneses are largest during JAS, so tracks are also the densest compared with other quarters. In July, the two regions of most frequent cyclogenesis are clusters 1 (Philippine Sea) and 4 (northern Marianas Island and central Micronesia) with 79% of the total TC genesis of the month and predominantly decay over Eastern China (cluster 2, 45%) while some TCs over the South China Sea, including mainland Southeast Asia and over Taiwan including Japan. Short straight tracks toward Eastern China are the most prevalent trajectory type in July and the short recurving tracks heading toward Japan are the second dominant trajectory type. The TC genesis in the domain reaches its northernmost position in August but the southernmost cyclogenesis also slightly shifts northward. Genesis cluster 1 (Philippine Sea) has the highest occurrence of TC formation in August corresponding to 43% of the August TCs with clusters 3 (South China Sea) and 4 (Northern Marianas and central Micronesia) as the next major regions of formation, both with 24% of TC genesis. The majority of the straight-moving TCs during this month decay over mainland Indochina and over Eastern China, while most of the recurving TCs dissipate over Taiwan and Japan.

In September, TC genesis starts to slightly shift southward and the number of TC geneses is also reduced. Genesis clusters 1 and 4 have a distinctive maximum during this month. Tracks are mainly short straight tracks toward Eastern China including the southern coast of Eastern China, and short recurving tracks heading toward Taiwan and Japan. In contrast, decay cluster 1 has the least frequent TC

dissipation; they are the TCs decaying over or near the Philippines. In September and October, recurving tracks extend farther northeast.

The plots of genesis and decay locations and the TC tracks are presented in Fig. 54 during the OND quarter. OND has lesser TC genesis than JAS and the latitudinal extent of birthplaces and tracks is not as large and dense but this has the greatest landfall probabilities and has more straight-moving TCs. Genesis points are predominantly seen in clusters 1 and 4, corresponding to TCs that form over the Philippine Sea and near Northern Marianas Islands including the central Micronesia. TC formation has significantly decreased in December. The TC tracks in OND occur mainly from clusters 3 and 4, characterized by straight trajectory crossing Philippines and South China Sea before hitting the Southeast Asia and Eastern China including its southern coast. In OND, TC geneses are much closer to the dateline and straight-moving TCs are observed during these months.

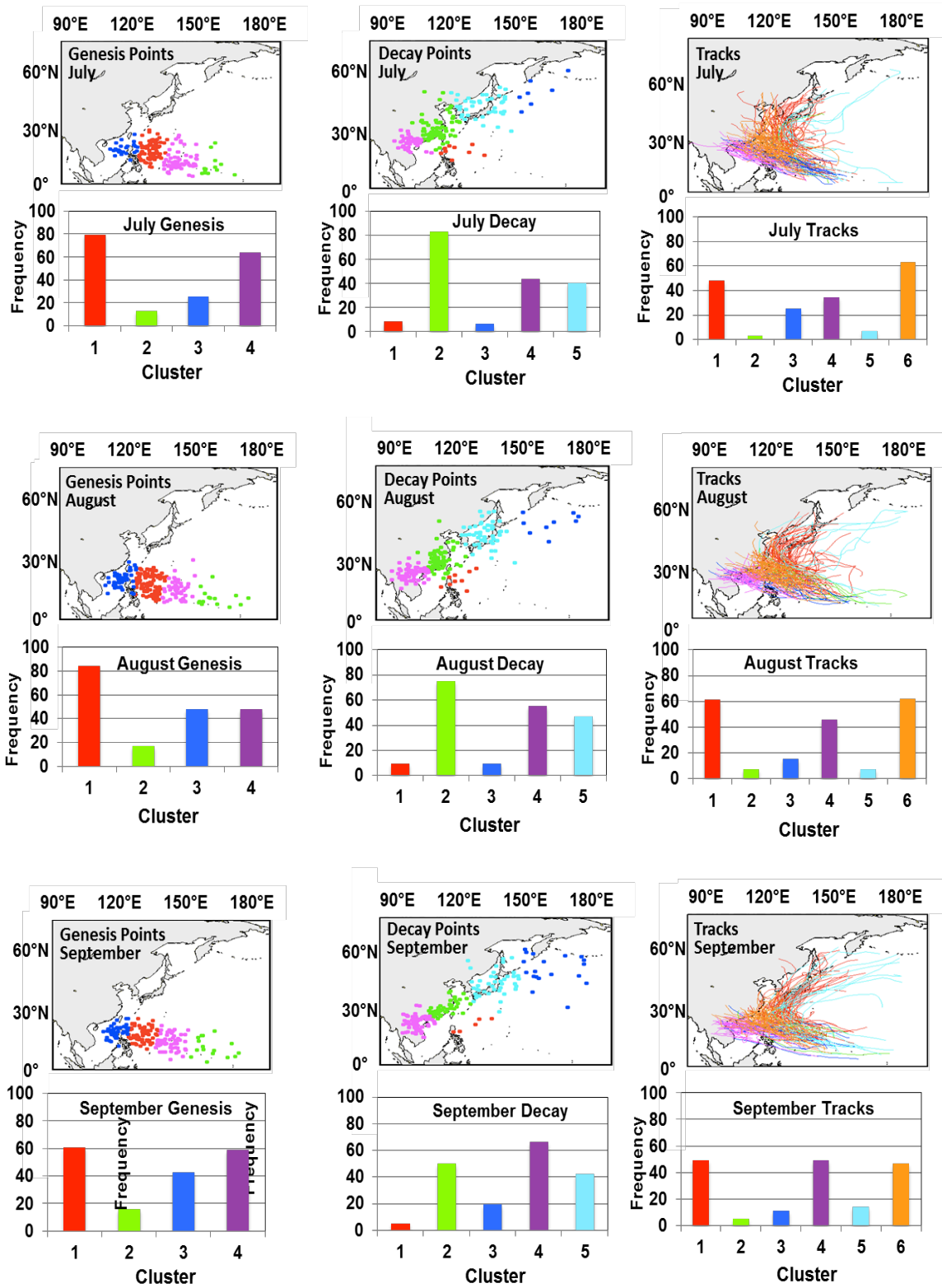


Fig. 53. Same as Fig. 51, but for JAS.

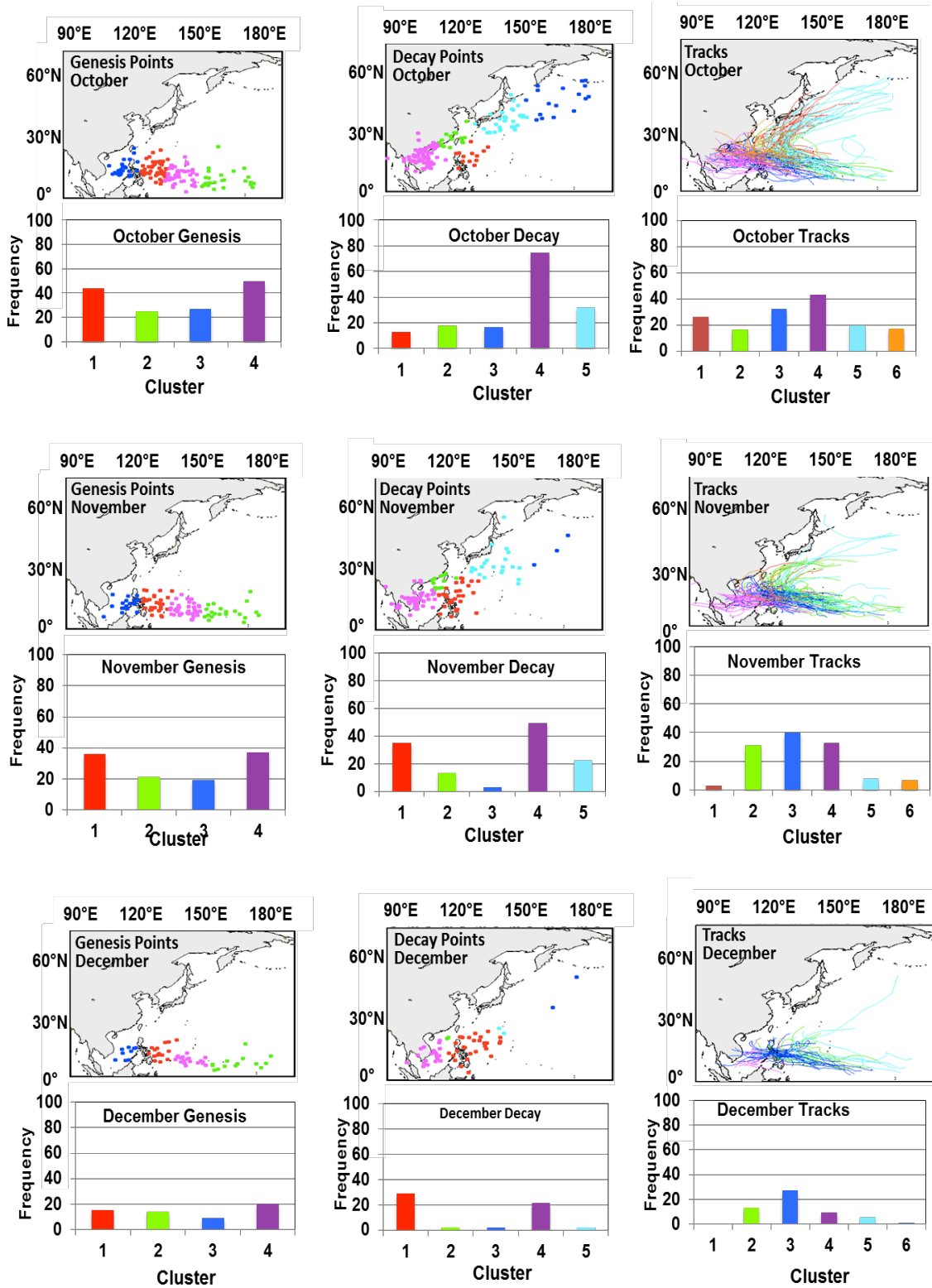


Fig. 54. Same as Fig. 51, but for OND.



## 5.4 Discussion and Conclusions

This study includes all the TCs that existed throughout the Philippine domain, regardless of intensity classification, providing a larger sample and more comprehensive statistical results, as opposed to other work that only include TCs with storm intensity (Elsner and Liu 2003) and TCs that occur in peak season, June-November (Harr and Elsberry 1991). Harr and Elsberry (1991) excluded the tracks considered as ‘odd’ in their classification. Here, we eliminate the TCs with negative silhouette value to improve the cluster cohesiveness.

The mean genesis location of the TCs in the WNP has a well-defined annual cycle (Chia and Ropelewski 2002; Camargo and Sobel 2005), with the average latitude reaching its northernmost position in August and its most equatorward position around February. This cycle is consistent and seen in the monthly analysis of the clusters; the genesis locations vary in latitude as the month progresses. The formation clusters of Philippine TCs occupy the western Pacific warm pool and lower latitudes and this is because of the presence of low values of vertical wind shear in that region. The cyclogenesis in fall and winter are found in the most equatorward latitudes while in summer TC genesis points are in northernmost latitudes. The cluster with highest TC genesis represents the Philippine Sea, just east of the Philippines, and this can be explained by more persistent warm sea surface temperature over this genesis region. The climatological SSTs in the Philippine Sea are above 26°C year round. In August, the cluster with the highest TC formation is just east of the Philippines. Harr and Elsberry (1991) also added that the combination of the broad

belt of anomalous equatorial westerlies between 75°E and 145°E and the anomalous easterlies between 20°N and 30°N from 120°E to 150°E form a large region of cyclonic horizontal shear. This may be associated with an enhanced monsoon trough, which is favorable environment for TC genesis (Love 1982). Anomalous easterlies between 20°N and 30°N then result from the enhanced gradient between the active monsoon trough to the south and the strong subtropical ridge to the north. The anomalous anticyclonic circulation over the East China Sea and southern Japan implies a strengthened subtropical ridge. In summary, these large-scale circulations provide a physically consistent pattern of an environment favorable for TC genesis in the monsoon trough. The probability that the Philippines are hit by TCs is also high; TCs cross the Philippines before hitting Eastern China and although some will pass north of the Philippines, the rain associated with the TC passage still affects the country.

TCs in genesis clusters close to the dateline are most likely to follow recurving tracks depending on the prevailing wind system affecting the Philippine domain. During the peak of the Northeast monsoon, TCs tend to have straight trajectories and hit or cross the Philippines, while during the peak of the Southwest monsoon, TCs are likely to recurve northeastward. TCs originating east of the Philippines over the Philippine Sea decay over mainland Indochina and Eastern China. Clusters (2 and 5) with TCs that developed closer to the dateline and equator have the longest tracks and presumably the longest mean duration compared to those in other clusters. Some of these TCs pass southern Japan while others pass east of Japan. Examination of genesis and track clusters suggests that some genesis clusters are associated with straight-

moving TCs, whereas recurving TCs are more likely to be associated with other genesis clusters. TC genesis locations contribute to the character of the intraseasonal variability in TC tracks, but the track itself is also influenced by the large-scale and synoptic –scale circulations.

The two main trajectory types identified in this study, namely recurving and straight-moving, are consistent with the two principal track types identified in previous studies (Sandgathe 1987; Harr and Elsberry 1995a; Lander 1996; Camargo 2007b). The six track clusters that present broader trajectory types are very similar with cluster results of Camargo (2007b) except for the cluster that represents the TCs outside the Philippine domain. Although the two studies used two different cluster methods, the results are almost the same. This proves that using K-means as the clustering method can still provide an accurate clustering, disputing earlier claims that K-means is not capable of clustering TCs with varying track shape and length.

The clustering of Philippine TC tracks has shown that 63% of the total TCs follow a straight-moving trajectory type and these corresponds to the TCs that belong in clusters 3, 4, and 6; other clusters are classified with recurving trajectory types. The clustering results also suggest that TCs originating east of about 150°E have a higher probability (67%) of following a recurving track, heavily dependent on the time of the year and the prevailing wind system affecting the Philippine domain, while the probability of straight-moving tracks remains higher for TCs that form west of 140°E, about 76%. The study of Nakamura et al (2009) suggests that straight-moving TCs are more frequently seen during the early or late seasons, whereas recurving TCs prevail during the peak TC season (July, August and September). This is not the case for

Philippine TCs, except in April the dominant trajectory type in the Philippine domain is straight-moving track.

The monthly distribution of each cluster of genesis, track, and decay demonstrates that the seasonality and general characteristics of TC activity differs from cluster to cluster. This variation in TC characteristics is attributed to the variations in the large-scale circulations. The Philippine TC genesis position shifts northward from June through August, but regresses southward in September. These seasonal variations reflect variations in the position of the monsoon trough and the North Pacific subtropical high (Chia and Ropelewski 2002). Monthly analyses of each cluster show which clusters of genesis, tracks, and decay dominate during a specific month; this is a potentially useful forecast tool. The patterns in genesis locations can possibly be used in track and landfall forecast, once the genesis location of a cyclone is known. Although analysis of seasonal variation of the genesis, tracks, and decay yields fundamental spatial/temporal characteristics in the entirety, it reveals some guiding results and thus aids prediction.

## **Chapter 6**

### **Future Work**

The first part of the study has identified gap or “quiescent period” between LAS and MAS, and vice versa. The length of the quiescent period is also related to the start and end dates of each TC season. What causing these varying length should be investigated. The conditions of the large-scale circulation associated with the transition period between the two seasons should be closely examined.

About 50% of the rainfall in the Philippines is associated with TC passages. The study on the impacts of ENSO to Philippine TCs shows the southeast (northwest) shift of TC genesis locations during El Niño (La Niña) years. Future work will include quantifying the influence on rainfall in relation with genesis displacement.

The application of cluster analysis to the Philippine TCs has classified various regions of TC formation and decay, and different patterns of trajectory type. The distinctly different and persistent condition for each cluster must be looked into to see which large-scale configuration can enhance or weaken TC genesis in certain cluster region, and favor or prevent certain track types. If these conditions could be identified, they could be used to produce outlooks of TC formation regions and likely track types.

It is vital to examine the intensity of TCs in each genesis and track cluster, the analysis will provide identification of where intense and weak TCs develop and how the intensity changes as the track veers or recurves. Although clustering algorithm has no access to the TC intensity, Camargo (2007) noted that recurving usually occur

when the TC move from a region of easterlies to a region of westerlies, emphasizing that the wind speed decreases near the recurving point. Shoemaker (1991) also added that the direction of TC motion depends on its intensity prior to landfall.

Lastly, it is of great importance to analyze the TC cluster characteristic as a function of large-scale circulation anomalies e.g. ENSO and MJO.

## Chapter 7

### References

- Aldenderfer, M. S. and R. K. Blashfield, 1984: Cluster analysis. Sage, Newbury Park, CA.
- Ash, K. D., and C. J. Matyas, 2012: The influences of ENSO and the subtropical Indian Ocean Dipole on tropical cyclone trajectories in the southwestern Indian Ocean. *Int. J. Clim.*, **32**, 41-56.
- Barnston, A.G., M. Chelliah, and S. B. Goldenberg, 1997: Documentation of a highly ENSO-related SST region in the equatorial Pacific. *Atmos. Ocean*, **35**, 367–383.
- Bell, G. D., and Coauthors, 2000: Assessment for 1999. *Bull. Amer. Meteor. Soc.*, **81**, 1–50.
- Bjerknes, J., 1969: Atmospheric teleconnections from the equatorial Pacific. *Mon. Wea. Rev.*, **97**, 163–172.
- Blender, R., K. Fraedrich, and F. Lunkeit, 1997: Identification of cyclone track regimes in the North Atlantic. *Quart J. Roy. Meteor. Soc.*, **123**, 727-741.
- Brand, S. and J. W. Blesloch, 1973: Changes in the characteristics of typhoons crossing the Philippines. *J. Appl. Meteor.*, **12**, 104-109.
- Briegel, L. M., and W. M. Frank, 1997: Large-scale influences on tropical cyclogenesis in the western North Pacific. *Mon. Wea. Rev.*, **125**, 1397-1413.
- Camargo, S. J., and A. H. Sobel, 2005: Western North Pacific tropical cyclone intensity and ENSO. *J. Clim.*, **18**, 2996–3006.
- , S. J., K. A. Emanuel, and A. H. Sobel, 2007a: Use of a genesis potential index to diagnose ENSO effects on tropical cyclone genesis. *J. Clim.*, **20**, 4819–4834.
- , S. J., A. W. Robertson, S. J. Gaffney, P. Smyth, and M. Ghil, 2007b: Cluster analysis of typhoon tracks. Part I: General properties. *J. Clim.*, **20**, 3635-3653.
- , S. J., A. W. Robertson, S. J. Gaffney, P. Smyth, and M. Ghil, 2007c: Cluster analysis of typhoon tracks. Part II. Large-scale circulation and ENSO. *J. Clim.*, **20**, 3654-3676.

- , S. J., A. W. Robertson, A. G. Barnston, and M. Ghil, 2008: Clustering of eastern North Pacific tropical cyclone tracks: ENSO and MJO effects. *Geochem. Geophys. Geosyst.*, **9**, Q06V05, doi:10.1029/2007GC001861.
- Carlson, T. N., 1971: An apparent relationship between the sea-surface temperature of the tropical Atlantic and the development of African disturbances into tropical storms. *Mon. Wea. Rev.*, **99**, 309-310.
- Chan, J. C. L., 1985: Tropical cyclone activity in the Northwest Pacific in relation to the El Niño/Southern Oscillation phenomenon. *Mon. Wea. Rev.*, **113**, 599-606.
- , J.C.L., 2000: Tropical cyclone activity over the western North Pacific associated with El Niño and La Niña events. *J. Clim.* **13**, 2960-2972.
- , J. C. L., and K. S. Liu, 2004: Global warming and western North Pacific typhoon activity from an observational perspective. *J. Clim.*, **17**, 4590–4602.
- , J. C. L., 2005: The Physics of tropical cyclone motion. *Ann. Rev. Fluid Mech.*, **37**, 99-128.
- , J.C.L., 2008: Decadal variations of intense typhoon occurrence in the western North Pacific. *Proceedings of the Roy. Soc.*, **464**, 249-272.
- , J.C.L., and M. Xu, 2008: Interannual and interdecadal variations of landfalling tropical cyclones in East Asia. Part I: time series analysis. *Int. J. Clim.*, **29**, 1285–1293.
- Chand, S. S., and K. J. E. Walsh, 2009: Tropical cyclone activity in the Fiji region: spatial patterns and relationship to large-scale circulation. *J. Clim.*, **22**, 3877-3893.
- , S. S., and K. J. E. Walsh, 2010: The influence of the Madden-Julian oscillation on tropical cyclone activity in the Fiji region. *J. Clim.*, **23**, 868-886.
- Chang, C. P., Z. Wang, J. McBride, and C. H. Liu, 2005: Annual cycle of Southeast Asia Maritime Continent rainfall and the asymmetric monsoon transition. *J. Clim.*, **18**, 287-301.
- Chen, S. Y. Wang, M. C. Yen, and W. A. Gallus Jr., 2004: Role of the monsoon gyre in the interannual variation of tropical cyclone formation over the western North Pacific. *Wea. Forecasting*, **19**, 776–785.
- Chen, T. C., S. P. Weng, N. Yamazaki, and S. Kiehne, 1998: Interannual variation in the tropical cyclone formation over the western North Pacific. *Mon. Wea. Rev.*,



126, 1080–1090.

- , T. C., S. Y. Wang, M. C. Yen, and A. J. Clark, 2009: Impact of the intraseasonal variability of the western North Pacific large-scale circulation on tropical cyclone tracks. *Wea. Forecasting*, **24**, 646–666.
- Chia, H. H., and C. F. Ropelewski, 2002: The interannual variability in the genesis location of tropical cyclones in the northwest Pacific. *J. Clim.*, **15**, 2934–2944.
- Choi, K. S., B. J. Kim, and H. R. Byun, 2008: Relationship between Korean Peninsula landfalling tropical cyclones and interannual climate variabilities. *J. Korean Earth Science Soc.*, **29**, 5, 375–385.
- Clark, J. D., and P. S. Chu, 2002: Interannual variation of tropical cyclone activity over the Central North Pacific. *J. Meteor. Soc. of Japan*, **80(3)**, 403–418.
- Colbert, A. J. Soden, B. J., 2012: Climatological variations in North Atlantic tropical cyclone tracks. *J. Clim.*, **25**, 657–673.
- Corbostero, K. L., and J. Molinari, (2003) The relationship between storm motion, vertical wind shear, and convective asymmetries in tropical cyclones. *J. Atmos. Sci.*, **60(2)**, 366–376. Doi:10.1175/1520-0469(2003)
- Dong, K., 1988: El Niño and tropical cyclone frequency in the Australian region and the northwest Pacific. *Australian Meteor. Magazine*, **36**, 219–225.
- , K., and G. J. Holland, 1994: A global view of the relationship between ENSO and tropical cyclone frequencies. *Acta. Meteor. Sin.*, **8**, 19–29.
- Elsner, J. B., K. B. Liu, B. Kocher, 2000: Spatial variations in major U.S. hurricane activity: statistics and physical mechanism. *J. Clim.*, **13**, 2293–2305.
- , J. B., 2003: Tracking hurricanes. *Bull. Amer. Meteor. Soc.*, **84**, 353–356.
- , J. B., and K. B. Liu, 2003: Examining the ENSO-typhoon hypothesis. *Clim. Research*, **25**, 43–54.
- Emanuel, K. A., 1999: Thermodynamic control of hurricane intensity. *Nature* **401**, 665–669.
- Fink, A. H. and P. Speth, 1998: Tropical cyclones. *Naturwissenschaften*, **85**, 482–493.
- Flores, J. F. and V. F. Balagot, 1969: Climate of the Philippines. In *Climates of Northern and Eastern Asia* (ed. H. Arakawa), Chapter 3, 159–213. Elsevier, *World Survey of Clim.*, Vol. 8.

- Frank, W. M., 1987: Tropical cyclone formation. In: A global view of tropical cyclones. Washington, DC, Elsberry, 53-90
- , W. M., and P. E. Roundy, 2006: The role of tropical waves in tropical cyclogenesis. *Mon. Wea. Rev.*, **134**, 2397-2417.
- Fudeyasu, H., S. Iizuka, and T. Matsuura, 2006: Impact of ENSO on landfall characteristics of tropical cyclones over the western North Pacific during the summer monsoon season. *Geophys. Res. Lett.*, **33**, L21815, doi:10.1029/2006GL027449.
- Gaffney, S. J., 2004: Probabilistic curve-aligned clustering and prediction with regression mixture models. Ph.D. thesis, University of California, Irvine, CA, 281 pp.
- Gaffney, S. J., A. W. Robertson, A. Smyth, S. J. Camargo, and M. Ghil, 2007: Probabilistic clustering of extratropical cyclones using regression mixture model, *Climate Dyn.*, **29**, 423-440.
- Garcia-Herrera, R., P. Ribera, E. Hernandez, and L. Gimeo, 2007: Northwest Pacific typhoons documented by the Philippine Jesuits, 1566-1900. *J. Geophys. Res.*, **112**, D06108.
- Gray, W.M., 1968: Global view of the origin of tropical disturbance and storms. *Mon. Wea. Rev.*, **96**, 669-700.
- , W. M., 1977: Tropical cyclone genesis in the western North Pacific. *J. of the Meteor. Soc. of Japan*, **55**, 465-482.
- , W. M., 1979: Hurricanes: Their formation, structure and likely role in the tropical circulation. *Meteorology over the Tropical Oceans*, D. B. Shaw, Ed., *Roy. Meteor. Soc.*, 155-218.
- , W. M., 1985: Tropical cyclones global climatology. Volume 1, WMO Tech Doc. WMO/TD-No. 7f2, World Meteorological Organization, 3-19.
- , W. M., 1993: Predicting Atlantic basin seasonal tropical cyclone activity by 1 August. *Wea. Forecasting*, **8**, 73-86.
- Hair, J. F., R. E. Anderson, R. L. Tatham and W. C. Black, 1992: Multivariate data analysis(3<sup>rd</sup> ed). Macmillan, New York.
- Hall, T. M., and S. Jewson, 2007: Statistical modeling of North Atlantic tropical cyclone tracks. *Tellus A*, **59**, 486-498.

- Harr, P. A. and R. L. Elsberry, 1991: Tropical cyclone track characteristics as a function of large-scale circulation anomalies. *Mo. Wea. Rev.*, **119**, 1448-1468.
- , P. A., and R. L. Elsberry, 1995a: Large-scale circulation variability over the tropical western North Pacific. Part I: Spatial patterns and tropical cyclone characteristics. *Mon. Wea. Rev.*, **123**, 1225–1246.
- , P. A., and R. L. Elsberry, 1995b: Large-scale circulation variability over the tropical western North Pacific. Part II: Persistence and transition characteristics. *Mon. Wea. Rev.*, **123**, 1247–1268.
- Ho, C. H., J. J. Baik, J. H. Kim, and D. Y. Gong, 2004: Interdecadal changes in summertime typhoon tracks. *J. Clim.*, **17**, 1767–1776.
- Hodanish, S., and W. M. Gray, 1993: An observational analysis of tropical cyclone recurvature. *Mon. Wea. Rev.*, **121**, 2665–2689.
- Holland, G. J., 1983: Tropical cyclone motion: Environmental interaction plus a beta effect. *J. Atmos. Sci.*, **40**, 328-342.
- , G. J., 1993: Tropical cyclone motion. Global guide to tropical cyclone forecasting, G. J. Holland, Ed., World Meteorological Organization, WMO/TD-500.
- , G. J., 1995: Scale interaction in the western Pacific monsoon. *Meteor. Atmos. Sci.*, **56**, 57-79.
- Hope, 1979: Tropical cyclone climatology. Operational techniques for forecasting TC intensity and movements. WMO *World Weather Watch*, **528**.
- Kalnay, E., and Co-authors, 1996: The NCEP/NCAR 40-year re-analysis project. *Bull. Amer. Meteor. Soc.*, **77**, 437-471.
- Kaufman, L. and P. J. Rousseeuw, 2005: Finding groups in data: An introduction to cluster analysis. ISBN: 978-0-471-73578-6
- Kim, H. S., J. H. Kim, C. H. Ho, and P. S. Chu, 2011: Pattern classification of typhoon tracks using the fuzzy c-means clustering method. *J. Clim.*, **24(2)**, 4889-508. doi: 10.1175/2011jcli3751.1
- Kim, J. H., C. H. Ho, H. S. Kim, C. H. Sui, and S. K. Park, 2008: Systematic variation of summertime tropical cyclone activity in the western North Pacific in relation to the Madden–Julian Oscillation. *J. Clim.*, **21**:6, 1171-1191.

- Kimberlain, T. B., 1999: The effects of ENSO on North Pacific and North Atlantic tropical cyclone activity. In *Preprints of the 23rd Conference on Hurricanes and Tropical Meteorology*, 250–253, Boston, American Meteorological Society.
- Kistler, R., and Coauthors, 2001: The NCEP–NCAR 50–year reanalysis: Monthly means CD–ROM and documentation. *Bull. Amer. Meteor. Soc.*, **82**, 247–267.
- Knaff, J. A., 1997: Implications of summertime sea level pressure anomalies in the tropical Atlantic region. *J. Clim.*, **10**, 789–804.
- Kossin, J. P., S. J. Camargo, and M. Sitkowski, 2010: Climate modulation of North Atlantic hurricane tracks. *J. Clim.*, **28**, 3057–3076.
- Kubota, H. and J. C. L. Chan, 2009: Interdecadal variability of tropical cyclone landfall in the Philippines from 1902 to 2005. *Geophys. Res. Lett.*, **36**, L12802.
- Lander, M. A., 1993: Comments on “A GCM simulation of the relationship between tropical storm formation and ENSO.” *Mon. Wea. Rev.*, **121**, 2137–2143.
- , M. A., 1994: An exploratory analysis of the relationship between tropical storm formation in the western North Pacific and ENSO. *Mon. Wea. Rev.*, **122**, 636–651.
- , M. A., 1996: Specific tropical cyclone tracks and unusual tropical cyclone motions associated with a reverse-oriented monsoon trough in the western North Pacific. *Wea. Forecasting*, **11**, 170–186.
- Landsea, C. W. 2000. El Niño–Southern Oscillation and the seasonal predictability of tropical cyclones. In *El Niño: Multiscale variability and global and regional impacts*, edited by H. F. Díaz and V. Markgraf, 149–181. Cambridge: Cambridge University Press.
- Lighthill, J., and Coauthors, 1994: Global climate change and tropical cyclones. *Bull. Amer. Meteor. Soc.*, **75**, 2147–2157.
- Love, G., 1982: The role of the general circulation in Western Pacific tropical cyclone genesis. Colorado State University Atmospheric Science paper no. 340.
- Lyon, B., and S. J. Camargo, 2008: The seasonally varying influence of ENSO on rainfall and tropical cyclone activity in the Philippines. *Climate Dyn.*, **32**, 125–141.
- McBride, J. L., 1996: Tropical cyclone formation. In: Global perspectives on tropical cyclones. WMO/Tech. Doc. 693, World Meteorological Organization, Geneva,

Elsberry, 63-105.

- MacQueen, J., 1967: Some methods for classification and analysis of multivariate observations. *Proc. Fifth Berkeley Symp. on Mathematical Statistics and Probability*, Berkeley, CA, University of California, 281–297.
- McCloskey, T. A., T. A. Bianchette, and K.B. Liu, 2013: Track patterns of landfalling and coastal tropical cyclones in the Atlantic Basin, their relationship with the North Atlantic Oscillation (NAO), and the potential effect of global warming. *Amer. J. Clim. Change*, 2013, **2**, 12-22.
- Milligan, G. W., 1980: An examination of the effect of six types of error perturbation on fifteen clustering algorithms, *Psychometrika*, **45**, 325-342.
- Nakamura, J., U. Lall, Y. Kushir, and S. J. Camargo, 2009: Classifying North Atlantic tropical cyclone tracks by their mass moments. *J. Clim.*, **22**, 5481-5494.
- Neumann, C. J., 1993: Global overview. In *Global Guide to Tropical Cyclone Forecasting*, edited by G. J. Holland, *WMO/TD No. 560*, 1.1-1.56.
- Perrone, T. J., Lowe, P. R., 1986: A statistically derived prediction procedure for tropical storm formation. *Mon. Wea. Rev.*, **114**, 165-177.
- Powell, M., G. Soukup, S. Cocke, S. Gulati, N. Morisseau-Leroy, S. Hamid, N. Dorst and L. Axe (2005). State of Florida hurricane loss projection model: Atmospheric science component. *J. of Wind Engineering and Industrial Aerodynamics.*, **93(8)**, 651-674.
- Pudov, V. D., and S. A. Petrichenko, 1998: Relationship between the evolution of tropical cyclones in the northwestern Pacific and El Niño. *Oceanology*, **38**, 447–452.
- , and ———, 2001: 1997–1998 El Niño and tropical cyclone genesis in the northwestern Pacific. *Izv. Atmos. Oceanic Phys.*, **37**, 576–583.
- Punji, G., and D. W. Stewart, 1983: Cluster analysis in marketing research: Review and suggestions for application. *J. Marketing Res.*, **20**, 134-148.
- Ramsay, H. A., S. J. Camargo, and D. Kim, 2011: Cluster analysis of tropical cyclone tracks in the southern hemisphere. *Clim. Dyn.*, **39**, 897-917.
- Rasmusson, E. M., and T. H. Carpenter, 1982: Variations in tropical sea surface temperature and surface wind fields associated with Southern Oscillation/El Niño. *Mon. Wea. Rev.*, **110**, 354– 384.

- Ribera, P., R. Garcia-Herrera, L. Gimeno, and E. Hernandez, 2005: Typhoons in the Philippine Islands, 1901-1934. *Clim. Res.*, **29**, 85-90.
- Ritchie, E. A. and G. J. Holland, 1999: Large-scale patterns associated with tropical cyclogenesis in the western Pacific. *Mon. Wea. Rev.*, **127**, 2027-2043.
- Sadler, J. C., 1967: On the origin of tropical vortex. *Proc. Working Panel on Tropical Dynamic Meteorology*, Norfolk, VA, Naval Wea. Res. Facility, 39-75.
- Sandgathe, S. A., 1987: Opportunities for tropical cyclone motion research in the northwest Pacific region. Tech. Rep. NPS-63-87-006, Naval Postgraduate School, Monterey, CA, 36 pp.
- Saunders, M.A., R.E. Chandler, C. J. Merchant, and F.P. Roberts, 2000: Atlantic hurricanes and NW Pacific typhoons: ENSO spatial impacts on occurrence and landfall. *Geophys. Res. Lett.*, **27**, 1147-1150.
- Shoemaker, D. N., 1991: Characteristics of tropical cyclones affecting the Philippine Islands. *NOCC/JTWC Technical Note 91-1*, 35 pp.
- Smith, T. M., and R. W. Reynolds, 2003: Extended reconstruction of global sea surface temperature based on COADS data (1854-1997). *J. Clim.*, **16**, 1495-1510.
- Smith, T. M., R. W. Reynolds, T. C. Peterson, and J. Lawrimore, 2008: Improvements to NOAA's historical merged land-ocean surface temperature analysis (1880-2006). *J. Clim.*, **21**, 2283-2296.
- Torrence, C., and G. P. Compo, 1998: A Practical guide to wavelet analysis. *Bull. Amer. Meteor. Soc.*, **79**, 61-78.
- Tuleya, R. E., and Y. Kurihara, 1981: A numerical study of the effects of environmental flow on tropical storm genesis, *ibid.*, **109**, 2487-2506.
- Saunders, M.A., R.E. Chandler, C. J. Merchant, and F.P. Roberts, 2000: Atlantic hurricanes and NW Pacific typhoons: ENSO spatial impacts on occurrence and landfall. *Geophys. Res. Lett.*, **27**, 1147-1150.
- Shoemaker, D. N., 1991: Characteristics of tropical cyclones affecting the Philippine Islands. *NOCC/JTWC Technical Note 91-1*, 35 pp.
- USCIA World Factbook, 2013, <https://www.cia.gov/library/publications/the-world-factbook/>
- Vincent, D. G., and J. M. Schrage, 1995: Thermodynamic and moisture variables. Vol.

2. Climatology of the TOGA-COARE and adjacent regions (1985–1990). Department of Earth and Atmospheric Sciences, Purdue University, 123 pp.

- Wang, B., and J. C. L. Chan, 2002: How strong ENSO events affect tropical storm activity over the western North Pacific. *J. Clim.*, **15**, 1643-1658.
- Wang, Y., and G. J. Holland, 1996: Tropical cyclone motion and evolution in vertical shear. *J. Atmos. Sci.*, **53(22)**, 3313-3332.
- Wendland, W. M., 1977: Tropical storm frequencies related to sea surface temperatures. *J. App. Meteor.*, **16**, 477-481.
- Wu, C. C., K. H. Chou, H. J. Cheng, and Y. Wang, 2003: Eyewall contraction, breakdown and reformation in a landfalling typhoon. *Geophys. Res. Lett.*, **30** (17), 1887, doi: 10.1029/2003 GL01765.
- Wu, M. C., W. L. Chang, and W. M. Leung, 2004: Impacts of El Niño-Southern Oscillation events on tropical cyclone landfalling activity in the western North Pacific. *J. Clim.*, **17**, 1419-1428.
- Wu, C. C., and K. A. Emanuel, 1993: Interaction of a baroclinic vortex with background shear: application to hurricane movement. *J. Atmos. Sci.*, **50(1)**, 62-76, doi:10.1175/1520-0469(1993)050<0062:ioabvw>2.0.co;2
- Wu, G., and N. C. Lau. 1992: A GCM simulation of the relationship between tropical storm formation and ENSO. *Mon. Wea. Rev.*, **120**, 958–977.
- Wu, L., and B. Wang. 2004: Assessing impacts of global warming on tropical cyclone tracks. *J. Clim.*, **17**, 1686-1698.
- Xue, Z., and C. J. Neumann, 1984: Frequency and motion of western North Pacific tropical cyclones. *NOAA Tech. Memo*, NWS NHC 23 (PB85106466), 89 pp.
- Zhang, W., H. F. Graf, Y. Leung, and M. Herzog, 2012: Different El Niño types and tropical cyclone landfall in East Asia. *J. Clim.*, **25**, 6510–6523.
- Zhang, W., Y. Leung, and Y. Wang, 2012: Cluster analysis of post-landfall tracks of landfalling tropical cyclones over China. *Clim. Dyn.*, September 2012.